

BEACH EROSION MODEL (EBEACH) USERS MANUAL
VOLUME II: THEORY AND BACKGROUND

by

David L. Kriebel

Department of Civil Engineering
University of Delaware
Newark, DE 19711

and

Department of Coastal and Oceanographic Engineering
University of Florida
Gainesville, FL 32606

through

Beaches and Shores Resource Center
Florida State University

BEACHES AND SHORES
TECHNICAL AND DESIGN MEMORANDUM NO. 84-5-II

COASTAL ZONE
INFORMATION CENTER

Reviewed by

Beaches and Shores Resource Center
Institute of Science and Public Affairs
Florida State University

and

Florida Office of Coastal Management
Florida Department of Environmental Regulation

Funded by

A grant from the U. S. Office of Coastal Zone Management
National Oceanic and Atmospheric Administration
(under the Coastal Zone Management Act of 1972, as amended)
through

Florida Office of Coastal Management
Florida Department of Environmental Regulation

and

Florida Department of Natural Resources

FOREWORD

This users manual describes the numerical computer model EBEACH which is designed to estimate the time-dependent beach-dune erosion associated with severe storm such as hurricanes or northeasters. The users manual is presented in two parts: volume I contains a description of program logic and variables used, volume II provides a more thorough discussion of background theory and model verification. The original research pertaining to the EBEACH model was conducted by the author under the direction of Robert G. Dean as part of the author's Master or Civil Engineering degree at the University of Delaware. The research phase was supported by the National Oceanic and Atmospheric Administration and the Delaware Sea Grant College Program.

The present work is presented in partial fulfillment of contractual obligations of the Federal Coastal Zone Management Program (subject to provisions of the Coastal Zone Management Improvement Act of 1972, as amended) subject to provisions of contract CM-37 entitled "Engineering Support Enhancement Program". Under provisions of DNR contract C0037, this work is a subcontracted product of the Beaches and Shores Resource Center, Institute of Science and Public Affairs, Florida State University. The document has been adopted as a Beaches and Shores Technical and Design Memorandum in accordance with provisions of Chapter 16B-33, Florida Administrative Code.

At the time of submission for contractual compliance, James H. Balsillie was the contract manager and Administrator of the Analysis/Research Section, Hal N. Bean was Chief of the Bureau of Coastal Data Acquisition, Deborah E. Flack Director of the Division of Beaches and Shores, and Dr. Elton J. Gissendanner the Executive Director of the Florida Department of Natural Resources.

Deborah E. Flack

Deborah E. Flack, Director
Division of Beaches and Shores

July, 1984

Property of CSC Library

U. S. DEPARTMENT OF COMMERCE NOAA
COASTAL SERVICES CENTER
2234 SOUTH HOBSON AVENUE
CHARLESTON, SC 29405-2413

JAN 21 1987

GB459. F56b no. 84-5-2
11321355

TABLE OF CONTENTS

<u>Chapter</u>		<u>Page</u>
I	INTRODUCTION	1
	1.1 Schematic Erosion Prediction Methods	3
	1.2 Proposed Method	12
II	EQUILIBRIUM BEACH PROFILE THEORY	17
III	SEDIMENTS TRANSPORT EQUATION	19
IV	NUMERICAL SOLUTION OF CONTINUITY EQUATION	26
V	INITIAL PROFILE AND SOLUTION DOMAINS	31
	5.1 Boundary Conditions	33
	5.2 Simulation of Erosion Process	35
VI	RESULTS-GENERAL BEHAVIOR	37
	6.1 Relative Effects of Water Level and Wave Height	39
	6.2 Relative Effects of Sand Grain Size and Beach Slope	42
VII	SIMULATION OF STORM SURGE HYDROGRAPH	45
VIII	RESULTS-SIMULATION OF HURRICANE ELOISE	55
	REFERENCES	71
	APPENDIX A	A1
	APPENDIX B	B1

LIST OF FIGURES

<u>Figure</u>		<u>Page</u>
1	Seasonal Change in Beach Profile	2
2	Bruun's Equilibrium Beach Profile	3
3	Bruun's Response of Equilibrium Profile to Sea Level Rise	4
4a	Edelman's Method Applied Natural Profile	6
4b	Edelman's Method Applied to Schematic Profile	6
5	Edelman's Method Applied to Concave-Upwards Profile	7
6	Swart's Schematic Beach Profile	8
7	Dean's Method for Determining Maximum Potential Erosion Due to Storm Surge Using Schematic Equilibrium Beach Profile	11
8	General Characteristics of the Beach Profile Before and After the Storm	13
9a	Schematic Beach-Dune Profile with Wide Berm	15
9b	Schematic Beach-Dune profile with no Berm	15
10	Particle Diameter Versus Shape Factor (A)	20
11	Particle Diameter Versus Equilibrium Energy Dissipation Based on the Smooth Average Curve Presented in Figure 10	21
12a	Equilibrium Profile Subjected to Increased Water Level Showing Decreased Surf Zone Width	22
12b	Equilibrium Profile Re-Established Relative to Increased Water Level	22
13a	Decreased Surf Zone Width Resulting From Beach Fill	23
13b	Beach Fill Distributed Over Surf Zone at Equilibrium	23
14	Effect of Varing the Sediment Transport Rate Coefficient on Cumulative Erosion During the Simulation of Saville's (1975) Laboratory Investigation of Beach Profile Evolution for a 0.2 mm Sand Size	25
15	Numerical Representation of Surf Zone Showing a Sediment Transport Over Imaginary Cell	27

<u>Figure</u>		<u>Page</u>
16	Time Dependent Solution for Berm Recession Due to Steady-State Forcing Conditions	38
17	Effect of Storm Surge Level on Volumetric Erosion	40
18	Effect of Wave Height on Volumetric Erosion	41
19	Effect of Sand Grain Size on Berm Recession	43
20	Effect of Beach Face Slope on Berm Recession	44
21	Method of Normalizing Axis to Represent Storm Surge Hydrograph and Maximum Potential Erosion	47
22	Schematic of Numerical Results Showing Predicted Erosion Curve Approaching Equilibrium for Smooth Increase to Static Peak Surge Level	48
23	Schematic of Numerical Results Showing Predicted Erosion Curve Reaching a Maximum as Water Level Decreases Following Peak Surge Level	48
24	Effect of Storm Surge Duration on Volumetric Erosion, 12 Hr. Storm Surge	50
25	Effect of Storm Surge Duration on Volumetric Erosion, 24 Hr. Storm Surge	51
26	Effect of Storm Surge Duration on Volumetric Erosion, 36 Hr. Storm Surge	52
27	Comparison of the Effects of 12, 24, and 36 Hr. Storm Surge on Volume Erosion	54
28	Estimated Storm Surge Hydrograph, Hurricane Eloise Bay-Walton County Line	57
29	Representative Profile, Bay-Walton County Line	59
30a	Steepening of Natural Dune Form	63
30b	Uniform Recession of Schematic Dune Form	63
31	Example of Predicted Post-Storm Beach-Dune Profile, Hurricane Eloise, Bay-Walton Counties, Florida	66
32	Comparison of Predicted Post-Storm Profile to Maximum Potential Erosion Due to Static Peak Surge Level, Hurricane Eloise, Bay-Walton Counties, Florida (Chiu, 1977)	67

<u>Figure</u>		<u>Page</u>
33	Contour Advance/Retreat Due to Hurricane Eloise Bay-Walton Counties, Florida (Chiu, 1977)	69
34	Volumetric Erosion Distribution and Beach Face Slope Variation, Bay-Walton Counties, Florida (Chiu, 1977)	70

LIST OF TABLES

<u>Table</u>		<u>Page</u>
I	HSTAR Values Versus Beach Slope and Sand Grain Sizes (Based on Moore's Sand Grain Size Versus Energy Dissipation)	32
II	Simulation of Schematic Profile of Bay-Walton County Hurricane Eloise	60
III	Observed Erosion Characteristics for Bay-Walton Counties	61
IV	Equilibrium Recession For Static Peak Surge Level Schematic Profile of Bay-Walton County	61

BEACH EROSION MODEL (EBEACH)

I. INTRODUCTION

At present, the mechanics of sand transport in the surf zone and on the foreshore are not known with certainty. Field measurements of beach profiles and plan forms have been widely used to identify erosion trends; however, few detailed pre-and post-storm profiles exist from which empirical relationships can be developed. Theoretical expressions have been developed to explain bed load and suspended load sediment transport for both the longshore and onshore-offshore modes. Again, however, field data from severe storms are not available to verify these theoretical equations. Laboratory experiments in small and large scale wave tanks have also been used to simulate prototype conditions, but the extension of these laboratory results, to predict erosion in nature, has not always been successful.

In general, it is known that as the water level rises during a severe storm, waves attack the berm or dune and large quantities of sand are transported offshore, either suspended in the turbulent water column or concentrated as bed load. At the seaward edge of the surf zone, the first breaking of the incoming waves effectively limits offshore sediment transport. While localized currents resulting from nearshore water surface gradients surely move some sediment beyond the breaking depth, most sand is deposited near the break point in the form of a bar. If no sand is gained or lost in the longshore direction, it may be argued that the idealized beach response results in a redistribution of sand over the surf zone, as the profile adjusts to a more stable form. If no overwash occurs, then the sand mass is conserved in the surf zone such that the volume deposited offshore equals the volume eroded onshore.

From this argument, several beach erosion prediction methods have been

developed. These methods are based on the assumptions that: (1) sand is conserved in the onshore-offshore direction and (2) the beach profile may be represented in schematic form, in which both the pre-and post-storm profile shapes are known. It is well known that beaches seem to reach seasonally stable shapes. In Figure 1, the "summer" or normal beach typically has a broad berm and a smooth profile, the result of onshore sand transport during a relatively mild wave climate. In contrast, the "winter" or storm beach may be characterized by a narrow berm and offshore bars, the result of offshore transport from the beach face to the seaward edge of the surf zone by larger waves from winter storms.

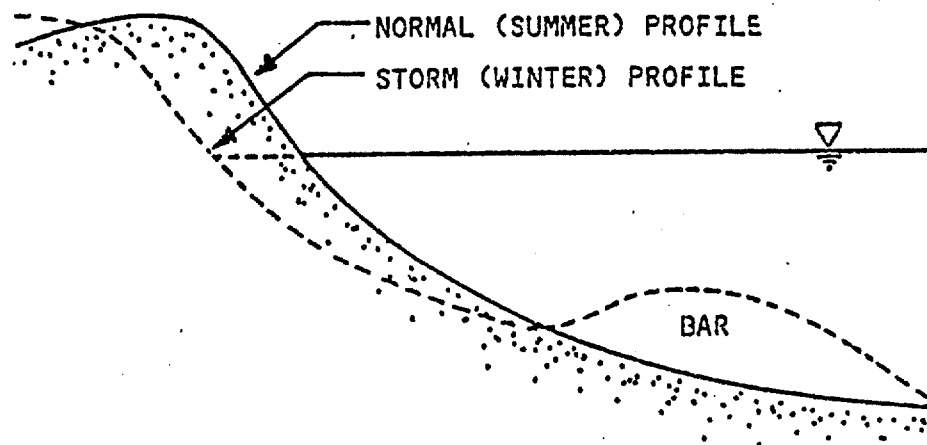


Figure 1 Seasonal Change in Beach Profile

Fenneman (1902) observed that beaches also exhibit a characteristic "profile of equilibrium", in which the entire beach profile reaches a state of equilibrium for the given sediment size, wave characteristics, and nearshore currents. If irregularities in the profile, such as troughs and bars, are smoothed, beaches may be considered to reach dynamic equilibrium, in which the

profile shape, relative to the mean water level is maintained as the entire profile slowly moves landward and seaward in response to changing hydraulic conditions. This concept of a unique equilibrium profile shape for any sediment size, has resulted in several highly idealized methods for predicting beach changes due to changing water levels and wave heights.

1.1 Schematic Erosion Prediction Methods

Bruun (1954) discovered that beach profiles from the coasts of California and Denmark exhibited similar shapes. From these profiles, an empirical expression relating water depth, h , to the distance offshore, x , was developed such that:

$$h = Ax^{2/3} \quad (1)$$

in which A is a coefficient that relates the steepness of the profile to the given sediment characteristics. This general profile form is represented in Figure 2.

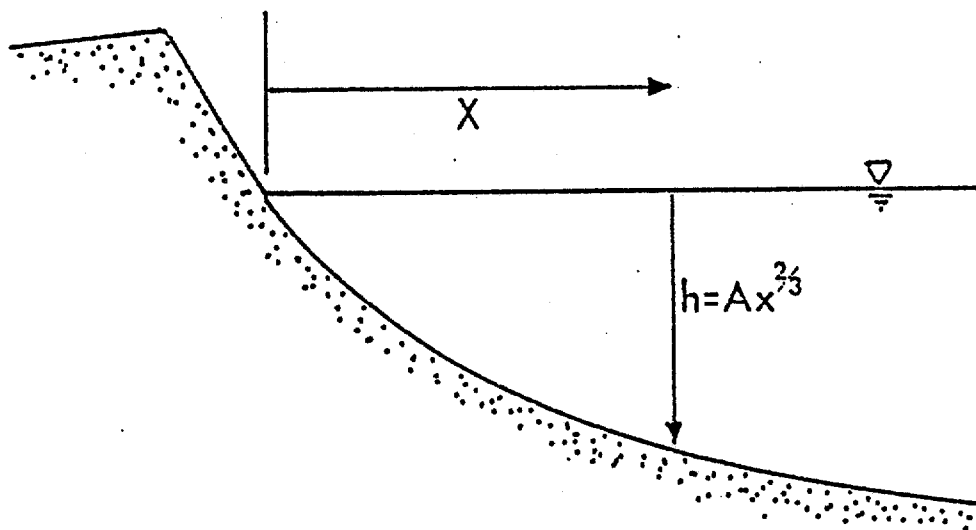


Figure 2 Bruun's Equilibrium Beach Profile

Bruun (1962) proposed that, for the two-dimensional case in which longshore sediment transport gradients do not exist, beach erosion due to a slow sea level rise is predictable since the profile geometry is always known relative to the still water line. As illustrated in Figure 3, for an increase in the water level, S , the profile must be shifted upward by an equal amount, S , to maintain the same relative vertical position. Since this net upward motion requires a considerable addition of sand in the offshore region out to the depth of closure (about 30 feet) the beach must recede by a distance, R , to provide the necessary sand volume. By equating the volume of sand eroded onshore with the volume of sand deposited offshore, the beach recession may be predicted for any given water level rise. Bruun estimated that for a 6 mm/yr rise in water level in southeast Florida, a 2.0 to 2.5 ft/yr recession is required to maintain equilibrium. This is in general agreement with the 1.0 to 3.0 ft/yr average recession observed on most of the East coast of Florida.

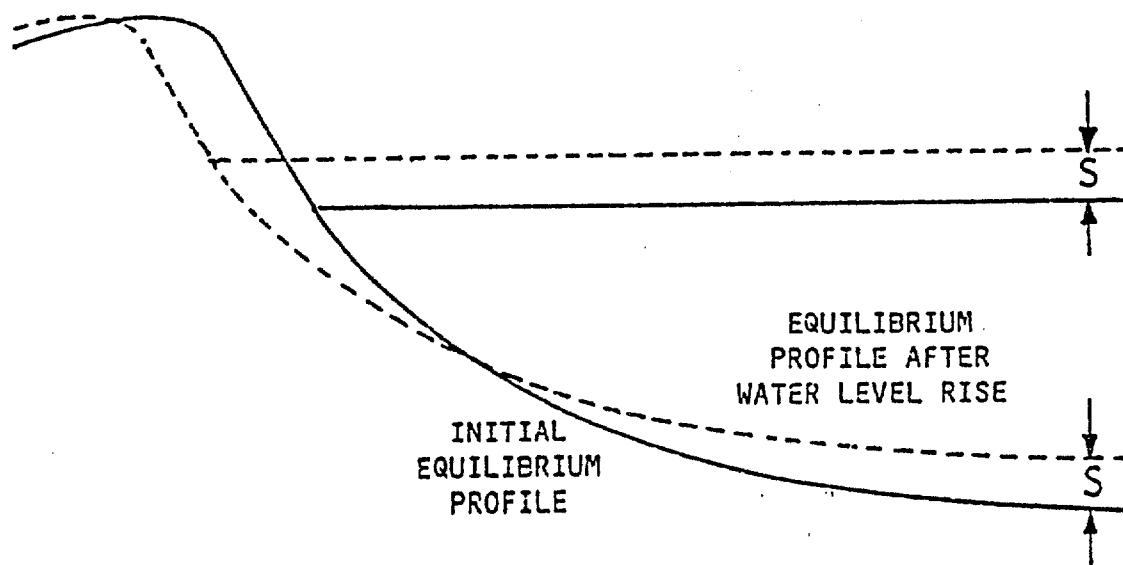


Figure 3 Bruun's Response of Equilibrium Profile to Sea Level Rise

Edelman (1968) observed many beach changes during storms in the Netherlands and suggested that: (1) the post-storm beach profile shape is mainly the result of wave transport of sand perpendicular to the coast, and (2) the short-term, ie. storm duration, transfer of sand occurs from the dunes offshore to the edge of the surf zone, where it is limited by the incoming shore-breaking waves. By using an idealized profile representations in Figures 4a and 4b, Edelman predicted maximum dune erosion due to specific storm conditions by balancing eroded and accreted volumes to satisfy continuity.

Edelman (1972) subsequently modified his earlier work to incorporate: (1) time dependent erosion, and (2) concave-upwards beach profiles as suggested by Brunn and as observed in nature. With a profile shape, given in Figure 5, which the curve AB can be determined empirically, Edelman theorized that the erosion process could be represented by shifting the profile horizontally, with velocity u , and vertically, with velocity v . By assuming that the profile "keeps up" with or moves at the same speed as the rising water level, the recession occurring during any time, Δt , is determined by balancing volumes. The results of this analysis yielded predicted recessions that were much larger than those observed during actual storms; Edelman concluded that erosion does not occur as fast as the water level rise.

Swart (1974) analyzed numerous small and large-scale laboratory experiments and combined the concept of a concave-upward equilibrium profile shape with a simple onshore-offshore sediment transport theory, in the first schematic erosion prediction method to include a time-dependent mechanism of sediment transport. In Figure 6, Swart defined three regions of sediment transport in the beach profile: (1) the backshore, above the wave run-up limit, in which only wind-blown transport occurs, (2) the transition area, seaward of the offshore limit of the surf zone, in which only bed load transport occurs, and (3) the developing or D-profile, including the surf zone and the swash zone, in which bed load and

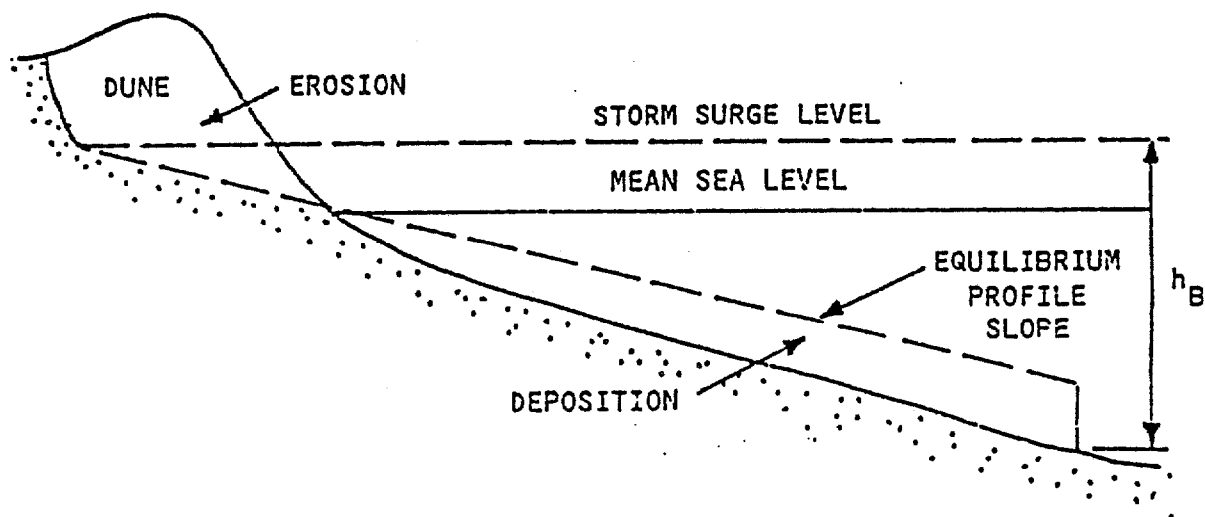


Figure 4a Edelman's Method Applied to Natural Profile

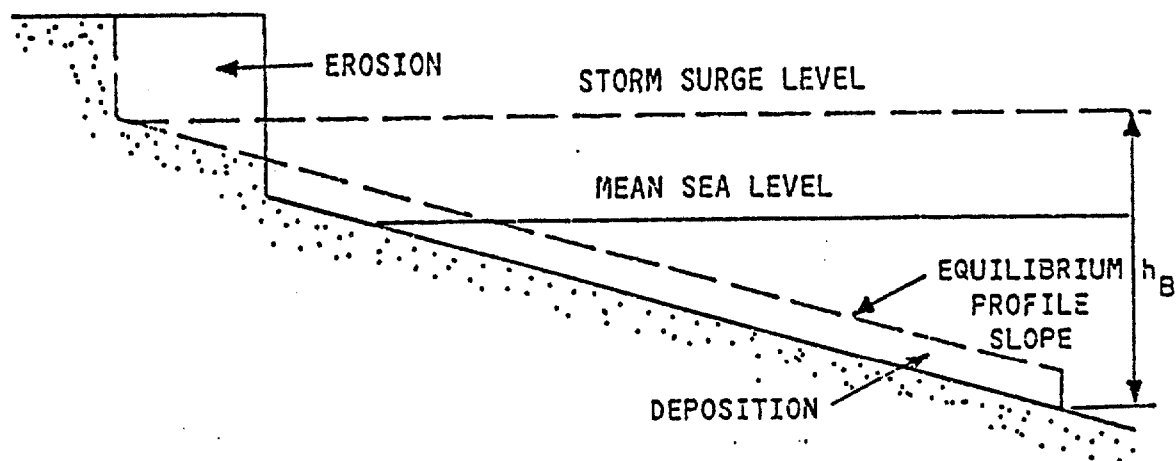


Figure 4b Edelman's Method Applied to Schematic Profile

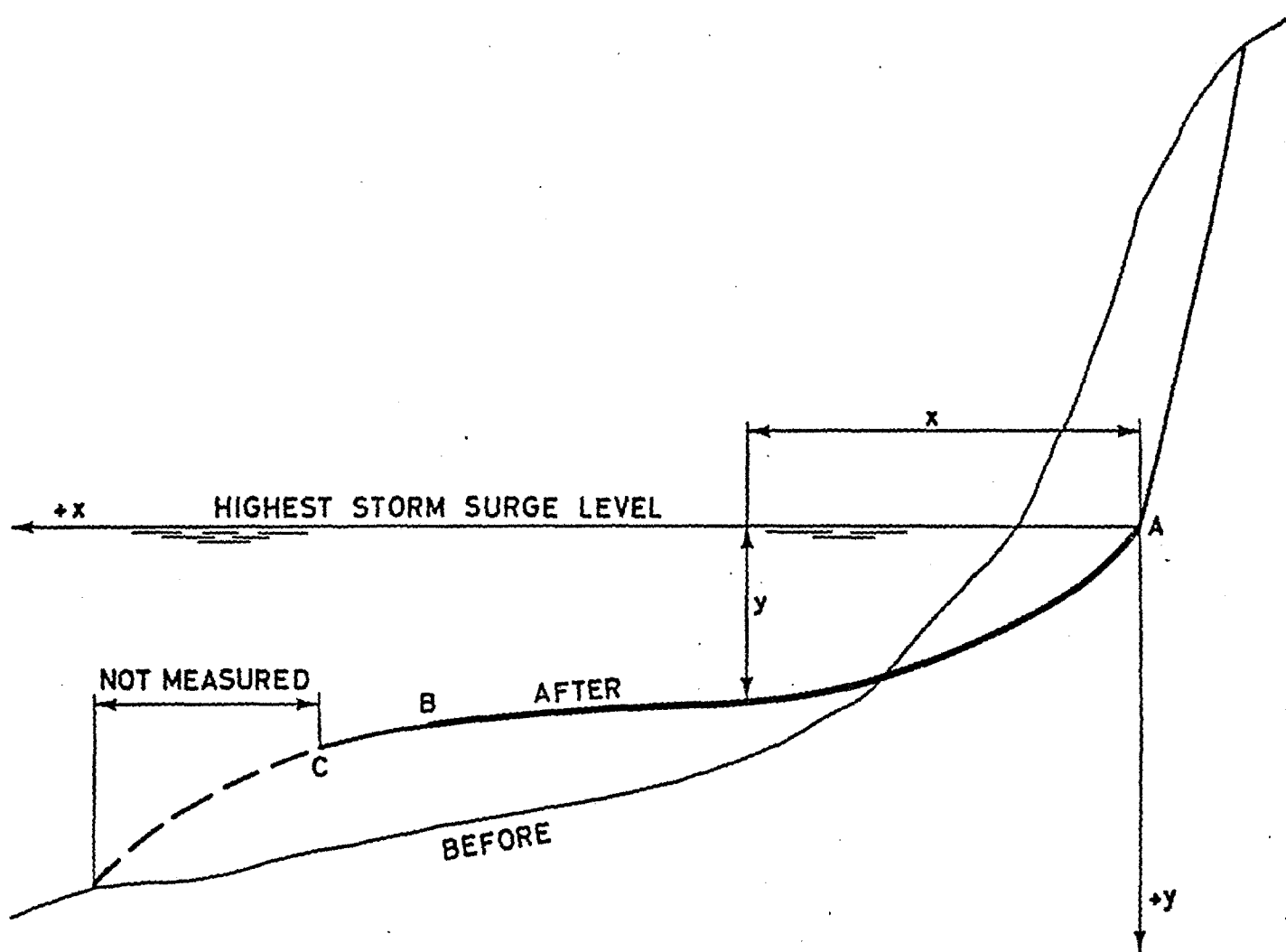


Figure 5 Edelman's Method Applied to Concave-Upwards Profile

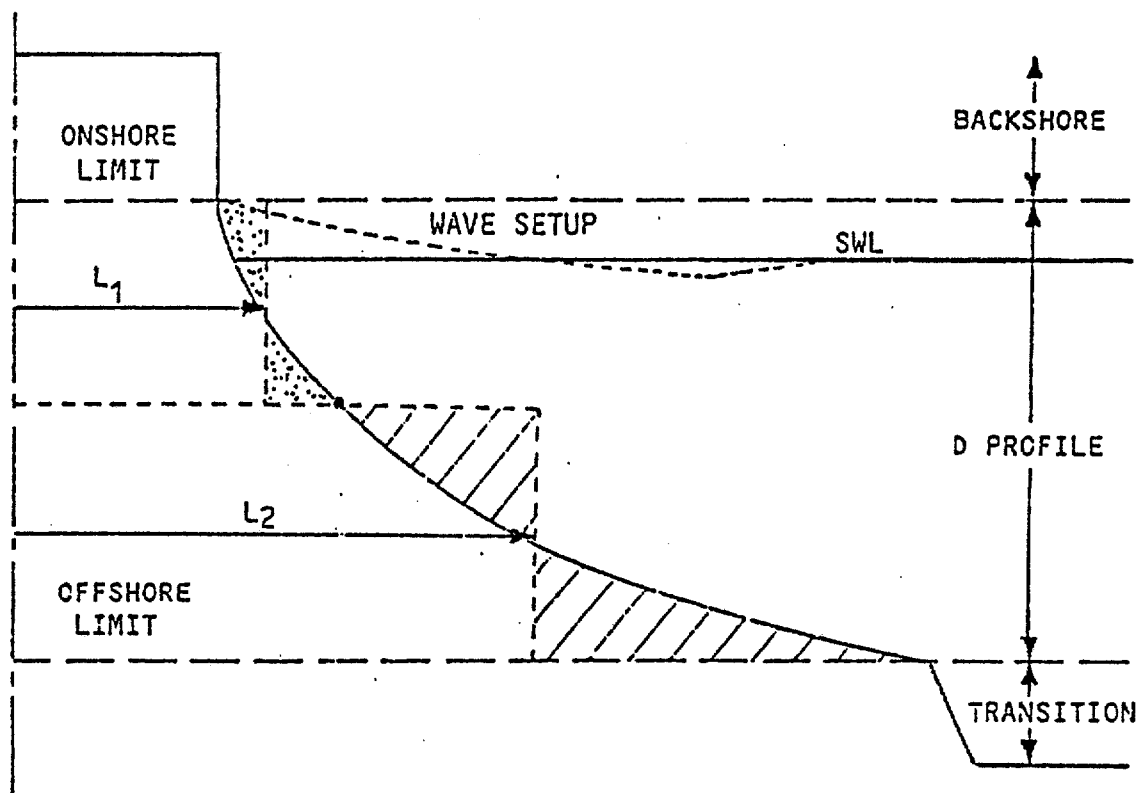


Figure 6 Swart's Schematic Beach Profile

suspended load transport due to breaking waves occurs.

By assuming that a stable, equilibrium profile is eventually attained, Swart developed a simple equation for sediment transport in the D-profile:

$$S_y = s_y(R_w - R_t) \quad (2)$$

in which S_y is a time dependent sediment transport flux in the D-profile, s_y is a transport rate coefficient dependent on specific boundary conditions, R_t is a time dependent parameter related to the sediment transport flux, and R_w is the equilibrium value of R_t . Note that in this expression Swart relates the total sediment transport flux to the disequilibrium of certain surf zone parameters. Swart then proposed that equation 2 could be defined in the D-profile of Figure 6, such that a schematic length $(L_2 - L_1)_t$ and an equilibrium value of $(L_2 - L_1)$, or W , represented the sediment transport mechanism, thus:

$$S_y = s_y [W - (L_2 - L_1)_t] \quad (3)$$

Swart (1974), (1976), developed lengthy, complex empirical relationships to define the D-profile, s_y , and W , in terms of deep water wave characteristics, sediment size, and berm height.

Dean (1977) developed theoretical expressions for possible mechanisms causing equilibrium beach profile shapes. Three possible causes were considered:

- (1) longshore shear stress in the surf zone;
- (2) uniform wave energy dissipation over the surf zone plan area;
- (3) uniform wave energy dissipation per unit volume of water in the surf zone.

Using linear wave theory, Dean found a theoretical form of the beach profile to be:

$$h = Ax^m \quad (4)$$

in which A is a shape factor dependent on sediment size, and m is an exponent

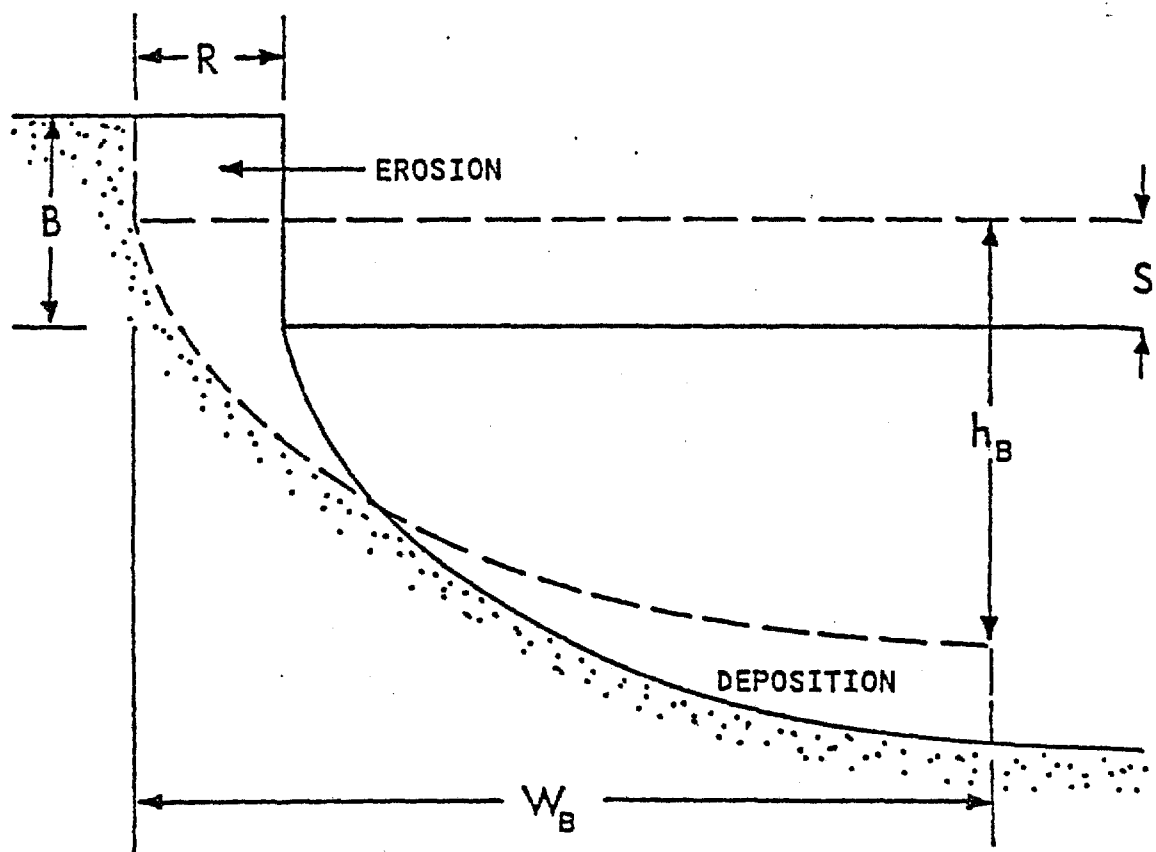
for the profile curvature, such that m equals 0.4 for causes (1) and (2) given previously, and 0.67 for (3).

Upon analysis of 502 beach profiles along the U.S. Atlantic and Gulf coasts, Dean determined the best-fit empirical exponent, m , to be 0.6 to 0.7. This seemed to confirm Bruun's original profile shape in Figure 1 and also identified uniform wave energy dissipation per unit volume as the best explanation of the profile shape.

In a geometric analysis similar to that used by Edelman (1972), but for a simple square-berm profile, Dean (1976) analytically integrated the eroded and accreted volumes, and found the maximum "potential" berm recession as a function of wave height, berm height, water level rise, and the A coefficient as in Figure 7. Dean plotted the dimensionless water level rise, $S' = S/B$, versus the dimensionless breaking depth, $h'_b = h_b/B$, and developed curves for the dimensionless berm recession, $R' = R/W_b$, in which W_b is the surf zone width defined by the breaking depth and the A coefficient. Dean's method allows fast prediction of the maximum berm recession for a highly idealized profile geometry but does not include time dependence.

For storm surge-erosion prediction, Chiu (1977), has found that both Dean's method and Edlman's method over-predicted the actual erosion occurring during Hurricane Eloise, by and much as a factor of five. It seems clear that the rise and fall of water level occurs too quickly for the maximum erosion potential of the peak surge height to be realized. Since most predictions are based on a steady-state maximum storm surge is not surprising that the predicted maximum erosion is often much greater than observed in nature.

Of the schematic beach erosion methods described, none is well verified or completely adequate for general practical application. As mentioned, Edelman and Dean do not include realistic time dependence of the erosion process. Dean



$$R' = S' - \frac{3}{2}h_B' \left[1 - (1-R')^{2/3} \right]$$

$$R' = \frac{R}{W_B}$$

$$h_B' = \frac{h_B}{B}$$

$$S' = \frac{S}{B}$$

$$W_B = \left[\frac{h_B}{A} \right]^{3/2}$$

Figure 7 Dean's Method for Determining Maximum Potential Erosion Due to Storm Surge Using Schematic Equilibrium Beach Profile

and Swart do not include realistic beach face representations and only Edelman's method may be applied to analyze dune erosion. While Swart makes significant advances with the inclusion of a time dependent sediment transport mechanism, the complex, interrelated empirical parameters used in the solution prohibit easy application.

In the state of Florida, another prediction method is also available. Chiu (1972) has developed a modified form of Edelman's (1968) scheme, in which the actual pre-storm profile is approximated by a linear offshore profile, a sloping beach face, and a vertical dune face, illustrated in Figure 8. To find the beach recession or eroded volume, the post-storm profile is represented by linear bottom slope that intersects in peak storm surge elevation. This solution is carried out by computer and has been found to be a good approximation for some storm conditions.

1.2 Proposed Method

This report summarizes the development of an alternative schematic method of predicting beach and dune erosion due to changes in water level and wave height associated with severe storms. This method differs from previous methods in that it is based on:

- (1) more realistic representations of the beach profile, including sloping beach and dune faces;
- (2) a general mechanism for onshore-offshore sand transport in the surf zone;
- (3) the time history of the storm surge, such that the time-dependent shoreline response is predicted.

From preliminary results, this model agrees both qualitatively with observed erosion from Hurricane Eloise.

In general, the model uses a steady state solution of simplified finite difference equations that describe equilibrium beach profile evolution. From

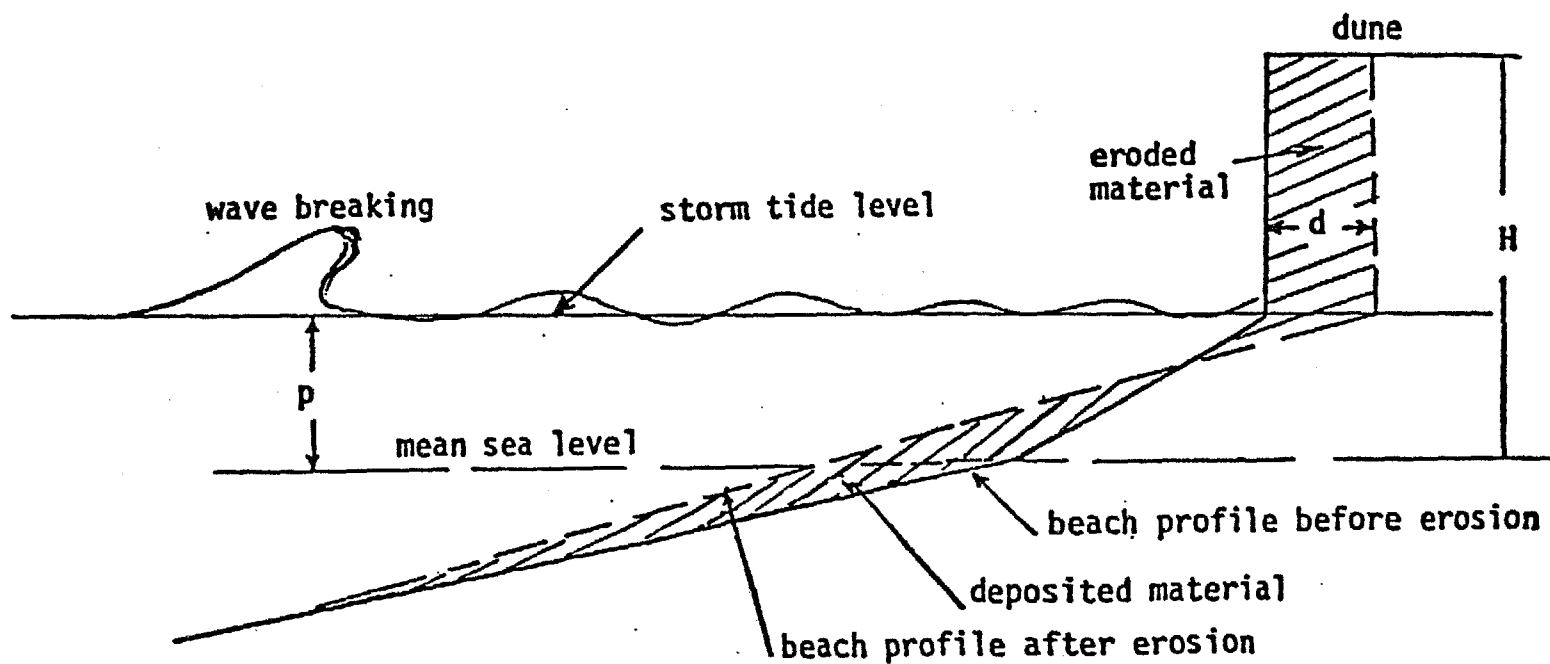


Figure 8 General Characteristics of the Beach Profile Before and After the Storm

Dean's theory, where wave energy dissipation per unit volume in the surf zone governs profile form, a sediment transport equation maybe proposed of the form:

$$Q_s = K (D - D_{eq}) \quad (5)$$

where Q_s is the volumetric sediment transport flux in the onshore-offshore direction, K is a transport rate parameter, and $(D - D_{eq})$ represents the excess energy dissipation per unit volume during storm conditions. This equation is solved simultaneously with the equation of continuity for sand transport normal to the shoreline:

$$\frac{\partial x}{\partial t} = - \frac{\partial Q_s}{\partial h} \quad (6)$$

This ensures that: (1) sand is conserved, i.e. the eroded volume equals the deposited volume and (2) time dependence is included.

Three general types of input are required. First, the actual pre-storm profile is represented in schematic form, as illustrated in Figures 9a and 9b. The initial dune profile is approximated by a constant dune height, h_D , and uniform dune face slope, M_D . Foreshore geometry is expressed as a uniform slope, M_B , and a berm height, h_B . To accomodate a variety of profile forms, the berm width, W_B , may be varied to simulate a wide berm or to simulate a concave profile form with a break in slope between the beach and dune faces. Offshore, the profile is approximated by the equilibrium profile shape

$$h = Ax^{2/3} \quad (7)$$

which is defined by Dean (1977). Second, for specific applications the storm surge hydrograph is required, since the water level at each time step governs profile change. As a third input requirement, wave height values may be input either at each time step or in the form of a constant design wave height. In terms of the

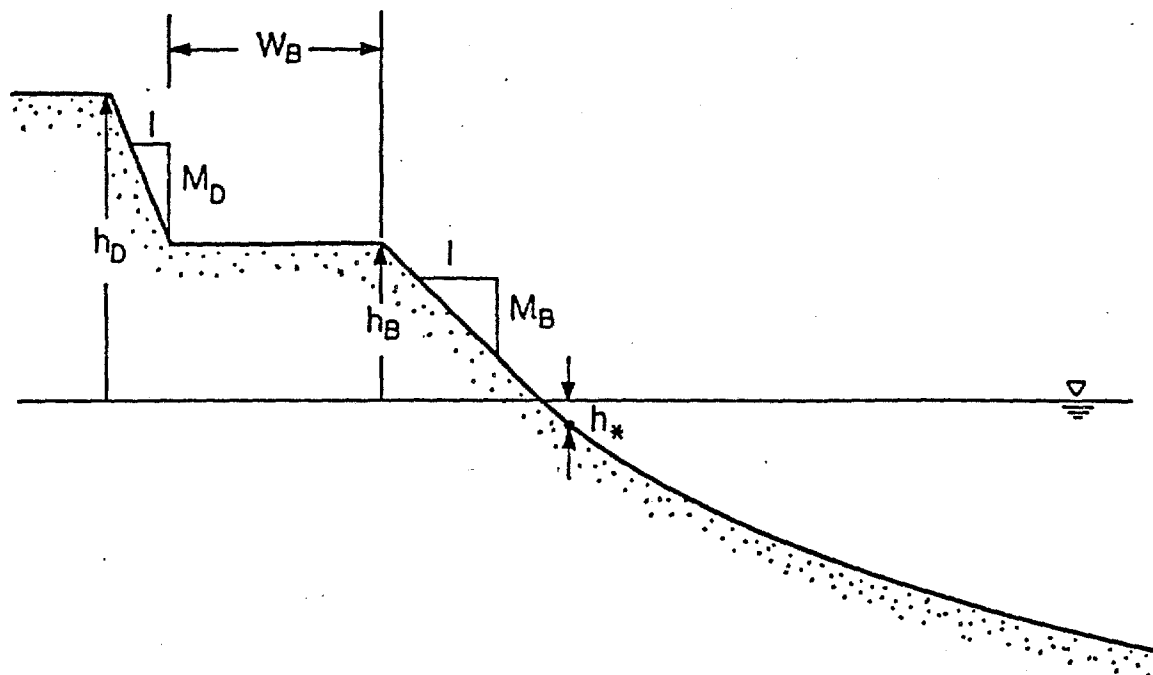


Figure 9a Schematic Beach-Dune Profile with Wide Berm

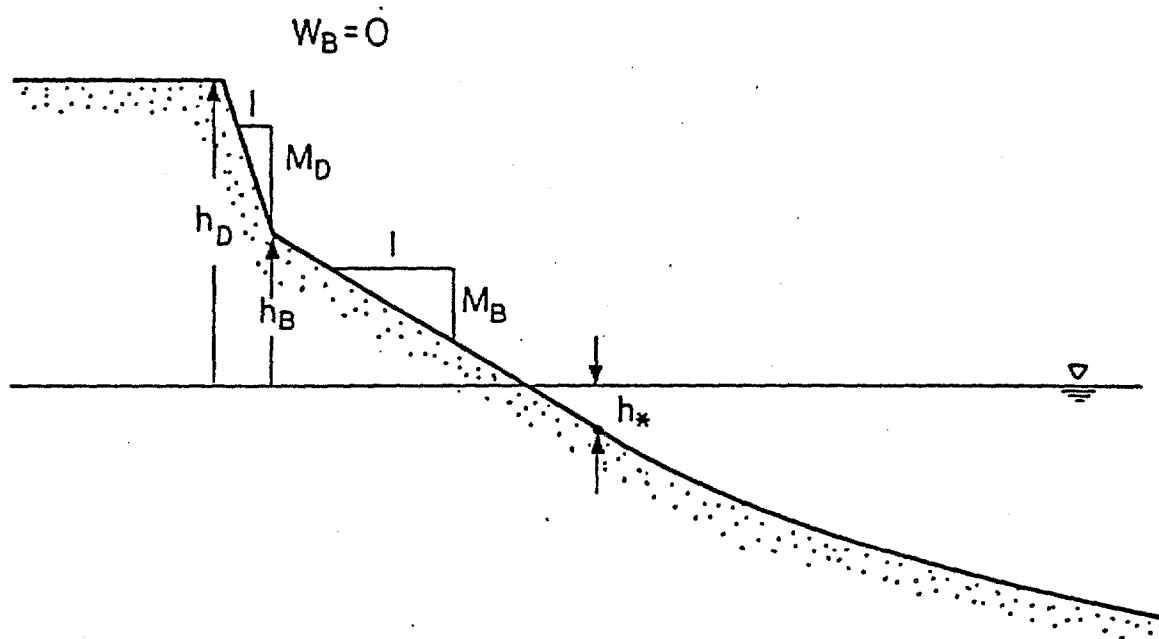


Figure 9b Schematic Beach-Dune Profile with no Berm

numerical solution, the total water level at each time step may be thought of as the driving force inducing profile change with the wave height serving as a boundary condition limiting the active surf zone width.

II. EQUILIBRIUM BEACH PROFILE THEORY

As a wave breaks over a sloping bottom, energy is dissipated in the form of turbulence and bottom friction. In general terms, this net energy loss in some control volume of unit width, $h \Delta x$, may be expressed by the change in energy flux over the volume. The energy dissipation per unit volume, D , may be expressed as:

$$D = \frac{F(x + \Delta x) - F(x)}{\bar{h} \Delta x} \quad (8)$$

where F is the energy flux at the volume boundary and is defined as positive in onshore direction, and \bar{h} is the average depth over the distance, Δx . In differential form, the energy dissipation may be given as:

$$D = \frac{1}{\bar{h}} \frac{\partial F}{\partial x} \quad (9)$$

From linear wave theory, the energy flux is equal to the total wave energy, E , times the speed at which the wave energy is transmitted, the group velocity, C_g . Thus,

$$F = EC_g \quad (10)$$

In the surf zone, the energy flux may be rewritten in terms of the water depth only. Employing both the shallow water and spilling breaker assumptions, Equation (10) is found to be:

$$F = \frac{1}{8} \gamma \kappa^2 g^{1/2} h^{5/2} \quad (11)$$

where κ is taken as 0.78 and γ is the specific weight of sea water.

By substituting this last expression for the energy flux into the differential form of the energy dissipation to be dependent on the water depth and bottom slope:

$$D = \frac{5}{16} \gamma \kappa^2 g^{1/2} h^{1/2} \frac{\partial h}{\partial x} \quad (12)$$

From this expression Dean determined the theoretical beach profile shape resulting from uniform wave energy dissipation per unit volume in the surf zone as:

$$h = Ax^{2/3} \quad (13a)$$

in which

$$A = \left[\frac{24}{5} \frac{D}{\gamma \kappa^2 g^{1/2}} \right]^{2/3} \quad (13b)$$

Dean's results seem to confirm the equilibrium profile shape suggested by Bruun where A is a shape parameter dependent on the sediment size.

Dean (1977) performed a least-squares analysis of 502 beach profiles from the East and Gulf coasts and determined the best-fit A parameter for each profile. In similar analysis, Hughes (1978) and Moore (1982) extended the empirical results to include a wide variety of sand grain sizes. In Figure 10, Moore (1982) presents a summary of these results in which the shape factor, A, is plotted versus grain size. In Figure 11 the equilibrium energy dissipation per unit volume is plotted versus grain size based on the A values in Figure 10 and Equation 13b. It is also possible to perform a least squares or similar analysis to determine A from a recorded offshore profile.

III. SEDIMENT TRANSPORT EQUATION

It was noted that Swart calculated the time-dependent profile change using a sediment transport relationship in which the sediment transport flux is dependent on the disequilibrium of the surf zone system. With Dean's theory that the equilibrium form of beach profiles results from uniform wave energy dissipation per unit volume, a similar sediment transport equation based on the disequilibrium of the energy dissipation may be proposed as:

$$Q_s = K(D - D_{eq}) \quad (14)$$

In this expression, Q_s is the volumetric flux of sand, K is a transport rate parameter, D is the actual energy dissipation, and D_{eq} is the equilibrium energy dissipation obtained from Figure 11.

With Equation (14), if D is greater than D_{eq} then Q_s is positive and offshore. For example, in Figures 12a and 12b, consider a profile initially in equilibrium with a constant breaking wave height, H_B and constant breaking depth h_B . If the water level is increased, then waves break closer to shore and the surf zone width is decreased, concentrating wave-energy into a smaller region. This causes the energy dissipation per unit volume to increase. Likewise, note in Equation (13a) that the energy dissipation is slope dependent. With a water level rise the local slope for any water level, h , is greater than the equilibrium slope, thus the calculated energy dissipation must be greater than equilibrium. Clearly, the original profile is not in equilibrium relative to the increased water level; thus, to regain an equilibrium position, the system requires offshore transport, such that sand is moved from the beach face to the offshore limit of the surf zone. Dean (1976) discusses many similar qualitative examples of the usefulness of the energy dissipation theory in predicting beach profile changes, for a variety of changes in water level and wave height. Equation (14) can be used to explain most of the profile changes, including onshore sediment transport

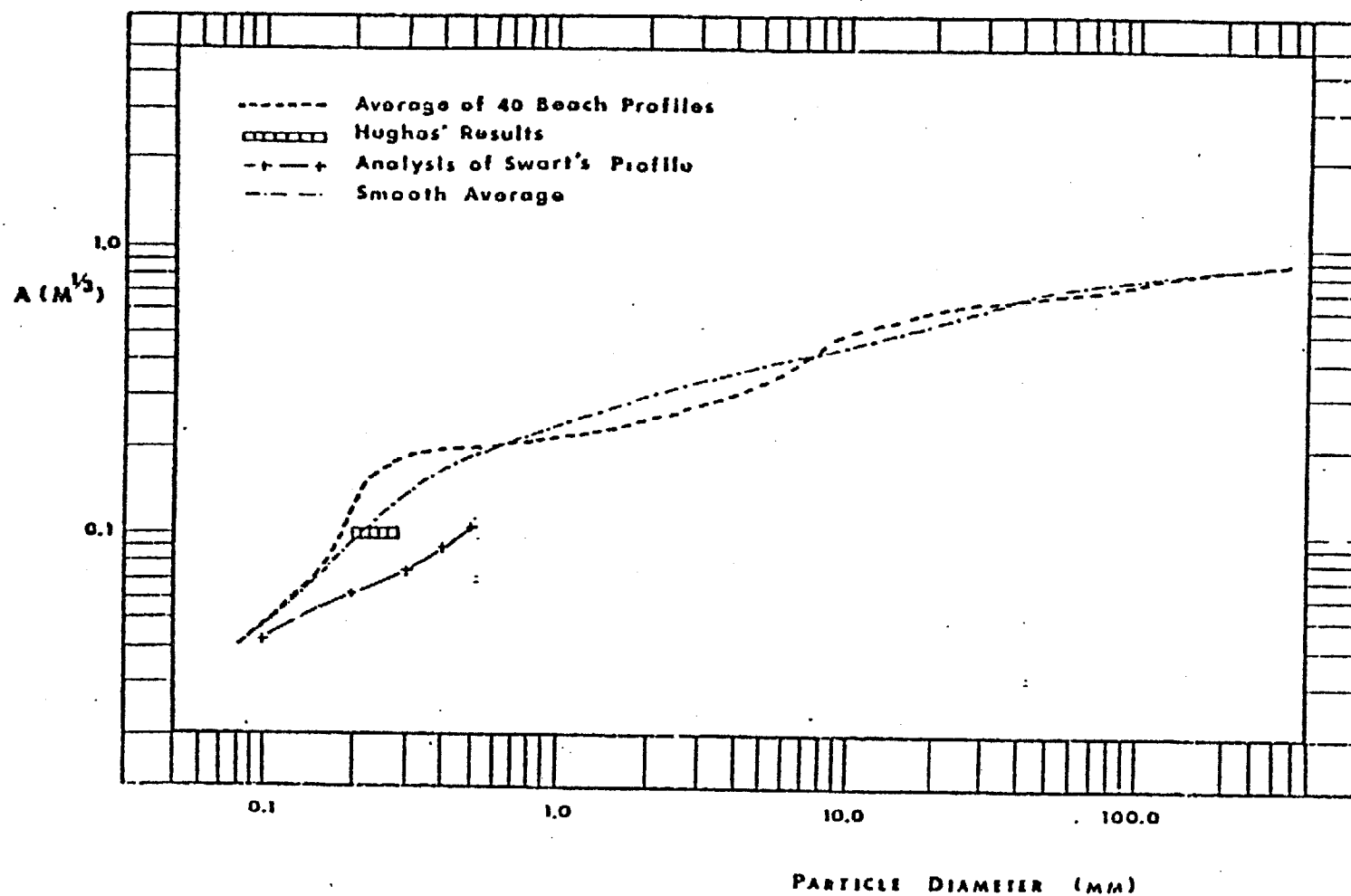


Figure 10 Particle Diameter Versus Shape Factor (A)

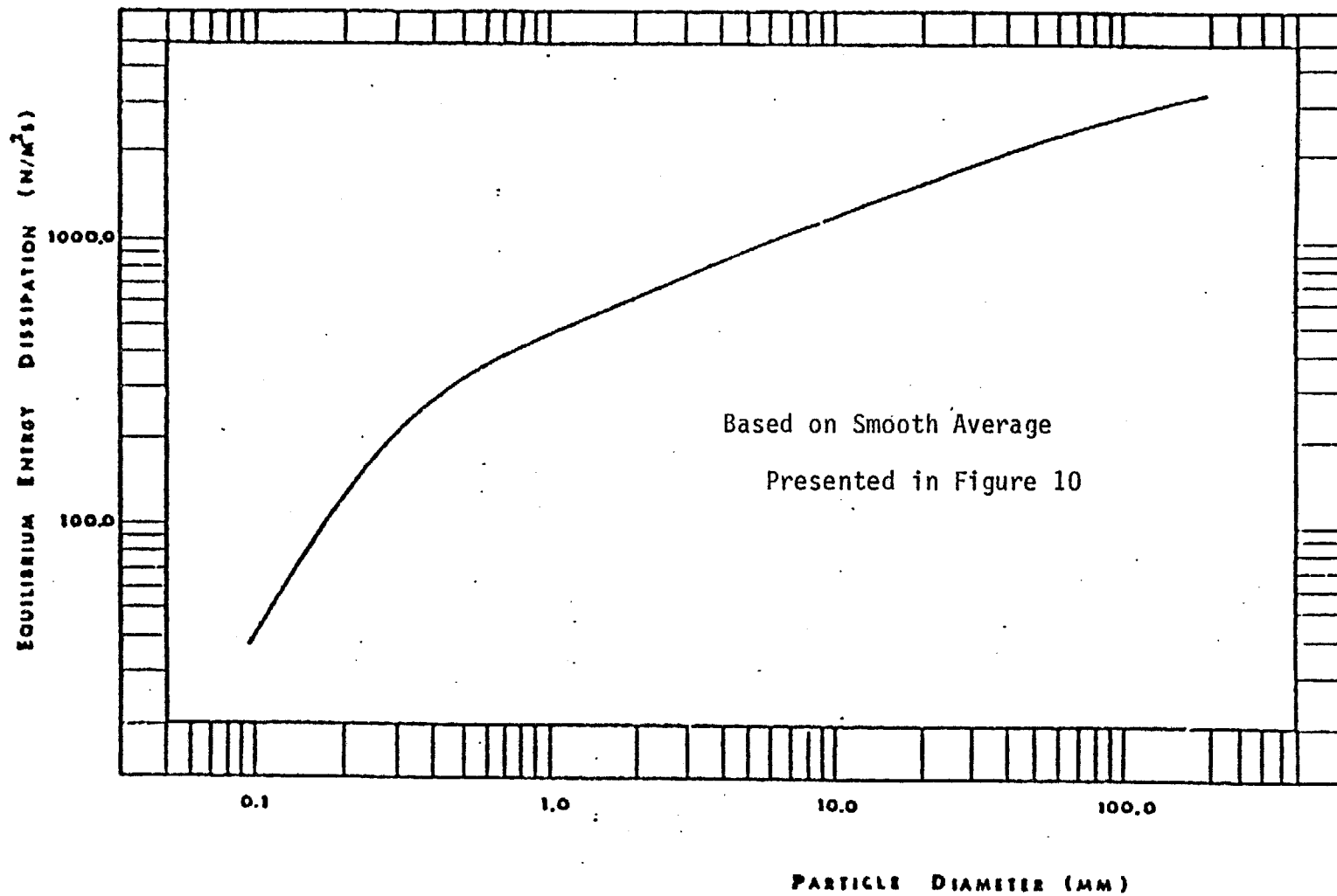


Figure 11 Particle Diameter Versus Equilibrium Energy Dissipation Based on the Smooth Average Curve Presented in Figure 10

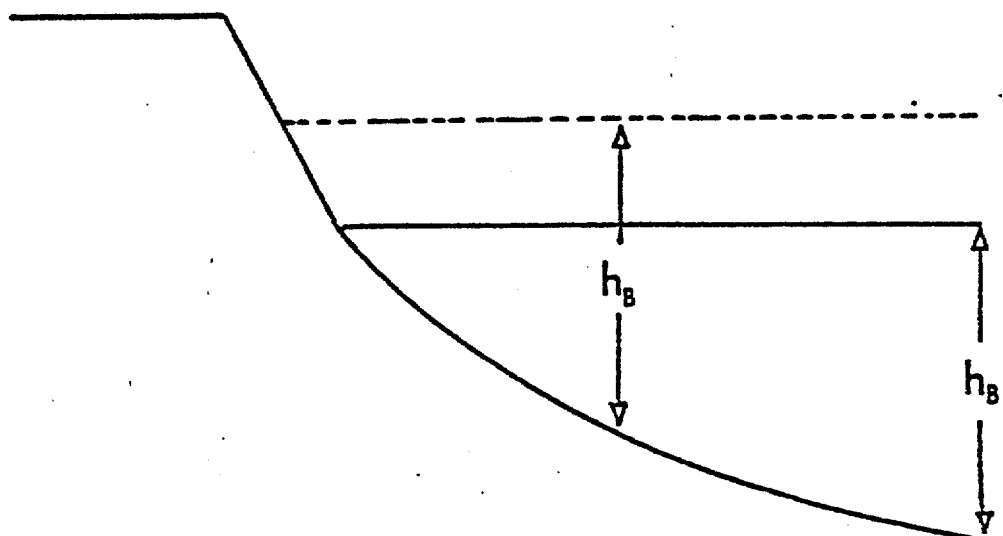


Figure 12a Equilibrium Profile Subjected to Increased Water Level Showing Decreased Surf Zone Width

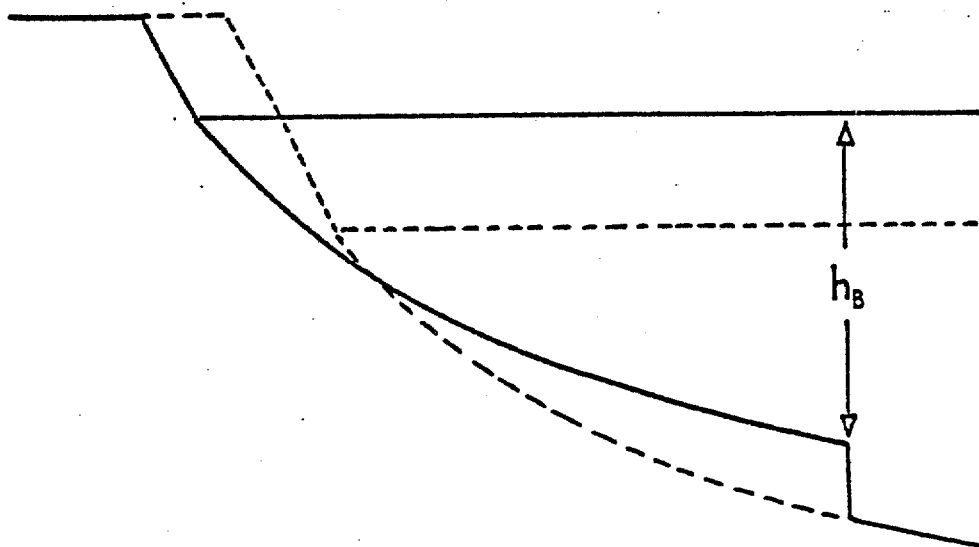


Figure 12b Equilibrium Profile Re-Established Relative to Increased Water Level

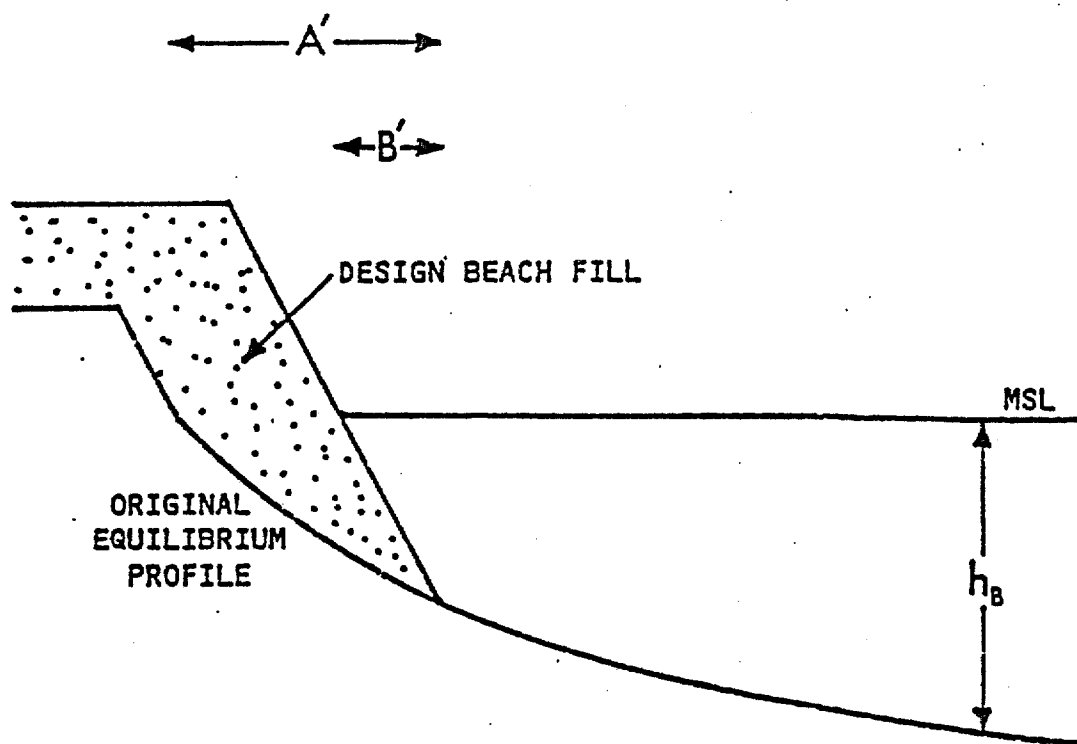


Figure 13a Decreased Surf Zone Width Resulting From Beach Fill

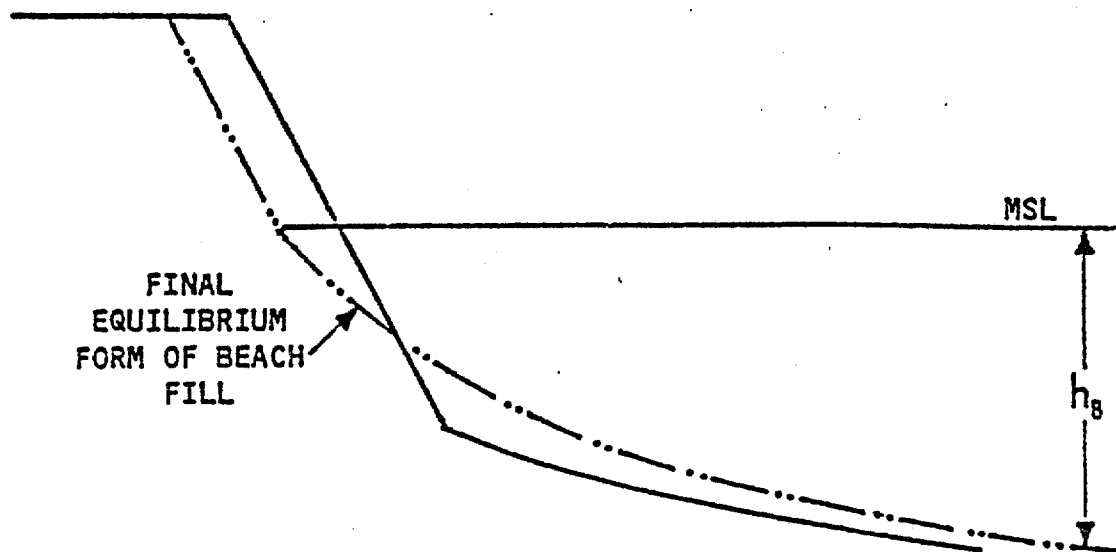


Figure 13b Beach Fill Distributed Over Surf Zone at Equilibrium

if the water level drops relative to the equilibrium profile, and evolution of a linear beach fill to an equilibrium shape, as in Figures 13a and 13b.

Assuming that the empirical determination of the A parameter and the equilibrium energy dissipation D_{eq} are valid, then only the transport rate parameter, K, must be determined to fully quantify the transport equation. It is evident in Equation (14) that K relates the excess energy dissipation to the combined suspended and bed load transport resulting from the destructive forces in the surf zone. Swart (1974) found the onshore offshore transport as a complex empirical function of both wave and sediment characteristics. Given the form of Equation (14), it appears that, since energy dissipation is a function of sediment size, water depth, and the breaking wave type, spilling breaker, the transport parameter must be either a constant or a function of other wave characteristics, i.e. period or steepness. Unfortunately, theoretical relationships or empirical results from pre-and post-storm profiles to determine K are beyond the present state-of-the-art.

Moore (1982) has determined empirical values of K that give good agreement with erosion rates found in the laboratory and in nature. Using a numerical model for onshore-offshore transport based on Equation (14), but that included a detailed simulation of breaking waves and bar formation, Moore simulated the large scale laboratory tests of beach profile evolution conducted by Saville (1957). These tests resulted in a constant value of K, $2.2 \times 10^{-6} \frac{m^4}{N}$ or $0.001144 \frac{ft^4}{lb}$ for both 0.2 mm and 0.4 mm sand, seemingly verifying that K is independent of sediment size of Figure 14. Likewise, Moore simulated profile changes occurring over one year at Santa Barbara, California, using daily average wave characteristics. These results seem to further indicate that K is independent of wave characteristics.

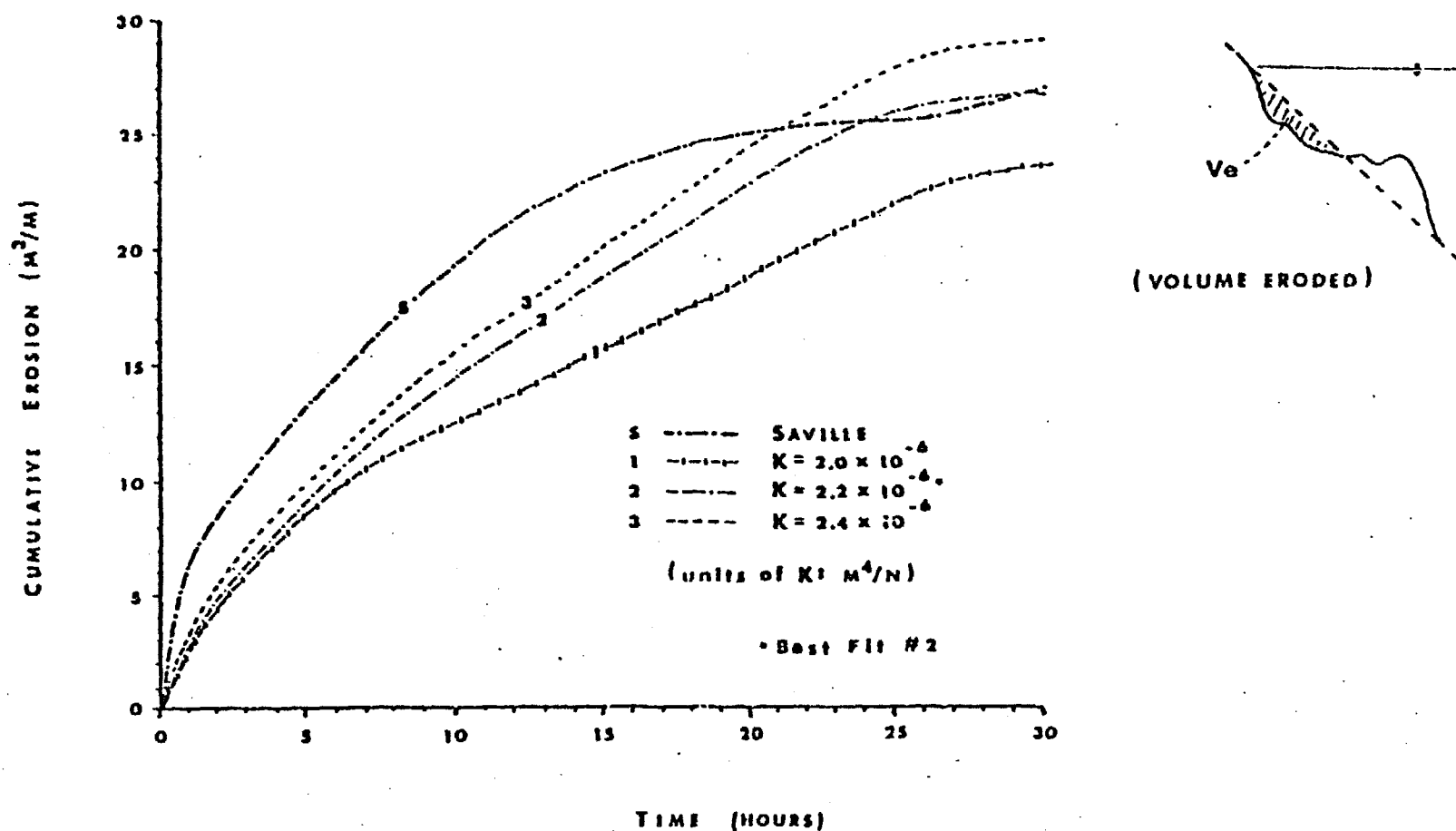


Figure 14 Effect of Varing the Sediment Transport Rate Coefficient on Cumulative Erosion During the Simulation of Saville's (1975) laboratory Investigation of Beach Profile Evolution for a 0.2 mm Sand Size.

IV. NUMERICAL SOLUTION OF CONTINUITY EQUATION

In addition to the transport equation, schematic beach profile changes are governed by the continuity equation for conservation of sand in the surf zone. In general, the change in depth of any point in the surf zone over time is the result of gradients in the flux of sediment which, for the onshore-offshore problem considered here may be given as:

$$\frac{\partial x}{\partial t} = - \frac{\partial Q_s}{\partial h} \quad (15)$$

where the minus sign is consistent with the definition of the sign of the depth, h . For numerical application, the surf zone may be represented by a series of cells in which the incremental change in depth, Δh , is uniform, as in Figure 15. With this definition, h_n is the water level, referenced to mean sea level, at the grid point, n . The storm surge, or departure from mean sea level, is represented by η_n and the total water depth at the grid point, h'_n , equals $h_n + \eta_n$. The distance from the shoreline datum to the grid point, x_n , is determined initially from the equilibrium profile form.

In finite difference form, Equation 15 can be expressed as:

$$\frac{\Delta x_n}{\Delta t} = \frac{Q_{s_n} - Q_{s_{n+1}}}{\frac{1}{2}(h'_{n+1} - h'_{n-1})} \quad (16)$$

where Δx_n is the change in position of the elevation contour as the water level remains constant over the time step. In this model, wave setup in the surf zone and wave runup on the beach face are not considered. Therefore, η is uniform throughout the surf zone and Equation 16 reduces to:

$$\frac{\Delta x_n}{\Delta t} = \frac{Q_{s_n} - Q_{s_{n+1}}}{\Delta h} \quad (17)$$

From this expression, it is clear that if $Q_{s_n} > Q_{s_{n+1}}$, there is a net addition of sand to the cell and the contour advance offshore, a Δx_n , is positive.

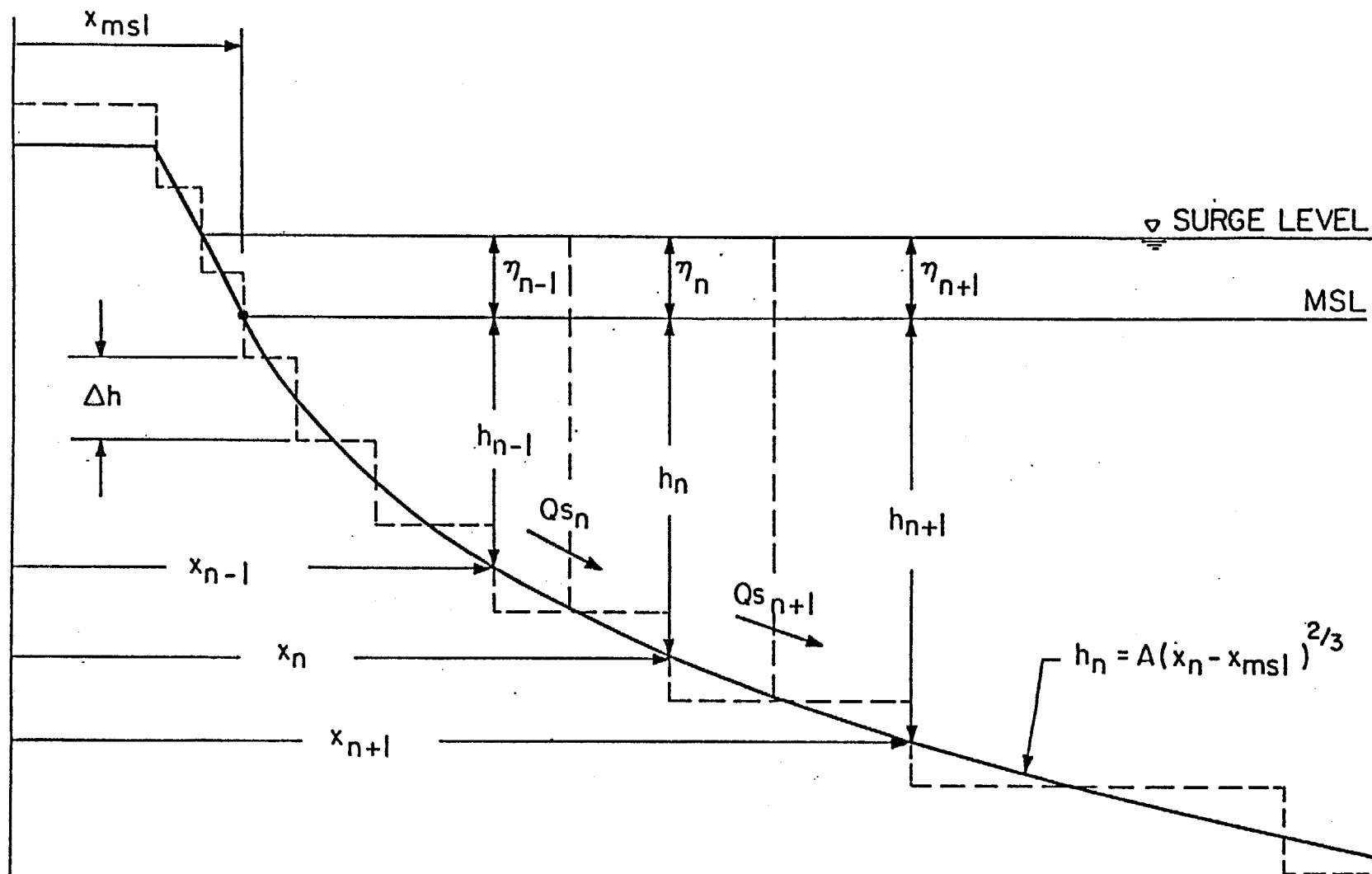


Figure 15 Numerical Representation of Surf Zone Showing a Sediment Transport Over Imaginary Cell

If $Q_{s_n} < Q_{s_{n+1}}$ there is a net loss of sand from the cell and the X_n contour recedes. As $Q_{s_n} = Q_{s_{n+1}} = 0$, the system reaches equilibrium and wave energy is effectively dissipated over the cell volume without a net gain or loss of sediment.

The solution for beach profile response may be obtained from the implicit solution of the two governing equations:

$$\frac{\Delta X_n}{\Delta t} = \frac{Q_{s_n} - Q_{s_{n+1}}}{\Delta h} \quad (18)$$

and

$$Q_{s_n} = K(D_n - D_{eq}) \quad (19)$$

Substituting Equation 19 into Equation 18, the contour retreat or advance can be expressed as:

$$\Delta X_n = \frac{K\Delta t}{\Delta h} [D_n - D_{n+1}] \quad (20)$$

While this form appears quite simple, the implicit numerical solution for the energy dissipation per unit volume is rather detailed.

First, it is convenient to rewrite the finite difference form of the energy dissipation per unit volume occurring in some cell:

$$D_{n+1} = \frac{F_{n+1} - F_n}{\frac{1}{2}(h_{n+1} + h_n)(X_{n+1} - X_n)} \quad (21)$$

From Equation 11 for the energy flux, this energy dissipation can then be expressed in terms of water depth and x distance only as:

$$D_{n+1} = Kd \frac{h_{n+1}^{5/2} - h_n^{5/2}}{(h_{n+1} + h_n)(X_{n+1} - X_n)} \quad (22a)$$

where

$$Kd = \frac{1}{4} \gamma \kappa^2 g^{1/2} \quad (22b)$$

Substituting Equation 22a into Equation 20, the solution for ΔX_n is now a function of both the position and depth of adjacent grid points:

$$\Delta X_n = \frac{K\Delta t}{\Delta h} \left[K_d \frac{h_n^{5/2} - h_{n-1}^{5/2}}{(h_n + h_{n-1})(X_n - X_{n+1})} - K_d \frac{h_{n+1}^{5/2} - h_n^{5/2}}{(h_{n+1} + h_n)(X_{n+1} - X_n)} \right] \quad (23)$$

It is important to note that in the solution scheme, water depths, h_{n+1} , h_n and h_{n-1} are constant over the time step in the steady state solution. However, horizontal positions, X_{n+1} , X_n and X_{n-1} vary as time progresses. Preliminary numerical solutions using constant X positions proved to be highly unstable; therefore, an average value of X over the time step

$$\bar{X}_n = X_n + \frac{\Delta X_n}{2} \quad (24)$$

was introduced in an effort to achieve unconditional stability.

In Appendix A, Equation 24 is substituted into Equation 23 and it is shown that the resulting solution is of the form:

$$A_n \Delta X_{n-1} + B_n \Delta X_n + C_n \Delta X_{n+1} = Z_n \quad (25a)$$

where

$$A_n = -\beta \frac{D_n}{(X_n - X_{n-1})} \quad (25b)$$

$$B_n = 1 + \beta \left[\frac{D_n}{X_n - X_{n-1}} + \frac{D_{n+1}}{X_{n+1} - X_n} \right] \quad (25c)$$

$$C_n = -\beta \frac{D_{n+1}}{X_{n+1} - X_n} \quad (25d)$$

$$Z_n = -\frac{2\beta}{K} (Q_{s_{n+1}} - Q_{s_n}) \quad (25e)$$

$$\beta = \frac{K\Delta t}{2\Delta h} \quad (25f)$$

This solution represents the matrix multiplication of the variables, ΔX_{n-1} , ΔX_n , and ΔX_{n+1} with known coefficients, A_n , B_n , C_n , and Z_n . While all

coefficients are dependent on the energy dissipation per unit volume, Z_n acts as the driving term in the equation and represents the net sediment flux over the cell. Thus, any perturbation in the system that causes gradients in the sediment transport also causes a change in the profile position.

To solve Equation 25a, a recursion formula must be introduced:

$$\Delta X_{n-1} = E_n \Delta X_n + F_n \quad (26)$$

in which one unknown ΔX_{n-1} is given in terms of another unknown, ΔX_n .

Substituting this form into Equation 25a results in:

$$\Delta X_n = \left[\frac{-C_n}{B_n + A_n E_n} \right] \Delta X_{n+1} + \left[\frac{Z_n - A_n F_n}{B_n + A_n E_n} \right] \quad (27)$$

Comparing Equation 27 to the recursion relationship, it is clear that

$$E_{n+1} = \frac{-C_n}{B_n + A_n E_n} \quad (28a)$$

and

$$F_{n+1} = \frac{Z_n - A_n F_n}{B_n + A_n E_n} \quad (28b)$$

Since all A_n , B_n , C_n , and Z_n coefficients are known, a double sweep solution may be employed as follows:

- (1) From an onshore boundary condition, specify E_1 and F_1 . In sweep number 1, all E_{n+1} and F_{n+1} coefficients are calculated according to Equations 28a and 28b.
- (2) From an offshore boundary condition, specify that some ΔX_{n+1} offshore equals zero. In sweep number all ΔX_n values may be determined according to the recursion relationship.

V. INITIAL PROFILE AND SOLUTION DOMAINS

As mentioned, this model allows schematic representations of a complex berm-dune system onshore and a concave-upwards profile shape offshore. In Figures 9a and 9b, the dune is approximated with a constant dune height, h_D , and a uniform dune slope, M_D . The berm with, W_B , may be varied to simulate a variety of initial profile configurations. Likewise, the constant berm height, h_B , and a uniform beach face slope, M_B are required. To achieve continuity in the profile, the linear beach face slope is assumed to intersect the equilibrium profile at some depth, h^* , such that there is a continuous decrease in slope in the offshore direction. Table I summarizes this depth of intersection for a variety of sand grain sizes and possible beach slopes.

With this basic profile definition, the double sweep solution is valid from h^* seaward to beyond the breaking depth. This region is governed by the energy dissipation and is termed the dynamic solution domain. From h^* onshore, any number of simulation schemes may be employed. In this model, this region is defined as the geometric solution domain and is governed by the continuity equation only, since the energy dissipation per unit volume is not defined above water line according to the governing equations. In a more advanced model, it is anticipated that a more complete swash zone transport relationship and a variable upper limit of wave induced transport may be introduced. For now, beach slope is kept constant as the beach face recedes uniformly. Similarly, for more severe storms, the dune slope is kept constant as the dune face recedes uniformly. This representation does not always represent nature, where the eroding profile steepens; however, it seems to give good agreement for eroded volume and an order magnitude agreement for contour erosion. It is anticipated that statistical or empirical corrections can be developed to adjust the uniform slope recession to better represent natural steepening.

Table I

HSTAR Values Versus Beach Slope and Sand Grain Sizes
(Based on Moore's Sand Grain Size Versus Energy Dissipation)

Sand Grain Size DIA (mm)	Beach Slope							
	$\frac{1}{6}$	$\frac{1}{8}$	$\frac{1}{10}$	$\frac{1}{12}$	$\frac{1}{15}$	$\frac{1}{20}$	$\frac{1}{30}$	$\frac{1}{40}$
0.2	0.0	0.0	0.0	0.0	0.0	0.5	0.5	1.5
0.3	0.0	0.0	0.5	0.5	1.0	1.5	4.0	---
0.4	0.0	0.5	0.5	1.0	1.5	3.0	---	---
0.5	0.5	0.5	1.0	1.5	2.5	---	---	---
0.6	0.5	1.0	1.5	2.0	---	---	---	---
0.7	0.5	1.0	1.5	2.5	---	---	---	---

5.1 Boundary Conditions

Two types of boundary conditions are required for the double sweep solution. In nature, onshore-offshore sediment transport is zero at the top of the berm (in the absence of overwash), is maximum somewhere between the swash zone and the break point, and is zero again at some point seaward of the breaking depth. Therefore, $Q_s = 0$ is the formal boundary condition for both onshore and offshore limits of the profile in the numerical model.

As mentioned, the dynamic solution extends from h^* offshore to the breaking depth. One feature of the finite-difference solution is that large discontinuities may exist in the sediment transport function at h^* , at the breaking depth, and near the peak of the Q_s curve. To eliminate these sharp jumps, a smoothing function is applied to the transport curve. This serves two purposes:

- (1) to spread, the sediment transport over adjacent cells, broadening the curve and reducing the peak;
- (2) to extend the transport curve beyond the breaking depth, helping to ensure a smooth transition in this region.

Onshore, uniform recession of the beach/dune face is ensured by extending the Q_s curve linearly from h^* to zero at the top of the berm/dune. This also serves two purposes:

- (1) providing a smooth transition in the Q_s curve at h^* ;
- (2) ensuring that all Z_n on the beach/dune face are equal.

In terms of the numerical model, the onshore and offshore boundary conditions may now be specified. First, in Sweep #1, the E and F coefficients are defined down to h^* as:

$$E_n = 0 \quad (29)$$

$$F_n = Z_n \quad (30)$$

From this condition, E_{n+1} and F_{n+1} may be determined by the dynamic calculations out to beyond the breaking depth. Offshore, at the point where $Q_s = 0$, there is no wave energy dissipation and no sediment transport. In Sweep #2, all ΔX_n for this point seaward are defined equal to zero. Then according to the recursion relationship, ΔX_{n-1} values are determined in the landward sweep.

At the end of each time step continuity requires that the total eroded volume must equal the total deposited volume. During the onshore sweep, the net change in volume from offshore up to the point $h^* + \Delta h$ determines the volume that must be eroded to achieve continuity at the top of the berm/dune. This volume is distributed equally among the grid points from h^* landward, ensuring that the beach/dune face recedes uniformly. This procedure is required because the discrete nature of the sediment transport function can cause the grid point at h^* to erode beyond adjacent, grid points, resulting in an unstable, and unreasonable, numerical solution.

As with most numerical solutions, a stability criteria can be found for selecting a stable time step. In Equation 23, the coefficients are dependent on the relationship of the time step to the horizontal grid spacing. Through extensive testing of the model it has been found that:

$$\frac{K\Delta t}{X_n - X_{n-1}} \leq 0.25 \quad (31)$$

is required to avoid numerical instability. In particular, with a linearly sloping beach/dune face, the minimum grid spacing in this region governs the stability. It might be noted, that while the implicit solution scheme was used to avoid instability, a Taylor series approximation used in the derivation in (Appendix A) seems to introduce the instability at large time steps. In program application, time steps must be reduced when simulating steep dune slopes.

5.2 Simulation of Erosion Process

With the complex berm-dune configuration in Figures 9a and 9b, several erosion scenarios may be simulated:

- (1) erosion of berm only, for cases with wide berm;
- (2) erosion of the berm which then exposes the dune to subsequent erosion;
- (3) erosion of entire beach face-dune face, for cases in which no berm is present.

Therefore, in the model two conditions are monitored:

- (1) the surge height, S , relative to the top of the berm elevation, h_B ;
- (2) the berm width, W_B .

Consider the case in which the berm width is wide and a distinct berm is present. In this case, any water level rise up to but not exceeding the top of the berm is assumed to cause only the beach face to recede, thus Q_s is set equal to zero at the top of the berm. If erosion proceeds until the berm crest reaches the base of the dune then it is assumed that the entire beach-dune face erodes uniformly as waves would now run up the face of the dune. Thus, Q_s is extended to zero at the top of the dune. In nature, waves may overtop the berm and erode the base of the dune before the berm recedes completely. In the model, the geometric solution approximates this dune erosion only after the berm has receded; however, it is believed that the critical nature of the berm and the dune, as reservoirs of sand, are included in a fairly rational fashion.

Now consider the case in which water level quickly rises above the berm height. First, if this occurs before the berm is eroded to the dune, then the numerical model will calculate the energy dissipation per unit volume

between the dune foot and the top of the berm to be less than equilibrium, implying onshore transport and accretion of the dune face. In nature, any water level above the berm would allow waves to reach dune foot in a turbulent bore. From field observations, this results in rapid smoothing of the berm crest while the dune erodes and steepens. In the model, this process must be approximated to avoid unrealistic dune accretion; therefore, the berm is again required to erode completely before dune erosion is initiated. Continuity is satisfied initially by setting $Q_s = 0$ at the dune foot such that the berm erodes quickly, then by setting $Q_s = 0$ at the top of the dune to allow uniform dune recession. If the original profile has no distinct berm width, then the entire beach-dune face is allowed to erode uniformly by setting $Q_s = 0$ at the top of the dune. Once again, exact processes are highly approximated; however, the essential characteristics of the berm-dune system seem to be represented.

As a final note, the recovery process is governed by the same numerical solution for energy dissipation and sediment transport. While berm recovery and rebuilding are permitted, dune erosion is considered permanent. Although the time dependent erosion-recovery process may be represented by the proposed transport equation little attention has been paid to the recovery process. This model is intended only for the prediction of beach recession due to severe storms and is not intended for simulation of beach recovery.

VI. RESULTS-GENERAL BEHAVIOR

To observe the general behavior of the numerical solution, consider a profile in which there is an instantaneous increase in the water level which is then maintained with a constant incoming wave height. Since the berm recession is dependent on the disequilibrium of the system, the time-dependent berm recession in Figure 16 shows that the recession is largest initially, then decreases as the system approaches equilibrium. With this behavior, the actual recession approaches the maximum potential recession, R_{∞} , asymptotically. This behavior has been verified in the laboratory by Saville (1957), Swart (1974), and Hughes and Chiu (1982).

Although this ideal behavior is quite simple, it is significant for several reasons. Because the transport parameter, K , is small, i.e. $0.001144 \text{ ft}^4/\text{lb}$, the actual berm recession requires considerable time to reach equilibrium. Many coastal scientists have observed that erosion occurs at a slower rate than the change in water level; however, little field data from severe storms is available to quantify erosion rates. As noted in Chapter I, the beach erosion prediction methods of Edelman and Dean yield only the maximum potential recession, here defined as R_{∞} . It is clear that without accounting for the time dependence indicated in Figure 16, these methods over predict the actual recession. Because the numerical solution accounts for the time-dependent recession toward the maximum potential recession, it should allow more realistic representations of natural beach response.

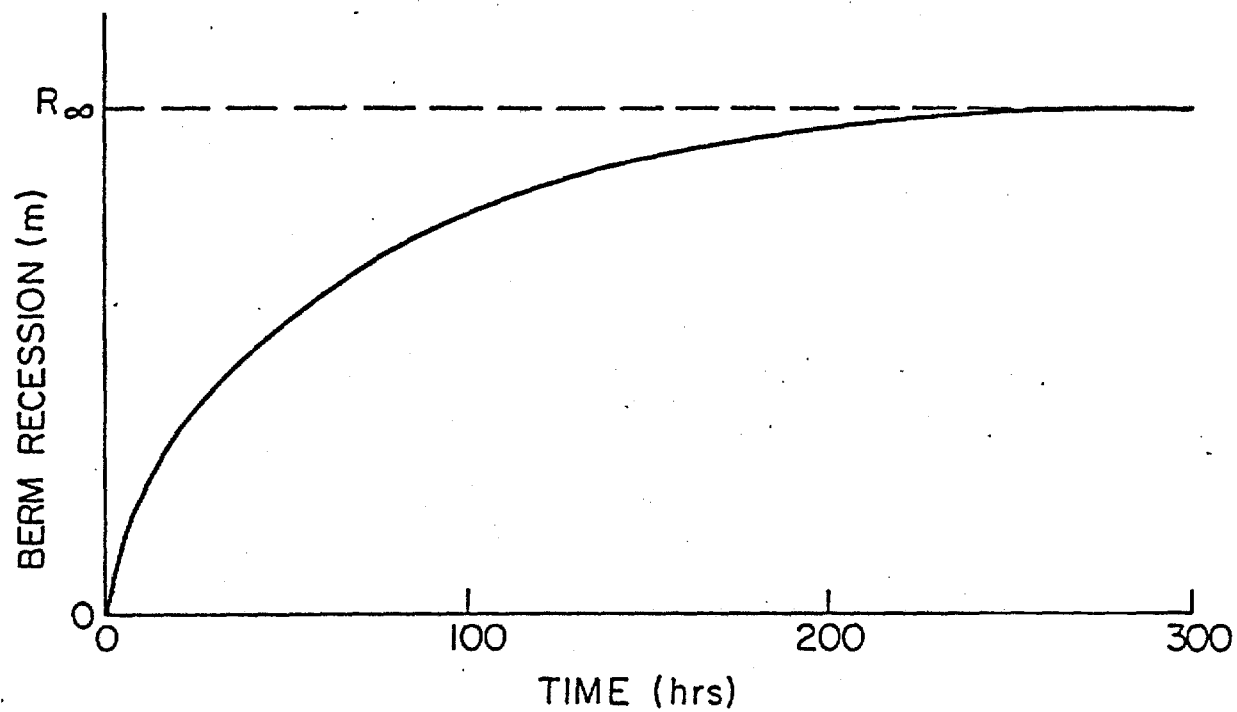


Figure 16 Time Dependent Solution for Berm Recession Due to Steady-State Forcing Conditions

6.1 Relative Effects of Water Level and Wave Height

Recalling the finite difference expression for the energy dissipation per unit volume in some cell:

$$D_{n+1} = Kd \frac{h_{n+1}^{5/2} - h_n^{5/2}}{(h_{n+1} + h_n)(X_{n+1} - X_n)} \quad (32)$$

it is clear that each incremental increase in the total water depth, h ; profoundly effects the energy dissipation, thus, the magnitude of the sediment transport in the cell. In Figure 17, a plot of the recession curves for several steady-state water levels with a given breaking wave height reveals that berm recession varies almost linearly with the water level. In fact, for a given wave height, the recession at any time is nearly proportional to the change in water level. This result is substantiated by the laboratory model tests of Hughes and Chiu (1982).

Now consider the same initial profile with a given steady-state water level but with several different breaking wave heights. The primary effect of increasing the wave height is to change the width of the surf zone and the offshore limit of the active profile. Since the onshore portion of the Q_s curve is not effected by a change in wave height, the berm recession in Figure 18 is initially the same for each wave height. Only after some length of time, does the increased surf zone width increase the berm recession, as the volume of sand required to reach equilibrium is greater for wider surf zones.

From these results, it is noted that water level behaves as the forcing function in the numerical solution while wave height acts essentially as a boundary condition controlling the surf zone width and the total volume of sand that must be moved to achieve equilibrium. This result agrees well with lab tests of Hughes and Chiu (1982) where water level was found to be the

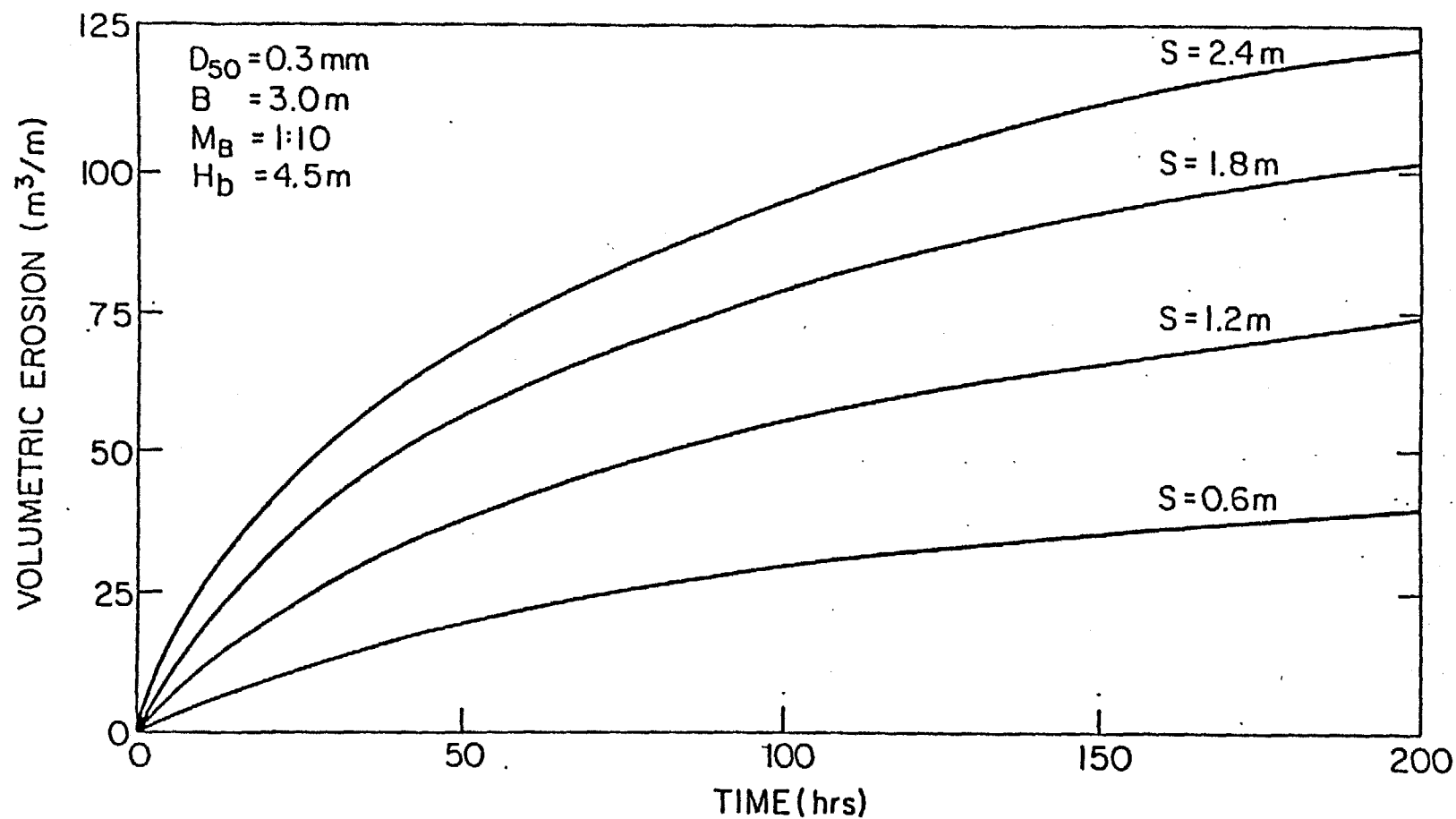


Figure 17 Effect of Storm Surge Level on Volumetric Erosion

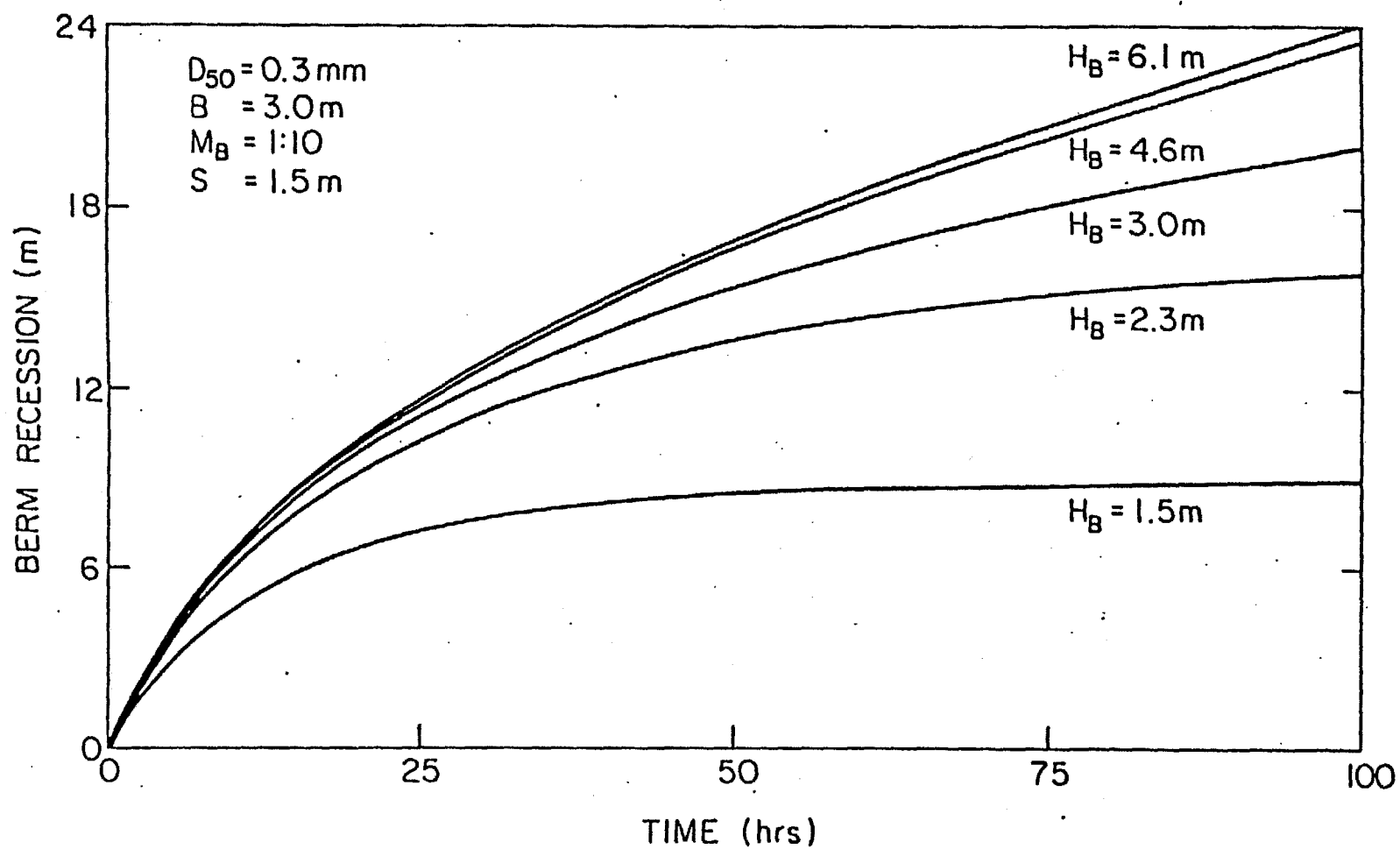


Figure 18 Effect of Wave Height on Volumetric Erosion

single most important parameter in the storm-surge erosion process. For the numerical simulation, this result indicates that exact wave height determination is not critical for data input.

6.2 Relative Effects of Sand Grain Size and Beach Slope

As further support that the numerical scheme correctly simulates natural profiles, at least qualitatively, consider two beach profiles, both subjected to the same storm surge level and wave height. In Figure 19, the berm recession may be compared for the case in which the two profiles have different mean grain sizes, but the same beach face slope. For this condition, the steeper profile ($D_{50} = 4$ mm) reaches equilibrium quickly with a fairly small recession indicating that beaches with larger sand grain sizes are relatively insensitive to peak surge duration. Conversely, it is evident that the milder profile ($D_{50} = 0.2$ mm) takes longer to reach equilibrium and that the equilibrium recession is much greater due to the wider surf zone. Thus, the model indicates that beaches with small sand grain size may experience significant variation in the magnitude of the erosion depending on the storm duration.

Now, in Figure 20, compare the berm recession for the two profiles with the same sand grain size but with different beach face slopes. This situation can occur over relatively short coastal segments where localized changes in bathymetry, shoreline orientation, or wave characteristics, can cause local changes in the beach face slope. For this case, the numerical results indicate that steeper beach faces erode both faster and farther than milder beach face slopes. This agrees with nature where steep beach faces often represent a more unstable profile formation with high erosion potential. This was confirmed by Chiu (1977) from field observations where steeper pre-storm profile experienced more erosion than milder pre-storm profiles.

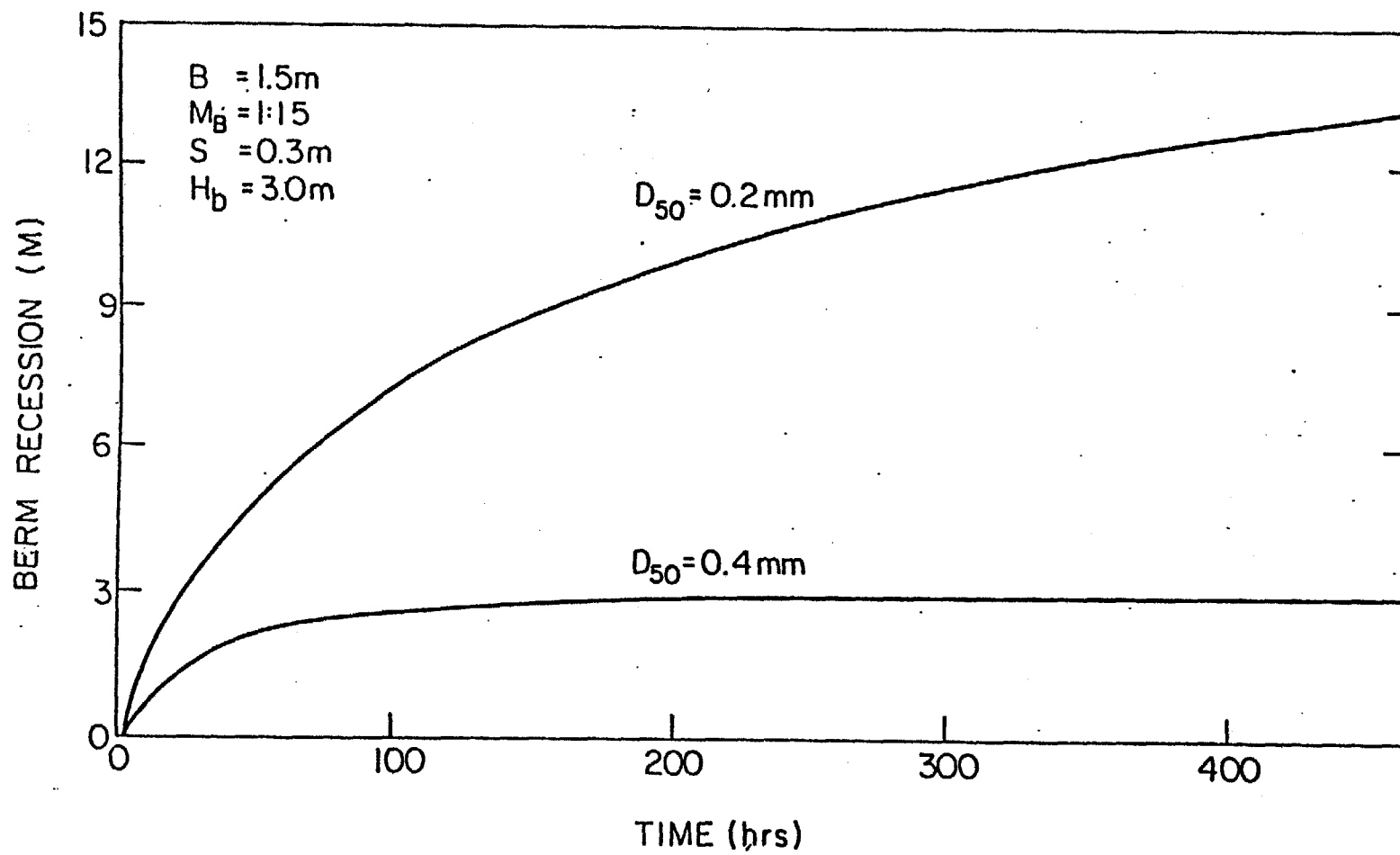


Figure 19 Effect of Sand Grain Size on Berm Recession

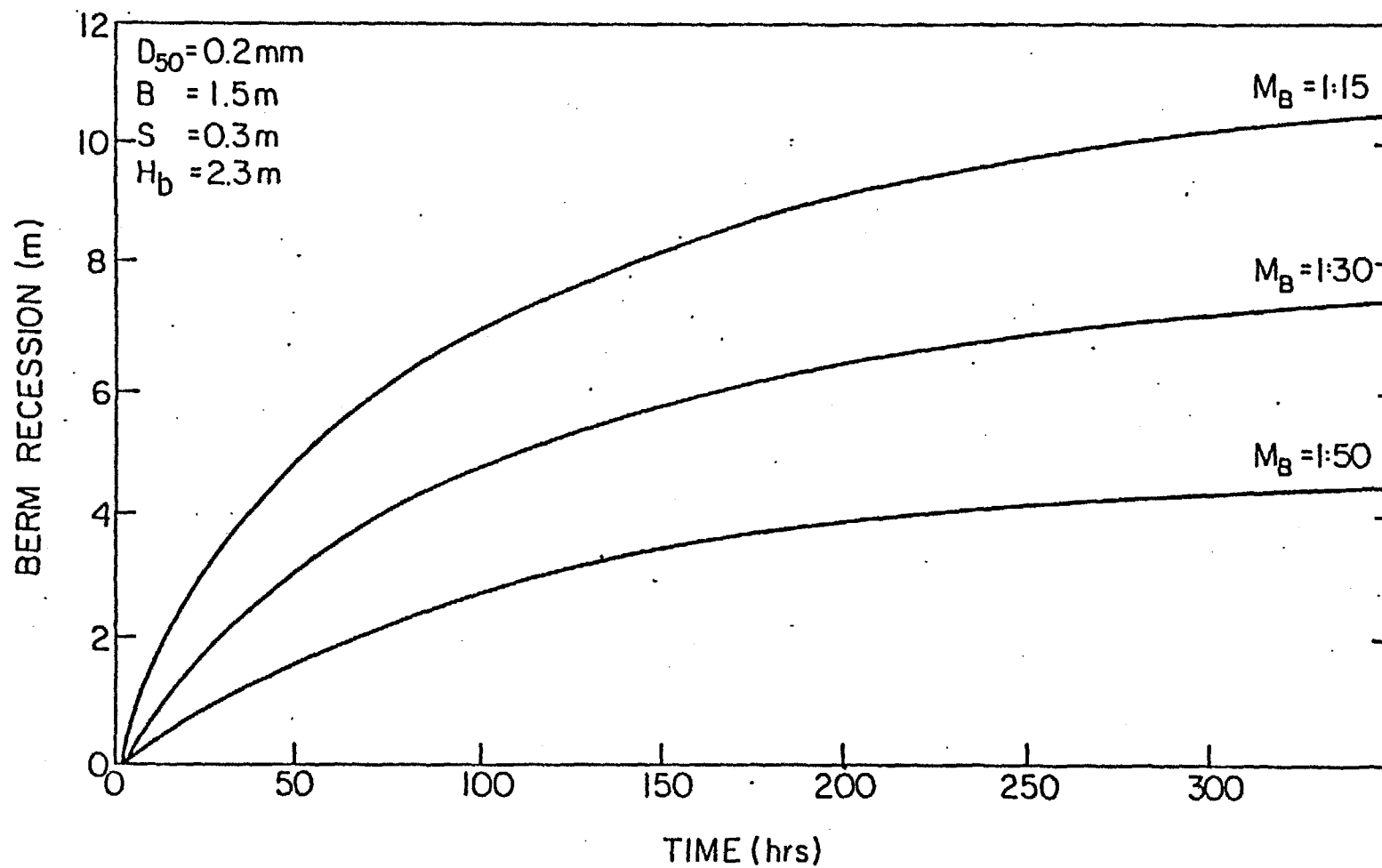


Figure 20 Effect of Beach Face Slope on Berm Recession

VII. SIMULATION OF STORM SURGE HYDROGRAPH

Prior discussions have considered only the beach response due to a simple instantaneous increase in the still water level; however, the time-dependent recession resulting from the complete storm surge hydrograph may also be simulated. Conceptually, the continuous surge hydrograph may be approximated by a series of discrete still water levels in a stair-step approximation. With this procedure, the solution at each time step is based on the total still water level during that time increment. As the incremental time step is decreased, the discrete representation more closely approximates a continuous function.

In the numerical model, the solution procedure is essentially unchanged. The energy dissipation and sediment transport flux are determined from the total water depth at each time step. Likewise, the breaking depth, h_b , and the transition depth, h^* , are determined relative to the new water level; therefore, these depths move onshore and offshore with each new water level and wave height. Referring to Equation 22a, it is clear that as the water level increases with a new time step, the energy dissipation and sediment transport values also increase. Since the dynamic system does not respond at the same rate as the change in water level, Q_s and D are maximum at the time of the peak surge. Thus, the beach erosion rate is also maximum at this time. Intuitively, since erosion occurs at a slow rate relative to the water level rise, the peak surge level represents the stage of the greatest disequilibrium in the system. From the continuity equation:

$$\frac{\partial x}{\partial t} = - \frac{\partial Q_s}{\partial h} \quad (33)$$

it is clear that since the slope of the transport curve, $\frac{\partial Q_s}{\partial h}$, is maximum everywhere in the profile at the peak surge level, the erosion rate, $\frac{\partial x}{\partial t}$, is also maximum.

Suppose for a moment that erosion occurs instantly such that the maximum potential erosion for any water level is realized immediately. The maximum potential erosion curve resulting from an idealized surge hydrograph may be represented as in Figure 21, where the temporal surge profile may define both the water level and the associated maximum potential erosion at each time step. With this representation, the time-dependent erosion may be plotted on the same graph for comparison to both the time-dependent storm surge and the maximum potential erosion associated with the peak surge level.

Consider the case, in Figure 22, in which the peak surge level is maintained indefinitely. In this case, the numerical results show that the actual erosion is much less than the maximum potential erosion for the duration of the water level rise. Only after the peak surge level is maintained for several hundred hours of simulation time does the profile "catch up" to the maximum potential value and attain complete equilibrium for the peak water level.

Now, in Figure 23, consider the case in which the water level decreases back to zero such that the peak surge level is maintained for a short time. For the duration of the water level rise, the recession characteristics are exactly equal to those noted above and the rate of recession is maximum at the time of the peak surge. However, as the water level decreases, the energy dissipation and the sediment transport flux also decrease as the system is brought back toward equilibrium. As the slope of the transport curve is decreased, the recession rate also decreases.

As some point, the instantaneous water level drops to a level at which the energy dissipation is nearly in equilibrium and the sediment transport curve is equal to zero in the nearshore region. At this time, $\frac{\partial Q_s}{\partial h}$ is equal to zero, therefore, the recession rate is equal to zero and the peak recession is attained. As the water level continues to drop, energy dissipation per unit volume decreases below the equilibrium value; hence, onshore sediment transport is initiated and

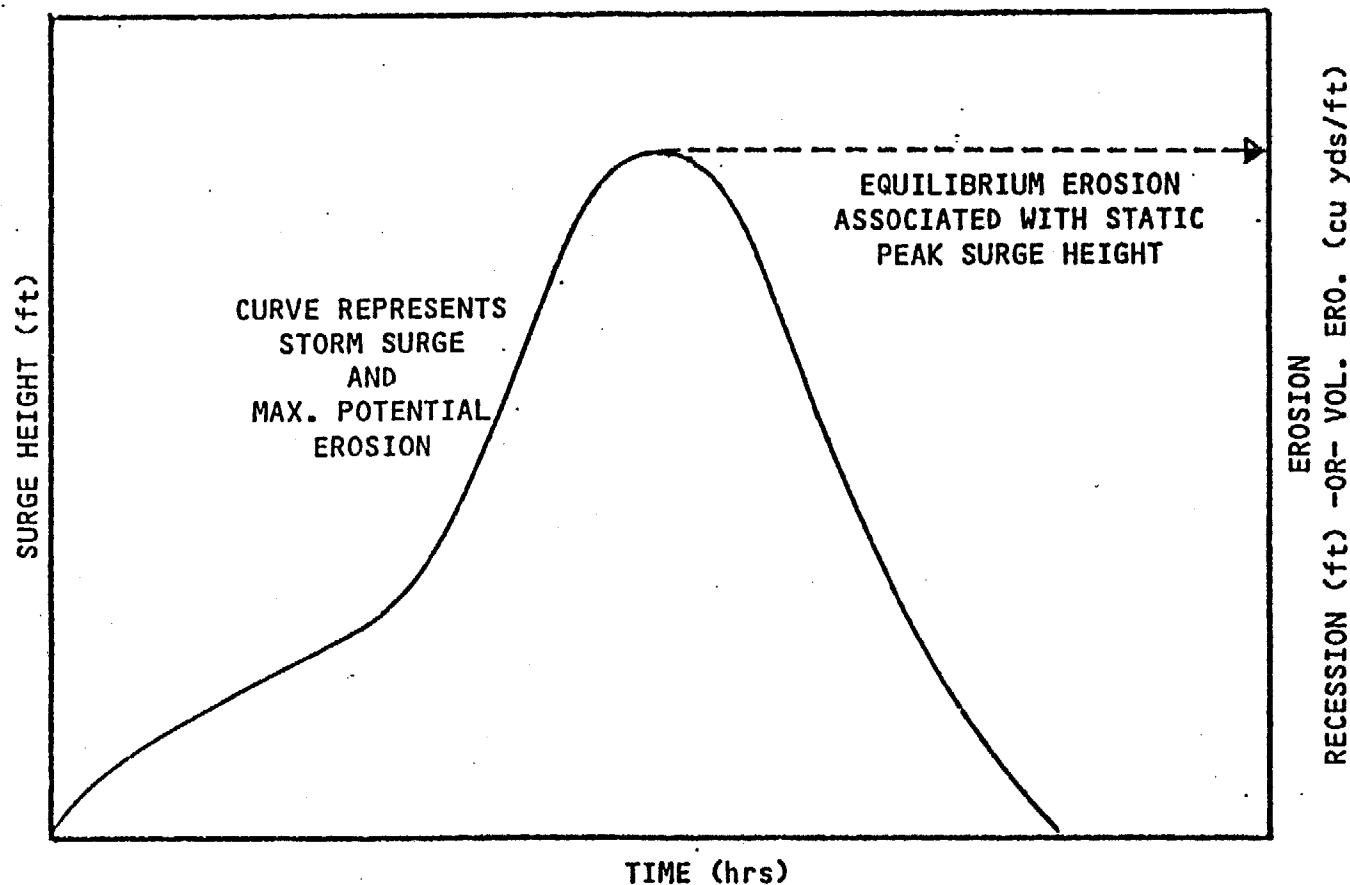


Figure 21 Method of Normalizing Axis to Represent Storm Surge Hydrograph and Maximum Potential Erosion

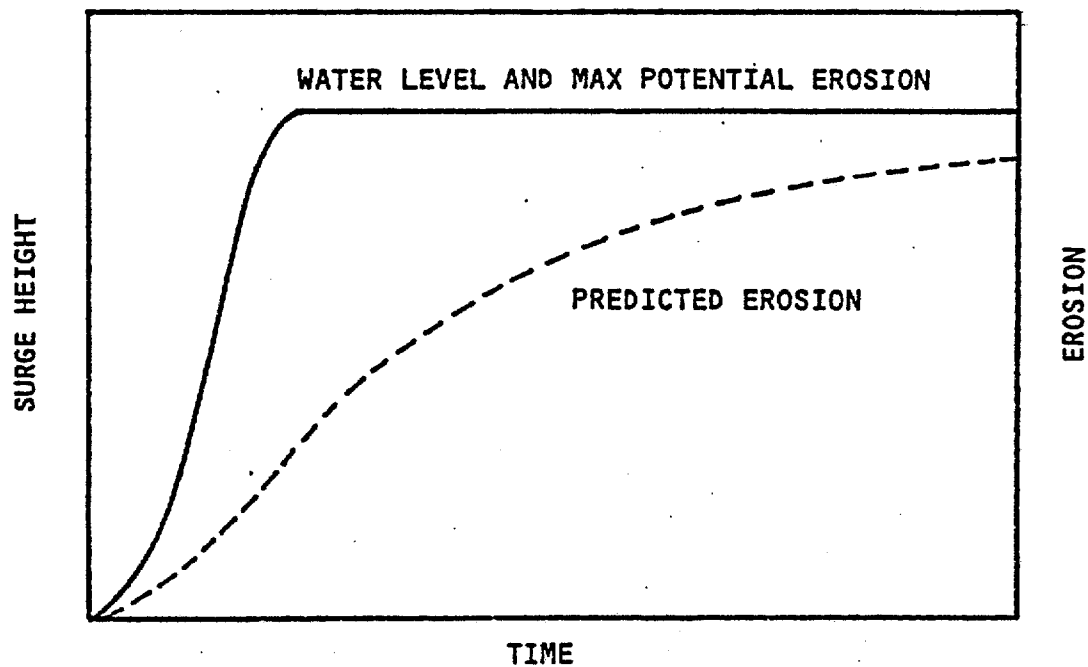


Figure 22 Schematic of Numerical Results Showing Predicted Erosion Curve Approaching Equilibrium for Smooth Increase to Static Peak Surge Level

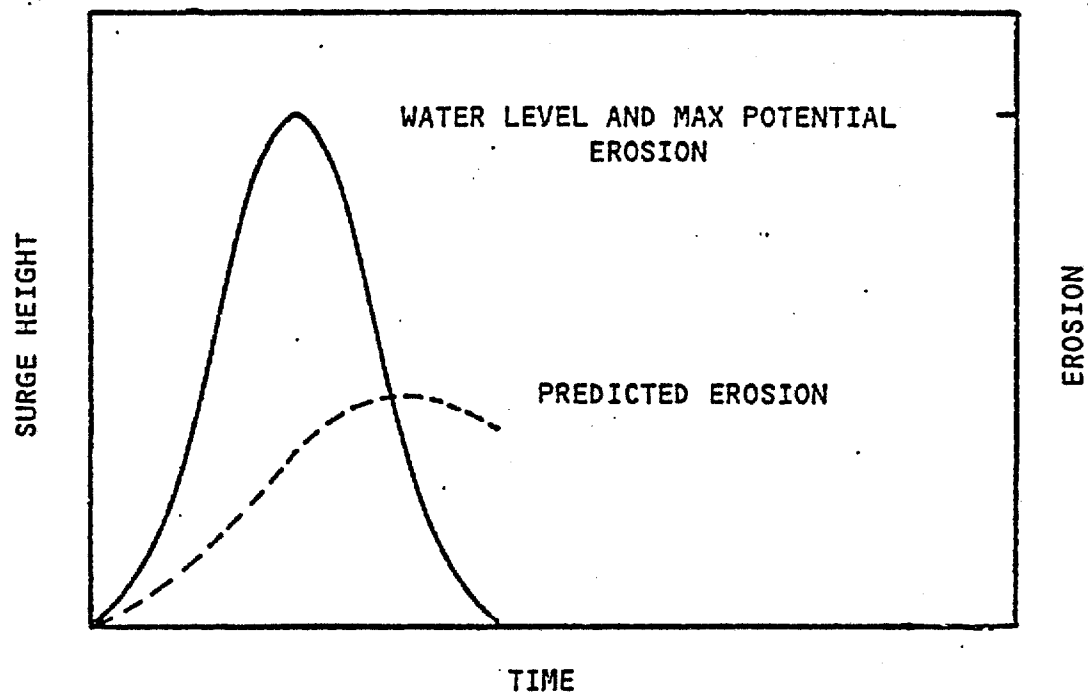


Figure 23 Schematic of Numerical Results Showing Predicted Erosion Curve Reaching a Maximum as Water Level Decreases Following Peak Surge Level

the profile begins rebuilding to a new equilibrium form. Hughes and Chiu (1981), have successfully modeled this behavior in small scale laboratory tests; concluding that the actual recession at the time of the peak surge is 60 to 90 percent of the peak recession.

In Figures 24 thorough 26, the dynamic erosion response of a beach-dune profile is illustrated for various storm surge durations. In these examples, the storm surge hydrograph is idealized by the relationship:

$$\eta = 4 \sin^2 \sigma t \quad (34)$$

where the peak surge level is 4 feet and σ equals π divided by the storm surge duration. Together with a breaking wave height of 10 feet, these ideal storm surge hydrographs are applied to a representative beach profile from the Bay-Walton county area of Florida.

In order to compare the response of the profile to the various storm surges, the equilibrium erosion conditions are first determined for a static water level of 4 feet and a constant wave height of 10 feet. From this analysis, the maximum potential volumetric erosion for an infinite storm duration, i.e. over 300 hours, is found to be about 28 cu yds/ft. Thus, the right hand axis of each figure is scaled to display this maximum potential erosion for the peak storm surge level.

It may be noted that Hughes and Chiu (1981) suggest that the maximum potential erosion resulting from a gradual water level increase is greater than that obtained from an instantaneous increase to a static water level. This may be attributed to increased deposition that occurs in the offshore region as the breaking depth migrates shoreward as the water level rises slowly. This effect is also evident in the numerical model results; however, for small increases in water level and for storm of short duration, the difference in volumes is insignificant.

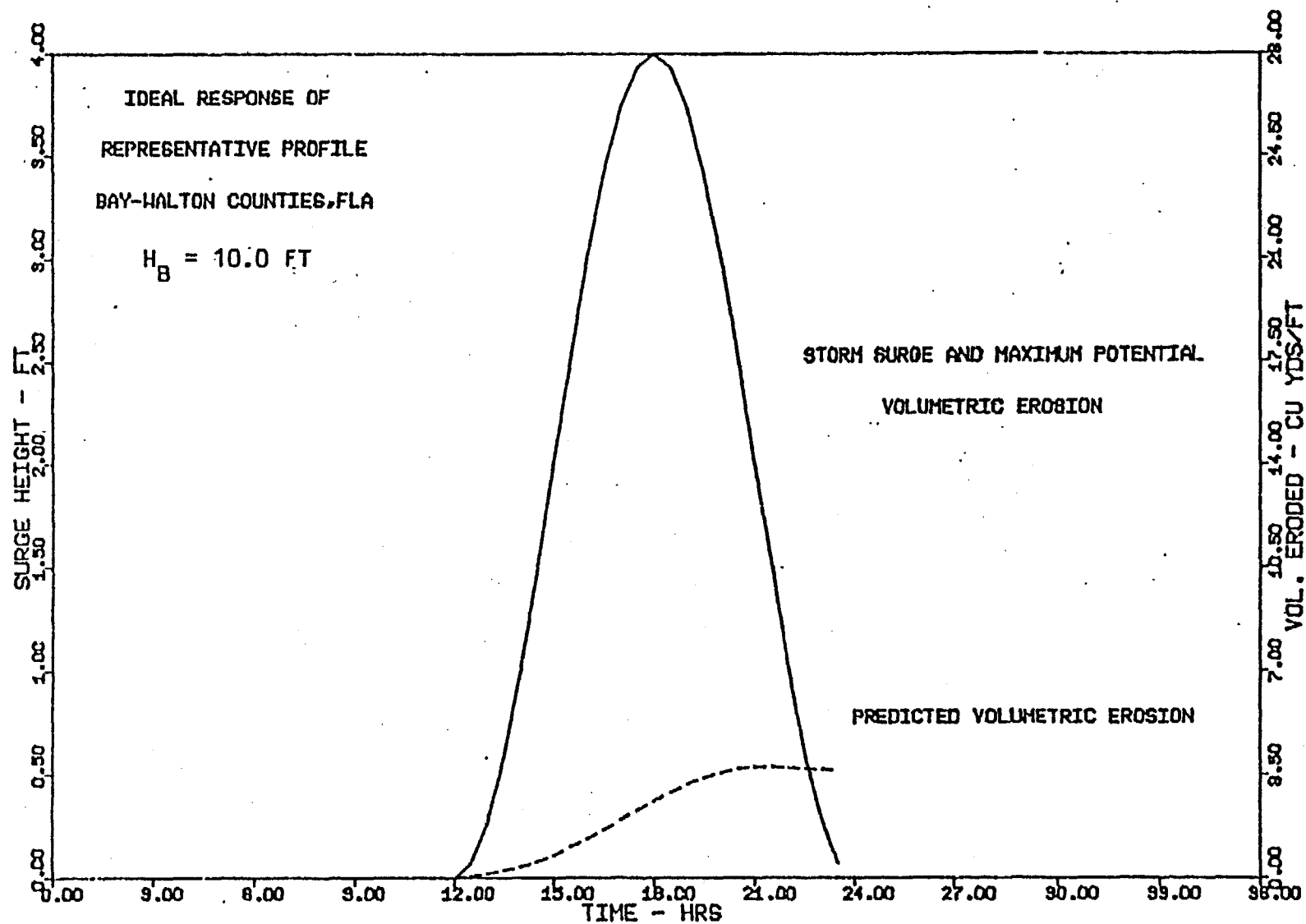


Figure 24 Effect of Storm Surge Duration on Volumetric Erosion, 12 Hr. Storm Surge

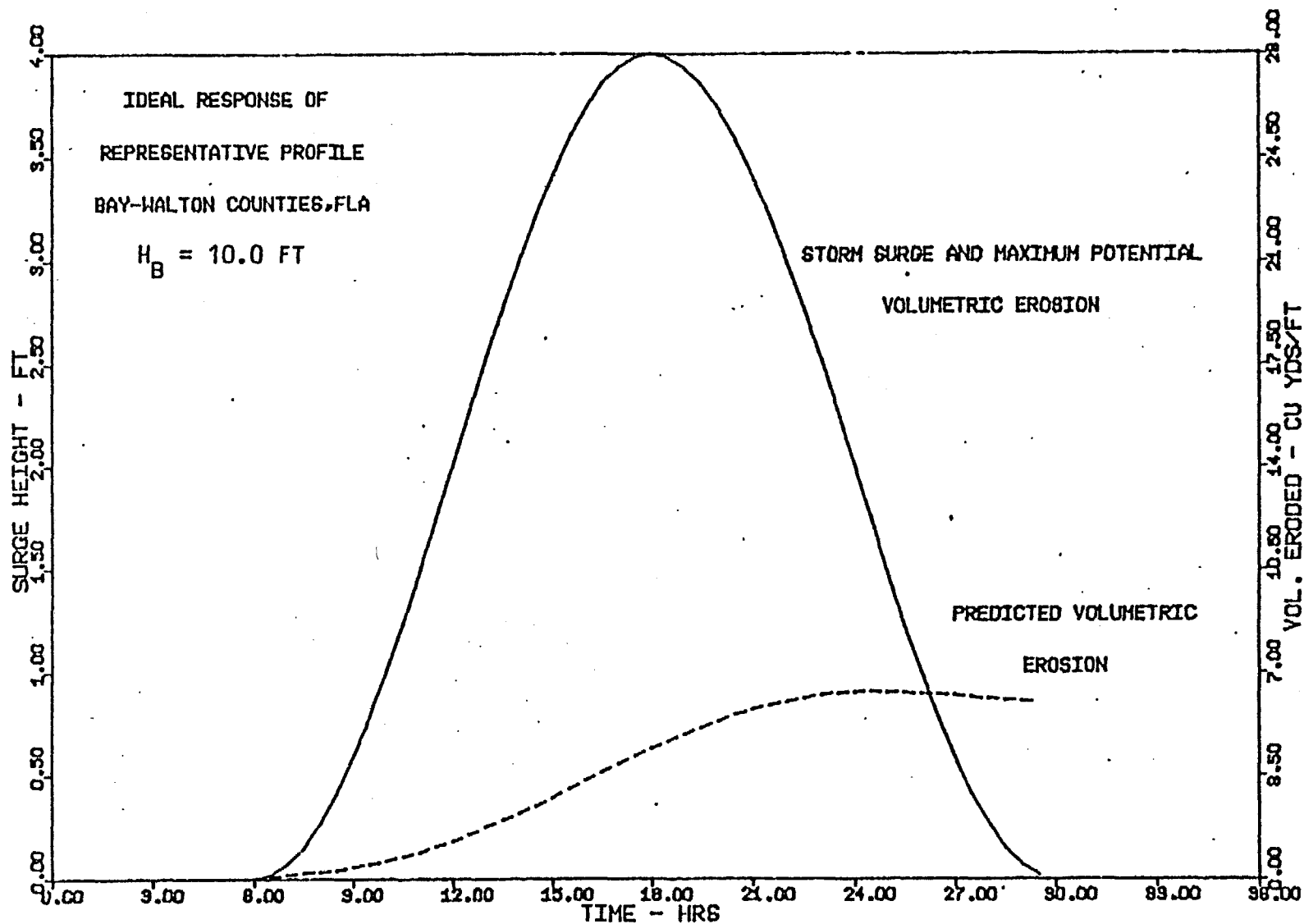


Figure 25 Effect of Storm Surge Duration on Volumetric Erosion, 24 Hr. Storm Surge

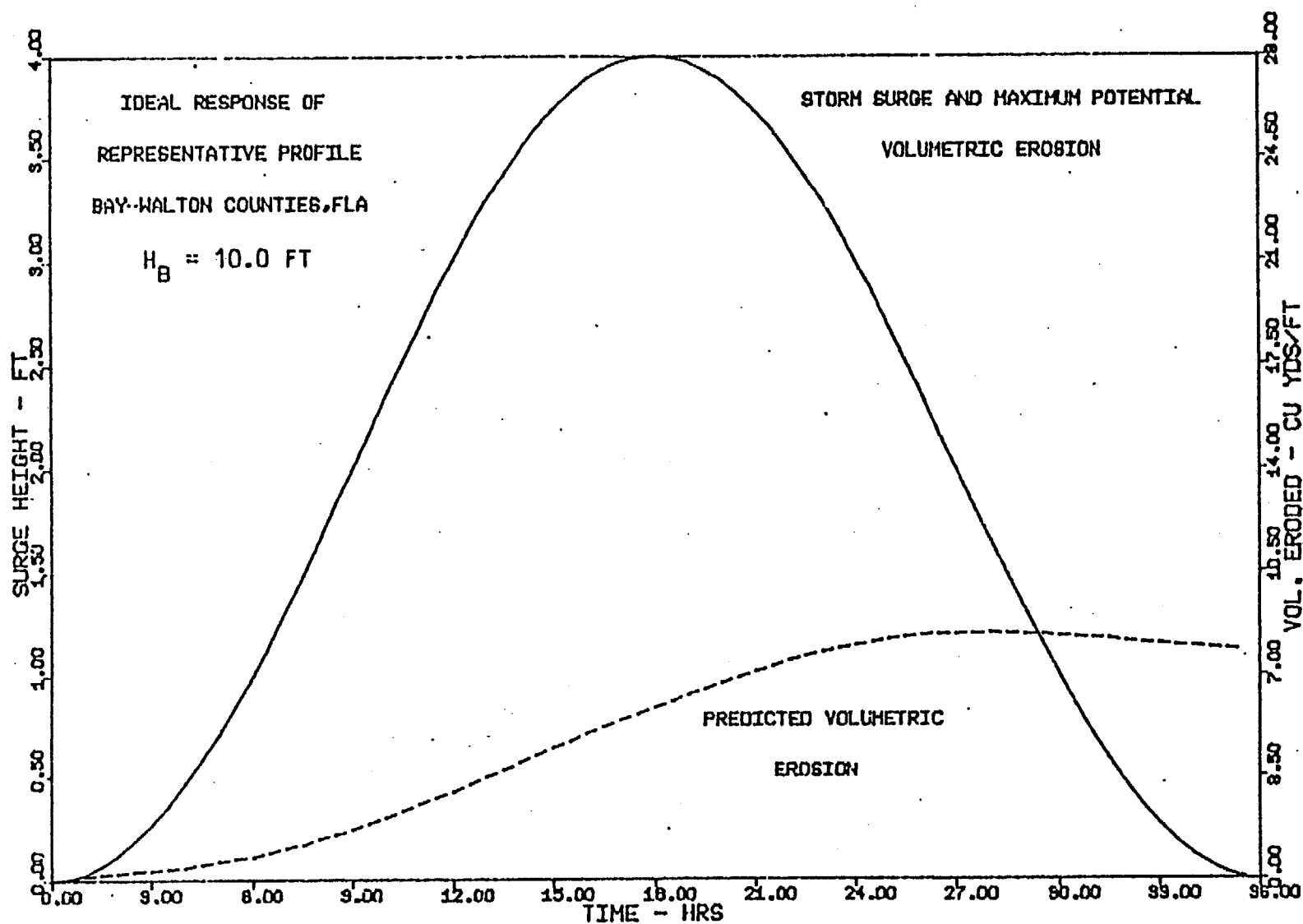


Figure 26 Effect of Storm Surge Duration on Volumetric Erosion, 36 Hr. Storm Surge

In Figures 24 through 26, the storm surge hydrograph and the maximum potential erosion are represented along with the predicted time-dependent volumetric erosion, for storms of 12, 24, and 36 hour durations respectively. In Figure 27, the results of the three simulations are compared directly to graphically depict the dynamic erosion response. It is important to note that the predicted maximum erosion is only 14.2 to 28.5 percent of the maximum potential erosion.

From these examples, the numerical analysis indicates that the time dependence of the storm surge erosion process is of fundamental importance in the prediction of storm related erosion. Specifically, it is evident that:

- (1) the actual maximum recession lags the peak storm surge;
- (2) the actual maximum recession is function of the storm duration as well as the peak surge height;
- (3) the erosion rate is dependent on the rate of increase of the water level;
- (4) the maximum potential recession predicted by Edelman and Dean is seldom attained during a typical storm surge duration.

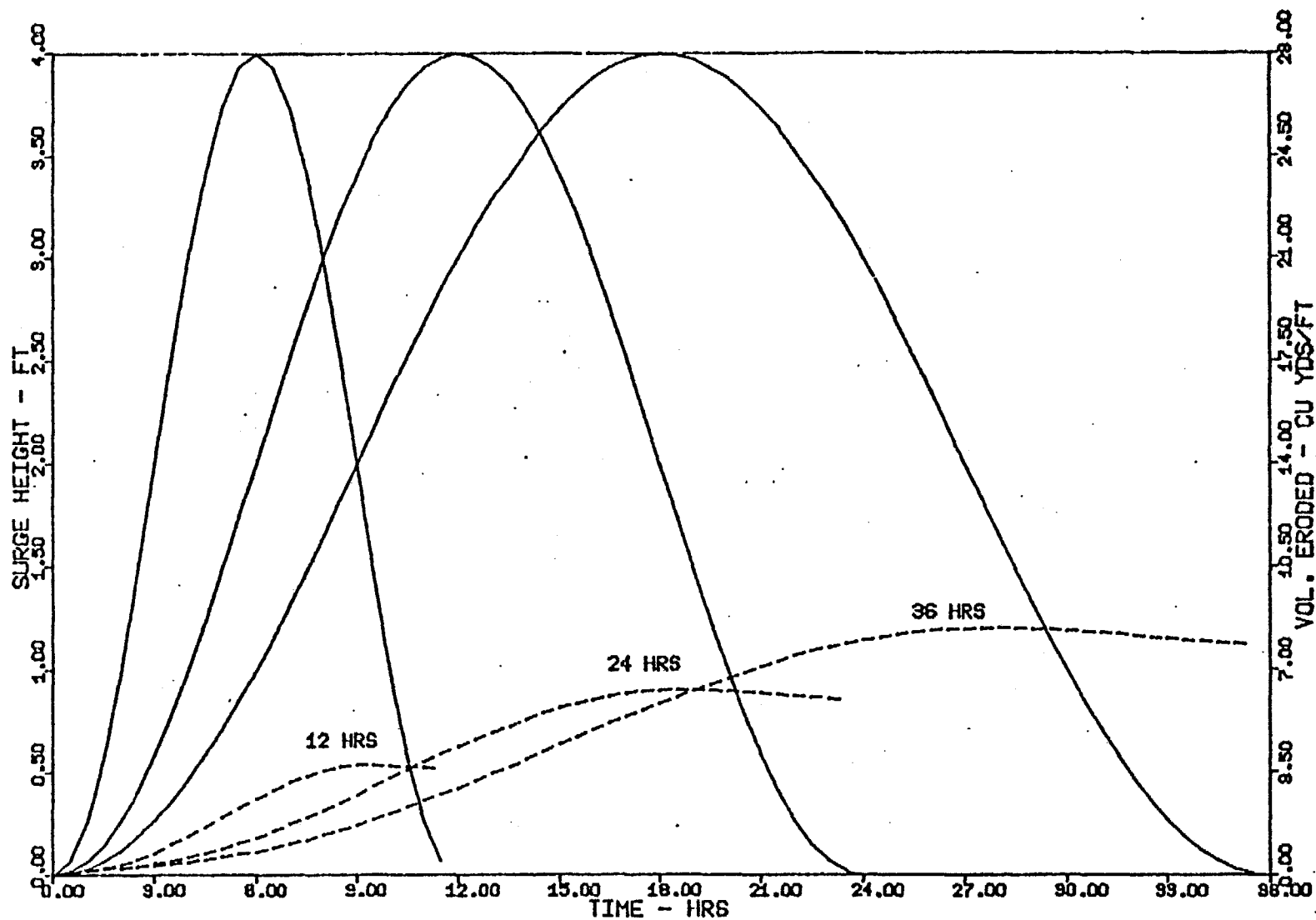


Figure 27 Comparison of the Effects of 12, 24, and 36 Hr. Storm Surge on Volume Erosion

VIII. RESULTS-SIMULATION OF HURRICANE ELOISE

As a preliminary verification of the numerical model, beach-dune erosion in Bay-Walton County area resulting from Hurricane Eloise is simulated. Hurricane Eloise crossed the Florida Panhandle on September 23, 1975 and was one of the most severe storms ever to strike the Bay-Walton County area. While no reliable tide gage records exist for this area, it appears that a peak storm surge of 8-12 feet occurred over much of the two-county area. Using numerical storm surge models, the National Weather Service has suggested the peak open coast storm surge to be about 10.5 feet above mean sea level at the Bay-Walton County Line. From high water mark, data, the Mobile District of the U.S. Army Corps of Engineers estimated peak surge elevations in the area to be 12-16 feet. While high water mark data does not correspond to the elevation of the peak surge, it seems clear that a peak surge of 10-12 feet occurred near the Bay-Walton County Line.

Chiu (1977) summarized beach erosion data from Bay and Walton counties, collected under the Florida Coastal Construction Setback Line Program. Two years prior to the storm, beach-dune profiles were taken at approximately 1,000 feet intervals. Also, aerial photographs at a scale of 1" = 100' were taken in the 1973 survey. This data provided the pre-storm profiles and, in the low energy environment of the Gulf of Mexico, were assumed to be representative of the actual pre-storm profiles. After the storm, similar data were collected; however, beach profiles were taken up to 3-4 weeks after the storm. By this time some recovery of the beach face had occurred. While dune erosion characteristics should be recorded accurately, Chiu notes that both the eroded volume and the contour advance/retreat of the contours near mean sea level reflect some beach recovery.

To simulate these beach-dune changes, three types of data are required:

- (1) the storm surge hydrograph;
- (2) the breaking wave height;
- (3) the pre-storm profile characteristics.

The storm surge hydrograph was estimated with a Bathystrophic Storm Surge Model written by the author. To simulate the storm surge on the open coast near the Bay-Walton County line, the characteristics of Hurricane Eloise at the time of landfall were supplied as input to the Bathystrophic model. Since Eloise made landfall almost normal to the coast, the peak storm surge was determined at the point of maximum wind, 20 to 22 miles from the storm center crossing. At this point, just east of the Bay-Walton County line, a peak surge height of 7.5 feet was calculated. Burdin (1977) shows a recorded storm surge record for Destin, Florida. While this tide gage is located in a bay and does not reflect the open coast surge directly, an initial water level rise of from 1.5 to 3 feet is evident up to 24 hours before the peak surge. By adding an initial rise of 1.5 to 3 feet, the predicted peak surge elevation agrees well with other predictions. The predicted storm surge hydrograph is shown in Figure 28.

The breaking wave height is extremely difficult to predict with any reliability. Because of this uncertainty, and because wave height is not of primary importance in this model, a constant breaking wave height is used for the duration of the model simulation. Numerical cases were run with breaking heights 7.5 and 15 feet.

Beach profiles for Bay-Walton County vary significantly in terms of dune height, beach slopes, and dune configurations. Chiu (1977) and Hughes and Chiu (1981) give several schematic beach-dune profiles from which a representative or,

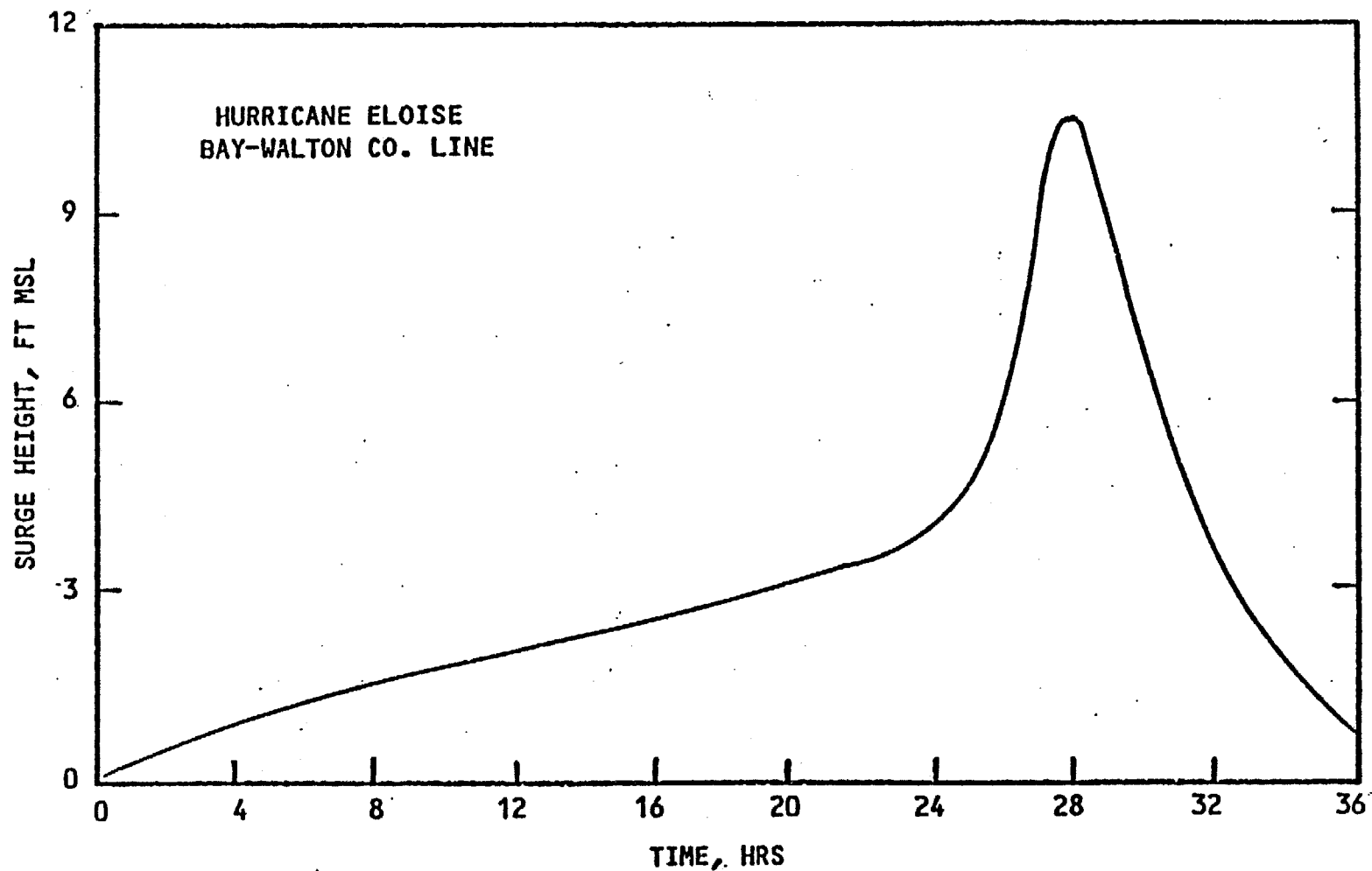


Figure 28 Estimated Storm Surge Hydrograph, Hurricane Eloise Bay-Walton County Line

perhaps, an average profile form can be determined. From these sources, the initial profile was assumed to have an average dune height of 18 feet above mean sea level and a break in slope at the vegetation line elevation, approximately 7 feet. Average dune face slopes appear to be between 1:4 and 1:2; beach face slopes average 1:15 to 1:10. This schematic profile is shown in Figure 29. After viewing actual pre-storm profiles from Walton County, this seems to be a very good approximation for several actual profiles. Offshore, the equilibrium profile shape was modeled with $A = 0.2055 \text{ ft}^{1/3}$ ($0.13 \text{ m}^{1/3}$) which is empirically determined for 0.3 mm sand. Hughes and Chiu (1982) found the representative A parameter for this area to be $0.19 \text{ ft}^{1/3}$.

In this preliminary verification, 20 test cases are simulated:

- (1) to determine the quantitative validity of the proposed model relative to observed erosion data;
- (2) in an effort to display some of the effects of the basic parameters on the erosion characteristics.

Since exact values of the peak surge, wave height, and beach slopes are not known, various combinations of 3 beach slopes, 2 dune slopes, 2 wave heights, and 2 peak surge elevations are tested. In Table II, the results from each test case are summarized, such that the maximum erosion, in terms of contour change and eroded volume, is shown. For comparison, average erosion statistics presented by Chiu (1979) are shown in Table III.

Upon inspection, the model results show good agreement with observed average erosion characteristics. First, consider the beach-dune change as measured by the volumetric erosion. From the 20 test cases, volumetric erosion varies from 8.3 to 15.3 cu yds/ft; this compares to average values of 7.3 and 8.14 for Bay and Walton counties respectively and an average of nearly 10 cu yds/ft near the point

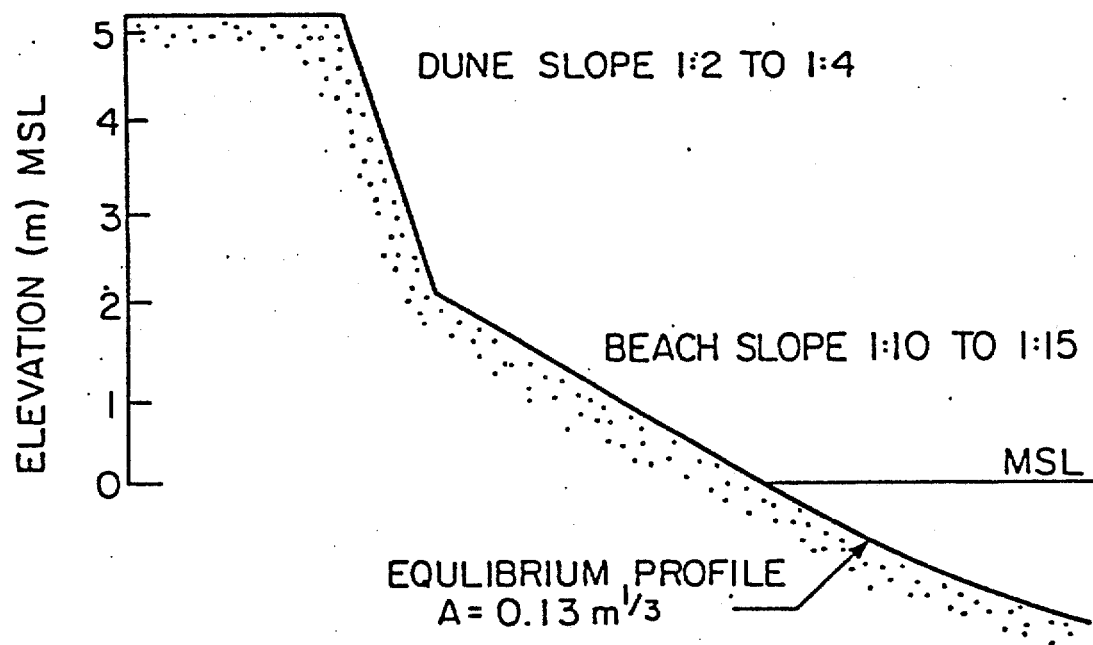


Figure 29 Representative Profile, Bay-Walton County Line

Table II
Simulation of Schematic Profile of Bay-Walton County
Hurricane Eloise

Beach Slope	Dune Slope	Wave Heights (ft)	Peak Surge (ft)	Contour Advance/Retreat				Volume Eroded (yd ³ /ft)
				15' (ft)	10' (ft)	5' (ft)	0' (ft)	
1:10	1:2	7.5	10.5	-22.4	-22.1	-12.7	+22.9	10.8
1:10	1:2	15.0	10.5	-23.0	-22.6	-15.9	+13.8	12.0
1:10	1:4	7.5	10.5	-20.1	-20.8	-15.2	+22.2	10.6
1:10	1:4	15.0	10.5	-20.6	-21.4	-18.4	+13.0	11.9
1:13	1:2	7.5	10.5	-19.1	-18.9	-10.3	+13.5	9.2
1:13	1:2	15.0	10.5	-19.6	-19.5	-12.9	+ 2.9	10.4
1:13	1:4	7.5	10.5	-17.0	-17.7	-12.6	+13.0	9.1
1:13	1:4	15.0	10.5	-17.5	-18.2	-15.1	+ 3.0	10.3
1:15	1:2	7.5	10.5	-17.5	-17.3	- 9.6	+ 7.5	8.3
1:15	1:2	15.0	10.5	-18.1	-17.8	-11.8	+ 1.9	9.6
1:15	1:4	7.5	10.5	-15.6	-16.2	-11.7	+ 5.8	8.3
1:15	1:4	15.0	10.5	-16.1	-16.7	-13.9	+ 3.1	9.6
1:10	1:2	7.5	11.5	-29.9	-28.2	-13.1	+29.7	13.3
1:10	1:2	15.0	11.5	-31.0	-29.4	-18.9	+16.0	15.3
1:10	1:4	7.5	11.5	-26.6	-27.7	-16.1	+29.2	13.1
1:10	1:4	15.0	11.5	-27.6	-28.8	-21.9	+14.8	15.1
1:15	1:2	7.5	11.5	-24.1	-22.2	- 8.4	+12.1	10.4
1:15	1:2	15.0	11.5	-25.1	-23.2	-13.1	+ 1.0	12.3
1:15	1:4	7.5	11.5	-21.1	-21.9	-11.1	+10.8	10.3
1:15	1:4	15.0	11.5	-22.2	-22.9	-15.8	- 1.7	12.4

Table III

Observed Erosion Characteristics For Bay-Walton Counties

Location	Avg. Contour Advance/Retreat				Volume Eroded (yd ³ /ft)
	15' (ft)	10' (ft)	5' (ft)	0' (ft)	
Bay County	- 8.9	-23.5	- 5.9	+26.5	7.30
Walton County	-12.8	-35.0	-11.3	+22.5	8.14
Bay-Walton County Line (20-22 miles from landfall)	-20.0	-42.0	- 5.0	+42.0	10.00

Table IV

Equilibrium Recession For Static Peak Surge Level

Schematic Profile of Bay-Walton County

Beach Slope	Dune Slope	Wave Height (ft)	Peak Surge (ft)	Contour Advance/Retreat				Volume Eroded (yd ³ /ft)
				15' (ft)	10' (ft)	5' (ft)	0' (ft)	
1:10	1:2	7.5	10.5	-115	-110	+ 20	+165	45
1:10	1:2	15.0	10.5	-225	-215	-110	+ 70	105
1:10	1:2	7.5	11.5	-130	-110	+ 45	+160	48
1:10	1:2	15.0	11.5	-250	-230	-100	+ 95	115

of the peak surge. While the predicted values are larger than observed eroded volumes, it should be remembered that the post-storm profiles reflect a partial rebuilding of the profile near the mean sea level line. Post storm profiles from Walton County show a well defined ridge of sand on the foreshore between the 0' and 3' elevations. Chiu notes the presense of this ridge and suggests that approximately 240,000 cu yds of sand were returned to the beach face in Walton County at the time of post-storm survey. Without this additional sand volume, the volumetric erosion at the time of the maximum erosion would be greater than the eroded volumes present in Table III; Chiu has estimated that perhaps an additional 2 cu yds/ft may have been eroded at the time of maximum erosion.

From this discussion, it appears that the model correctly includes time-dependent erosion such that the magnitude of the eroded volume is essentially preserved. To further illustrate this, the maximum potential erosion resulting from static water level and wave height conditions is presented in Table IV, for a 1:10 beach slope and a 1:2 dune slope. Comparing these results to the observed erosion statistics in Table II, it is clear that the maximum potential volumetric erosion is 5 - 10 times the actual observed values. In contrast, when the time dependent storm surge levels are considered, predicted erosion is, to the first order, in agreement with observed values. Thus, it seems that erosion rates are simulated accurately such that the eroded volume is conserved in the time-dependent simulation.

Now, consider the profile response as measured by the contour advance or retreat. First, it is well known that in nature, an eroding dune face steepens considerably, sometimes approaching a vertical slope. In Figure 30a, it is clear that for a water level of about 10 feet the 10' contour would erode further than the 15' contour, as the latter is subjected to less direct wave

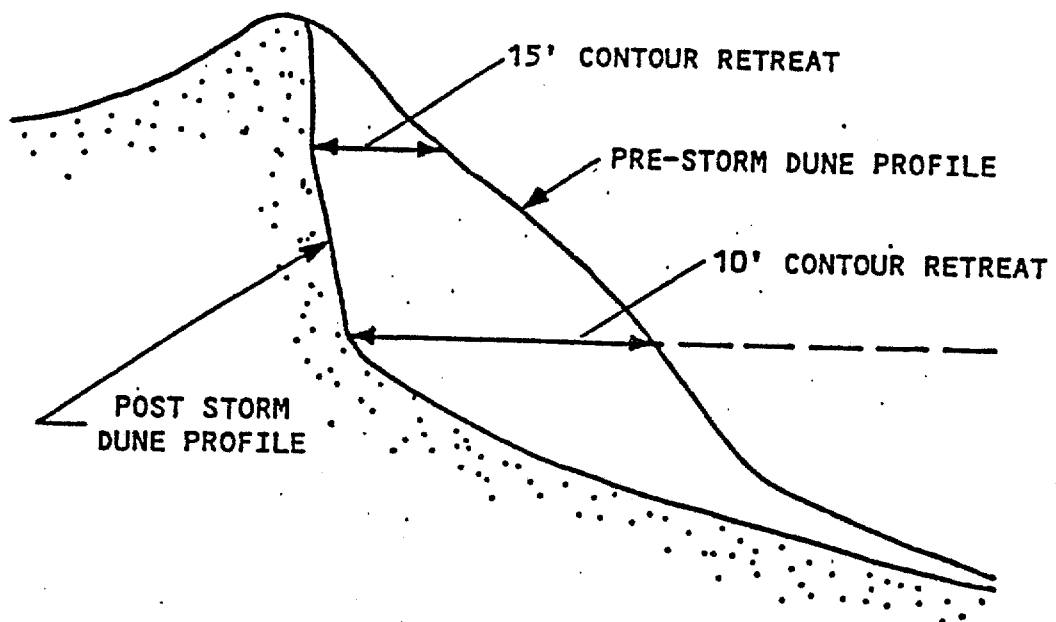


Figure 30a · Steepening of Natural Dune Form

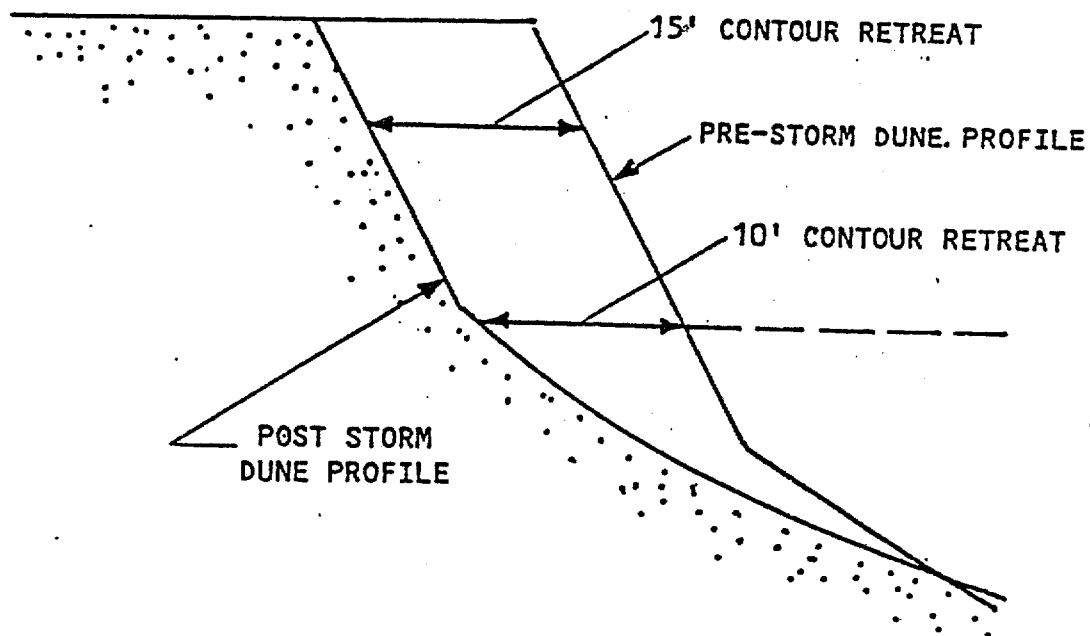


Figure 30b Uniform Recession of Schematic Dune Form

attack. This behavior is quite evident in the observed erosion data from Hurricane Eloise, both in Table III and in Figure 33 from Chiu (1977).

In the numerical model, it has been noted that the dune face is approximated by a linear slope which is maintained as the dune erodes. Therefore, in Figure 30b, the numerical solution results in equal recession of the 10 and 15 foot contours for a water level rise of up to 10 feet. For a slightly larger water level rise, as in the simulated storm surge hydrograph in Figure 28, the dynamic solution begins to affect the 10' contour as the concave profile shape is established below the still water level. Thus depending on the initial dune slope and the peak storm surge duration, the 10' contour recession may be greater than or less than the 15' contour recession by a small amount.

In the present model, without a rational method of including dune steepening, the numerical results for dune recession cannot be compared directly to the observed dune erosion. However, in analyzing the predicted results in Table II with respect to the observed dune recession in Table III, it may be argued that since the eroded volume is conserved, then the parallelogram approximation of dune erosion represents an average retreat of the dune face. In other words, since the volume eroded from the dune face in the model is essentially equal to the volume eroded from the dune face in nature, then the predicted dune recession should equal the average dune recession observed in nature. If the recession of the 10' and 15' contours in Table III are averaged, then the "average" dune retreat is 16.9 feet in Bay County, 23.9 feet in Walton County, and 31 feet in the region of the peak surge. Clearly this simple averaging has little physical significance, however, it does suggest that the model results are of the correct order-of-magnitude; numerical results range from 15.6 to 31 feet.

Again, it is emphasized that the proposed numerical solution accounts for time-dependent erosion effects in a rational fashion. In Table IV, the maximum

potential dune recession due to static peak surge conditions varies from 120 to 250 feet and requires more than 500 to 1,000 hours to reach equilibrium. In contrast, use of the storm surge hydrograph to determine the erosion for the duration of the storm surge, results in predicted values of dune recession that are 5-10 times less than the maximum potential recession. In Figure 31, the characteristics of the beach-dune erosion predicted for Hurricane Eloise are illustrated. Graphically, the difference between this predicted erosion and the maximum potential erosion for the static peak surge level is depicted in Figure 32.

In Table II, the results of the numerical simulation of erosion due to Hurricane Eloise reinforce earlier conclusions that:

- (1) the time-dependence of the storm surge-erosion process is critical for valid predictions of hurricane related beach erosion;
- (2) steeper beach/dune slopes erode farther and faster than mild slopes;
- (3) the change in water level is the dominant forcing function in the hurricane-related erosion process, while changes in wave height have less effect on storm induced dune erosion.

In the previous discussion, it has been noted that the inclusion of the time-dependent change in the water level represents a significant improvement in the ability to predict dune erosion associated with the hurricane storm surge. While the results in Table II represent the solution for idealized test cases, the close agreement between these results and observed erosion characteristics in Table III are encouraging. Likewise, the results in Table IV clearly suggest that use of the maximum potential erosion may greatly overpredict storm-induced erosion, especially for a fast moving storm such as Hurricane Eloise.

Aside from the storm surge duration, the magnitude of the storm surge has a significant effect on the storm related erosion. In Table II, storm durations

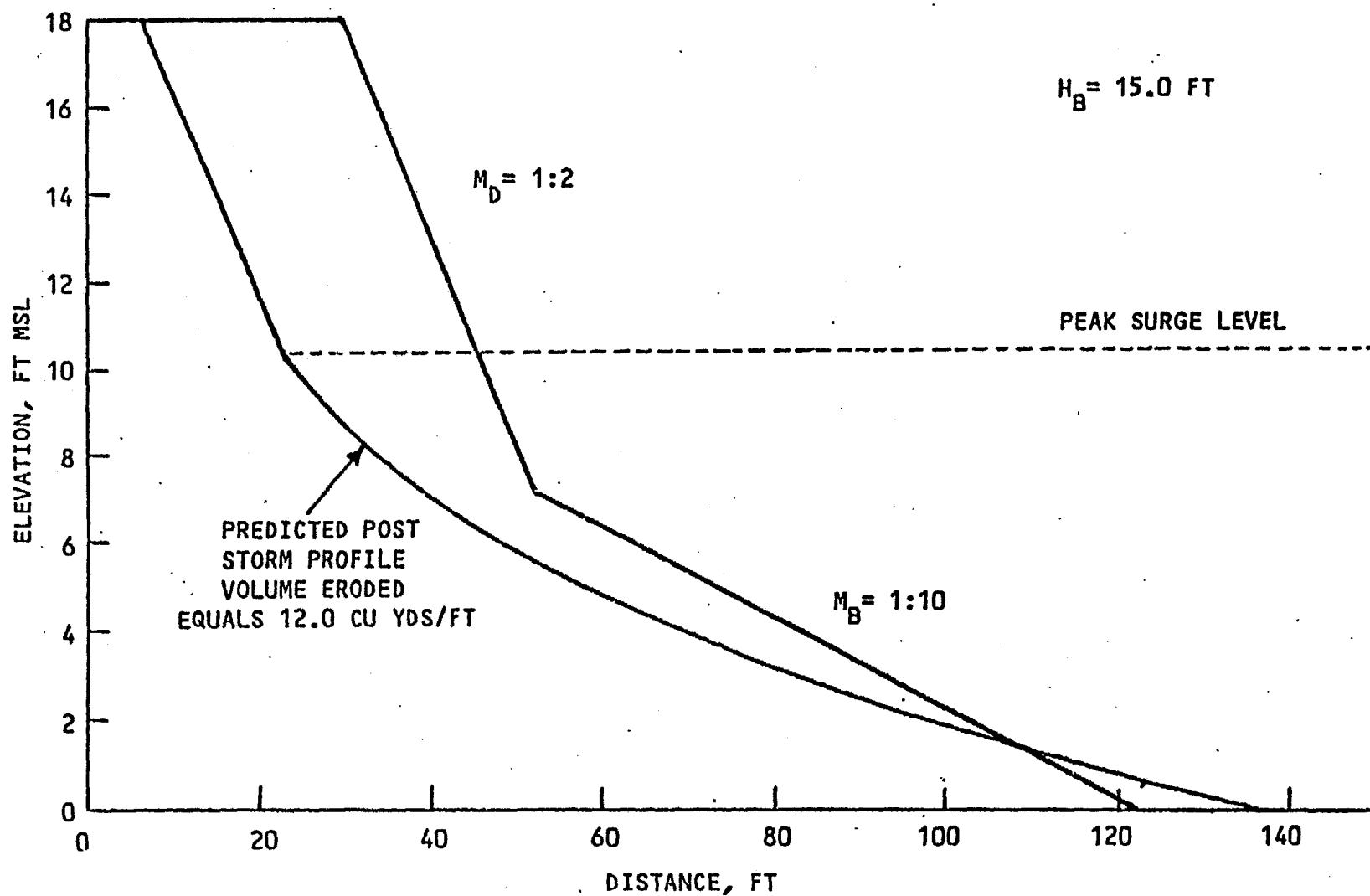


Figure 31 Example of Predicted Post-Storm Beach-Dune Profile, Hurricane Eloise, Bay-Walton County, Florida

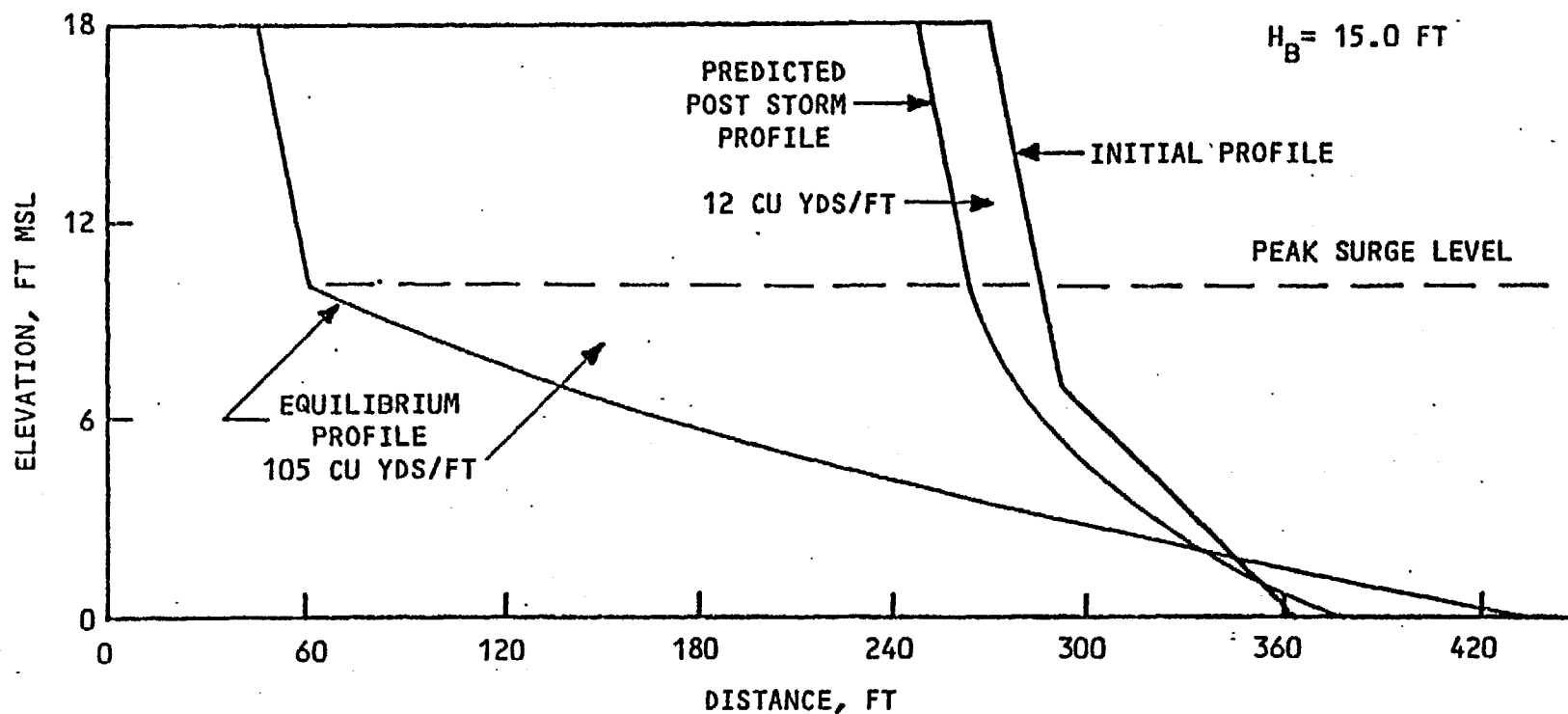


Figure 32 Comparison of Predicted Post-Storm Profile to Maximum Potential Erosion Due to Static Peak Surge Level, Hurricane Eloise, Bay-Walton County, Florida

are equal for both 10.5 and 11.5 ft. peak surge levels; however, it is clear that both volumetric erosion and contour recession are greater for the larger storm surge. This result is significant when compared to the erosion changes that result from a doubling of the wave height from 7.5 to 15 feet. While the equilibrium or maximum potential erosion is greatly affected by the wave height, for representative storm surge durations, wave height has a small impact on erosion.

Finally, the numerical results in Table II show that the beach face slope is a major parameter in determining the extent of the profile change. For any given water level and wave height, the steepest profile, a 1:10 beach slope and a 1:2 dune slope, exhibits the greatest dune recession and volumetric erosion. Likewise, the steepest profile shows the greatest advance of the 0' contour, as the contour must build seaward a greater distance to reach a stable position.

Chiu compared volumetric erosion directly to the beach slope and found a general trend toward increased erosion in areas of the greatest beach face slope. While local variations exist, possibly due to the presence of structures due to the variability in dune heights, it is clear in Figure 34 that volumetric erosion exhibits a distinct variation with beach slope. Likewise, comparing Figure 34 to Figure 33, it is evident that contour advance or retreat is greatest in areas of steepest beach slopes.

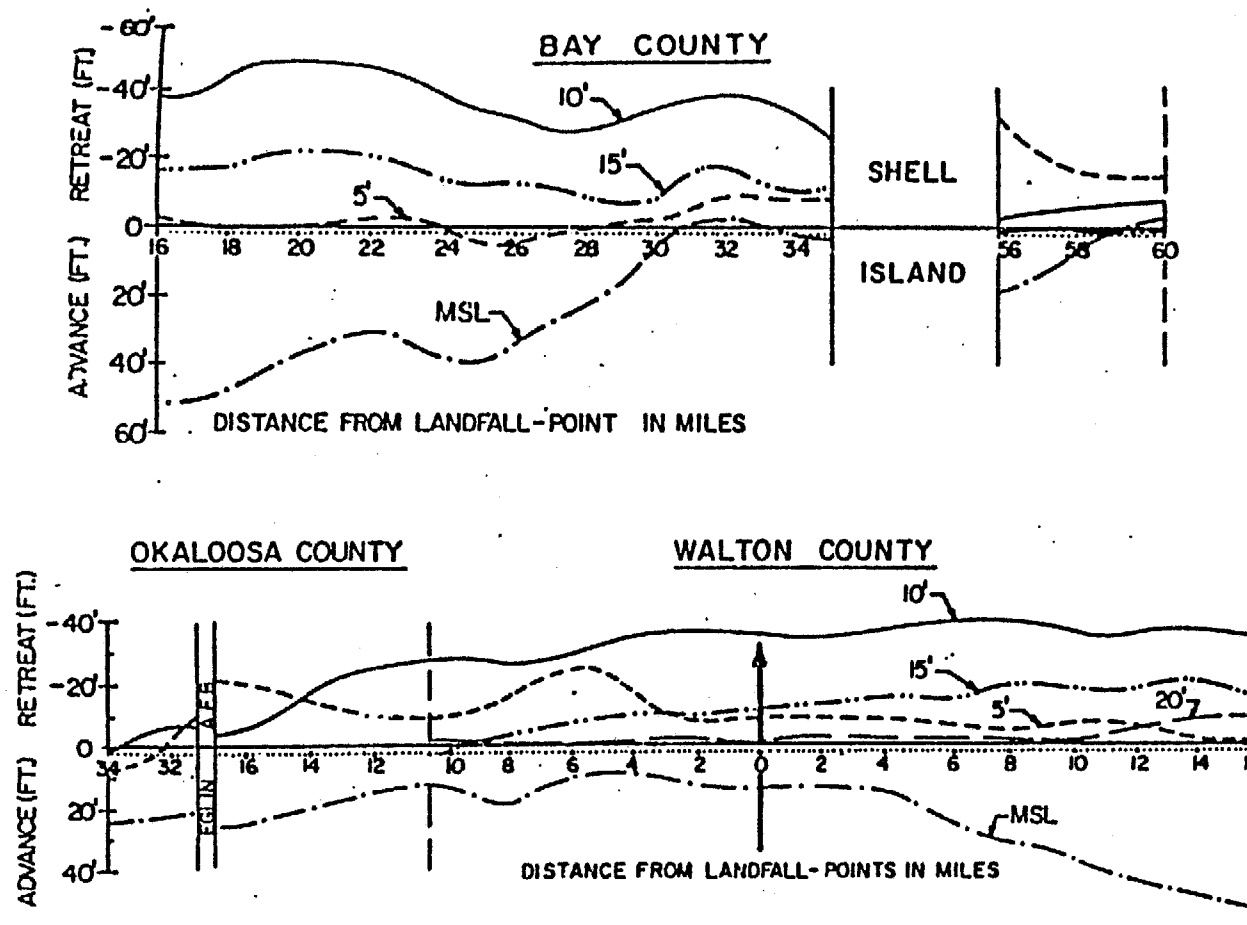


Figure 33 Contour Advance/Retreat Due to Hurricane Eloise Bay-Walton Counties (Chiu, 1977)

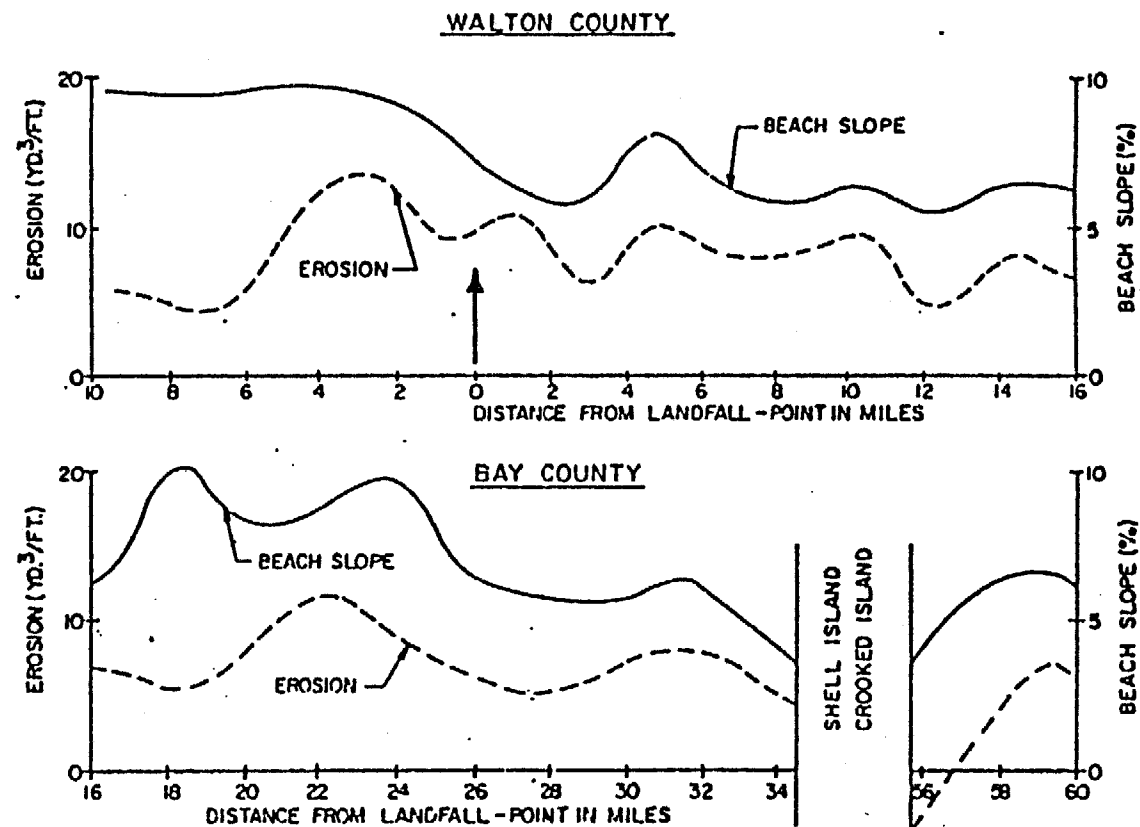


Figure 34 Volumetric Erosion Distribution and Beach Face Slope Variation, Bay-Walton Counties (Chiu, 1977)

REFERENCES

1. Bruun, P., "Coast Erosion and the Deveolpment of Beach Profiles," U.S. Army Corps of Engineers, Beach Erosion Board, Technical Memorandum No. 44, 1954.
2. Bruun, P., "Sea Level Rise as a Cause of Shore Erosion," Journal of Waterways and Harbors Division, ASCE, Vol. 88, WW1, February 1962.
3. Burdin, W.W., "Surge Effects from Hurricane Eloise," Shore and Beach, Vol.45, No. 2, April 1977.
4. Chiu, T.Y., "Beach and Dune Response to Hurricane Eloise of September 1975," Coastal Sediments '77, ASCE, 1977.
5. Chiu, T.Y., "Dune Erosion During Storm Conditions," Unpublished, Dept. of Coastal and Oceanographic Engineering, University of Florida, 1972.
6. Chiu, T.Y. and Dean, R.G., "Combined Total Storm Tide Frequency Analysis for Dade County, Florida," Dept. of Coastal and Oceanographic Engineering, University of Florida, 1981.
7. Dean, R.G., "Beach Erosion: Causes, Processes, and Remedial Measure," CRC Reviews in Environmental Control, CREC Press, Inc., Vol. 6, Issue 3, 1976.
8. Dean, R.G., "Equilibrium Beach Profiles: U.S. Atlantic and Gulf Coasts," "Ocean Engineering Report No. 12, Dept. of Civil Engineering, University of Delaware, Jan. 1977.
9. Edelman, T., "Dune Erosion During Storm Conditions," Proc. 11th Conf. on Coastal Engineering, London, 1968.
10. Edelman, T., "Dune Erosion During Storm Conditions," Proc. 13th Conf. on Coastal Engineering, Vancouver, 1972.
11. Fenneman, N.M., "Development of the Profile of Equilibrium of the Subaqueous Shore Terrance," Journal of Geology, Vol. X, 1902.
12. Hughes, S., "The Variation of Beach Profiles when Approximated by a Theoretical Curve," M.S. Thesis, University of Florida, 1978.
13. Hughes, S.A. and Chiu, T.Y., "Beach and Dune Erosion During Severe Storms," UFL/COEL-TR/043, Dept. of Coastal and Oceanographic Engineering, University of Florida, 1981.
14. Moore, B., "Beach Profile Evolution in Response to Changes in Water Level and Wave Height," M.S. Thesis, University of Delaware, 1982.
15. Saville, T., "Scale Effects in Two-Dimensional Beach Studies," Trans. 7th Meeting of Intl. Assoc. of Hydraulic Research, Lisbon, 1957.
16. Swart, D.H., "Offshore Sediment Transport and Equilibrium Beach Profiles," Publication No. 131, Delft Hydraulics Lab., Delft University of Technology, 1974.

17. Swart, D.H., "A Schematization of Onshore-Offshore Transport," Proc. 14th Conf. on Coastal Engineering, Copenhagen, 1974.
18. Swart, D.H., "Predictive Equations Regarding Coastal Transports," Proc. 15th Conf. on Coastal Engineering, Honolulu, 1976.

APPENDIX A

DERIVATION OF IMPLICIT EQUATION OF CONTINUITY GOVERNING ONSHORE-OFFSHORE BEACH PROFILE EVOLUTION

In Chapter III, an implicit finite-difference formulation for beach profile evolution was developed from a consideration of: (1) the offshore sediment transport, based on the excess energy dissipation per unit volume in the surf zone, and (2) the onshore-offshore continuity equation for conservation of sand in the surf zone. This solution involves a space staggered numerical scheme where the change in position of an elevation contour, or horizontal cell of height Δh , over time Δt , is given as:

$$\Delta x_n = \frac{K\Delta t}{\Delta h} \left[\frac{Kd(h_n'^{5/2} - h_{n-1}'^{5/2})}{(h_n' + h_{n-1}')(\bar{x}_n - \bar{x}_{n-1})} - \frac{Kd(h_{n+1}'^{5/2} - h_n'^{5/2})}{(h_{n+1}' + h_n')(\bar{x}_{n+1} - \bar{x}_n)} \right] \quad (A.1)$$

Also, it is recognized that for a static water level, the position of each contour, n , varies over the time step, such that the average position, \bar{x}_n , is given as:

$$\bar{x}_n = x_n + \frac{\Delta x_n}{2} \quad (A.2)$$

Substituting Equation (A.2) into Equation (A.1) results in the rather lengthy expression:

$$\Delta x_n = \frac{K\Delta t}{\Delta h} \left[\frac{Kd(h'_n)^{5/2} - h'_{n-1}^{5/2})}{(h'_n + h'_{n-1})(x_n + \frac{\Delta x_n}{2} - x_{n-1} - \frac{\Delta x_{n-1}}{2})} - \frac{Kd(h'_{n+1})^{5/2} - h'_n)^{5/2})}{(h'_{n+1} + h'_n)(x_{n+1} + \frac{\Delta x_{n+1}}{2} - x_n - \frac{\Delta x_n}{2})} \right] \quad (A.3)$$

where the interdependence of adjacent contours is evident.

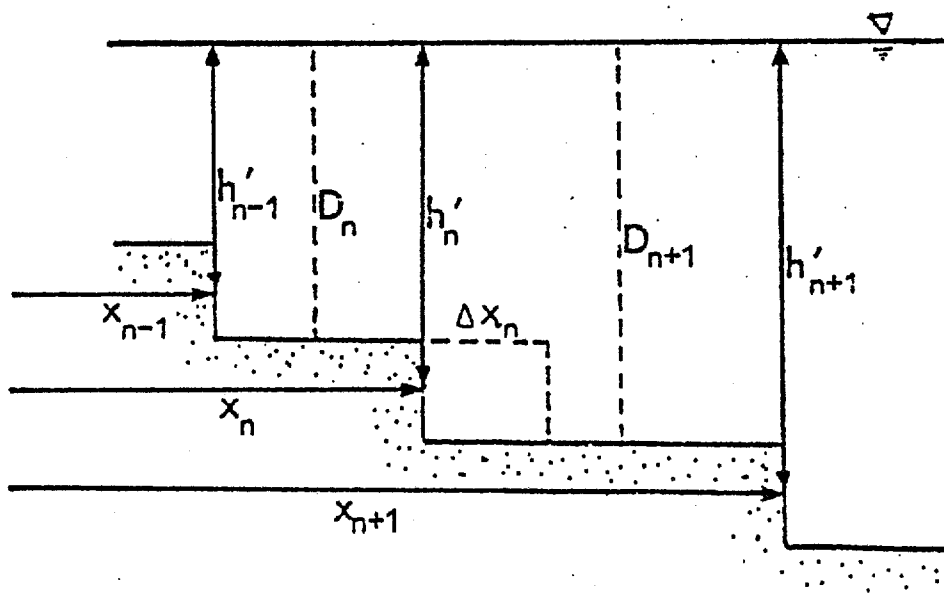


FIGURE A.1 DEFINITION SKETCH OF ENERGY DISSIPATION AT VERTICAL CELL BOUNDARY

From Figure (A.1), the change in position of the nth contour over a time step is defined by the excess energy dissipation in the water column associated with a vertical cell containing the nth contour. In Equation (A.3), the energy dissipation terms at the beginning of the time step may be identified as:

$$D_n = \frac{Kd(h_n'^{5/2} - h_{n-1}'^{5/2})}{(h_n' + h_{n-1}')(x_n - x_{n-1})} \quad (A.4)$$

Therefore, the implicit form of the continuity equation may be expressed as:

$$\Delta x_n = \frac{K\Delta t}{\Delta h} \left[\frac{D_n}{\left(1 + \frac{\Delta x_n - \Delta x_{n-1}}{2(x_n - x_{n-1})}\right)} - \frac{D_{n+1}}{\left(1 + \frac{\Delta x_{n+1} - \Delta x_n}{2(x_{n+1} - x_n)}\right)} \right] \quad (A.5)$$

where it is clear that Δx_{n-1} , Δx_n , and Δx_{n+1} are the only unknowns.

With these unknowns in the denominator of the right hand side of Equation (A.5), an analytical solution is difficult, if not impossible, to obtain. However, if a Taylor series expansion is introduced, namely:

$$\frac{1}{1 + \alpha} = 1 - \alpha + \alpha^2 - \alpha^3 + \alpha^4 \dots \quad (A.6)$$

then, to the first order:

$$\frac{1}{1 + \frac{\Delta x_n - \Delta x_{n-1}}{2(x_n - x_{n-1})}} = 1 - \frac{\Delta x_n - \Delta x_{n-1}}{2(x_n - x_{n-1})} \quad (\text{A.7})$$

Now, Equation (A.5) may be rewritten as:

$$\Delta x_n = \frac{K\Delta t}{\Delta h} \left[D_n - D_n \left(\frac{\Delta x_n - \Delta x_{n-1}}{2(x_n - x_{n-1})} \right) - D_{n+1} + D_{n+1} \left(\frac{\Delta x_{n+1} - \Delta x_n}{2(x_{n+1} - x_n)} \right) \right] \quad (\text{A.8})$$

where the unknowns are in the numerator. This form may be rearranged, such that:

$$\begin{aligned} \Delta x_n = \frac{K\Delta t}{\Delta h} & \left[D_n - D_{n+1} + \frac{D_n \Delta x_{n-1}}{2(x_n - x_{n-1})} - \frac{D_n \Delta x_n}{2(x_n - x_{n-1})} \right. \\ & \left. - \frac{D_{n+1} \Delta x_n}{2(x_{n+1} - x_n)} + \frac{D_{n+1} \Delta x_{n+1}}{2(x_{n+1} - x_n)} \right] \quad (\text{A.9}) \end{aligned}$$

and a constant coefficient may be defined as:

$$\beta = \frac{K\Delta t}{2\Delta h} \quad (\text{A.10})$$

By grouping like terms, with the unknowns on the left hand side, the final form of the continuity equation is:

$$\begin{aligned} & \left[-\frac{\beta D_n}{x_n - x_{n-1}} \right] \Delta x_{n-1} + \left[1 + \frac{\beta D_n}{x_n - x_{n-1}} + \frac{\beta D_{n+1}}{x_{n+1} - x_n} \right] \Delta x_n \\ & + \left[-\frac{\beta D_{n+1}}{x_{n+1} - x_n} \right] \Delta x_{n+1} = 2\beta(D_n - D_{n+1}) \end{aligned} \quad (A.11)$$

which may be more clearly given as:

$$A_n \Delta x_{n-1} + B_n \Delta x_n + C_n \Delta x_{n+1} = Z_n \quad (A.12)$$

where

$$A_n = -\frac{\beta D_n}{x_n - x_{n-1}} \quad (A.12a)$$

$$B_n = 1 + \frac{\beta D_n}{x_n - x_{n-1}} + \frac{\beta D_{n+1}}{x_{n+1} - x_n} \quad (A.12b)$$

$$C_n = -\frac{\beta D_{n+1}}{x_{n+1} - x_n} \quad (A.12c)$$

$$Z_n = 2\beta(D_n - D_{n+1}) \quad (A.12d)$$

As a final note, the expression, $D_{eq}-D_{eq}=0$, may be added to both sides of Equation (A.12); thus, the driving term, Z_n , may be defined as:

$$Z_n = 2\beta \left(D_n - D_{eq} - D_{n+1} + D_{eq} \right) \quad (A.13)$$

or

$$Z_n = - \frac{2\beta}{K} \left(Q_{s_{n+1}} - Q_{s_n} \right) \quad (A.14)$$

where the sediment transport flux across the vertical cell boundaries is now included for convenience.

APPENDIX B

LISTING OF COMPUTER PROGRAM

[illegible]

DAVID KRIEBEL--UNIVERSITY OF DELAWARE--APRIL 1982

$$H = A * (X ** (2/3))$$

QS = K*(D-DISSE)

$$(DX/DT) = (DQS/DH)$$

(1) SCHEMATIC REPRESENTATION OF INITIAL BEACH PROFILE, WITH:

- A) CONSTANT DUNE HEIGHT
- B) UNIFORM LINEAR DUNE FACE SLOPE
- C) INITIAL BERM HEIGHT -OR- ELEVATION OF CHANGE IN SLOPE FROM DUNE FACE TO BEACH FACE (USUALLY THE VEGETATION LINE ELEVATION)
- D) UNIFORM LINEAR BEACH FACE SLOPE
- E) OFFSHORE PROFILE OF THE FORM $A*(X^{2/3})$ WHICH INTERSECTS THE LINEAR BEACH FACE AT SOME DEPTH, HSTARI, SUCH THAT THE PROFILE SLOPE CONTINUOUSLY DECREASES IN THE OFFSHORE DIRECTION.

A) SURGE LEVEL FROM MSL RECORDED AT ONE-HALF HOUR INTERVALS

A) CONSTANT ESTIMATE OF DESIGN WAVE HEIGHT, -OR-
B) OBSERVED OR ESTIMATED WAVE HEIGHT AT ONE-HALF HOUR
INTERVALS.

- (1) BEACH PROFILE CROSS-SECTION AT TIME OF MAXIMUM EROSION,
- (2) CONTOUR ADVANCE OR RETREAT FOR SPECIFIC ELEVATIONS,
- (3) VOLUMETRIC EROSION IN CUBIC YARDS PER LINEAR FOOT.

B4

- (1) DISTANCES (X DIRECTION) ARE POSITIVE SEAWARD OF SOME ARBITRARY BASELINE DATUM
- (2) ELEVATIONS (Y DIRECTION) ARE POSITIVE BELOW THE WATER LINE
- (3) A DISCRETE PROFILE REPRESENTATION IS USED WITH UNIFORM VERTICAL CELLS OF WIDTH, $\Delta H = 0.5$ FEET. MIDPOINT OF EACH CELL IS DEFINED BY THE GRID NUMBER, N, SUCH THAT $N=1$ AT THE TOP OF THE DUNE, $N=N_{MAX}$ AT LAST POINT OFFSHORE.

INPUT VARIABLES:

DISSE = EQUILIBRIUM ENERGY DISSIPATION PER UNIT VOLUME, OBTAINED FROM THE "A" PARAMETER FROM THE PROFILE SHAPE.

HDUNET = AVERAGE INITIAL ELEVATION OF TOP OF DUNE IN FEET RELATIVE TO MSL; NOTE: MUST HAVE NEGATIVE SIGN.

HBERM = AVERAGE INITIAL ELEVATION OF TOP OF BERM -OR- BREAK IN SLOPE BETWEEN DUNE AND BEACH SLOPES (USUALLY THE ELEVATION OF THE VEGETATION LINE); NOTE: MUST HAVE NEGATIVE SIGN

XDUNET = INITIAL HORIZONTAL DISTANCE FROM BASELINE DATUM TO CREST OF DUNE IN FEET; NOTE: MUST BE POSITIVE NUMBER.

XBERM = INITIAL HORIZONTAL DISTANCE FROM BASELINE DATUM TO CREST OF BERM -OR- BREAK IN SLOPE BETWEEN DUNE AND BEACH FACE, IN FEET

NBERM = GRID NUMBER OF BERM CREST -OR- BREAK IN SLOPE IF NO BERM IS PRESENT IN THE INITIAL PROFILE. NOTE: MUST BE AN INTEGER; $N=1$ AT TOP OF DUNE AND INCREASES BY 1 FOR EACH 0.5' DECREASE IN ELEVATION.

EXAMPLE: IF $HDUNET = -18.0'$ AND $HBERM = -7.0'$, THEN
 $NBERM = 1 + \text{INTEGER}((18-7)/0.5) = 23$

XMD = UNIFORM LINEAR DUNE FACE SLOPE IN DECIMAL FORM (FT/FT)

XMB = UNIFORM LINEAR BEACH FACE SLOPE IN DECIMAL FORM (FT/FT)

HSTARI = DEPTH OF INTERSECTION OF LINEAR BEACH FACE SLOPE AND EQUILIBRIUM PROFILE; ESTABLISHED AT THE POINT OF TANGENCY SUCH THAT SLOPE DECREASES IN OFFSHORE DIRECTION; USED TO DEFINE THE TRANSITION BETWEEN DYNAMIC AND GEOMETRIC SOLUTION REGIONS. NOTE: MUST BE ROUNDED TO NEXT GREATER DEPTH IN 0.5' INCREMENT.

LTMAX = MAXIMUM VALUE OF THE TIME COUNTER, LTIME, USED TO IDENTIFY TIME DEPENDENT STORM SURGE ELEVATION.
 $LTIME=0$ AT $T=0$ HOURS, $LTIME=LTMAX$ FOR FINAL WATER LEVEL DATA POINT. LTIME INCREASES BY 1 FOR EACH ONE-HALF HOUR INCREASE IN REAL TIME.

WSEL(LTIME) = STORM SURGE LEVEL RELATIVE TO MSL AT TIME STEP LTIME;
 NOTE: POSITIVE FOR WATER LEVEL INCREASE

```

C      WH      = DESIGN BREAKING WAVE HEIGHT IN FEET; CONSTANT VALUE.
C
C      WAVE(LTIME)= BREAKING WAVE HEIGHT AT TIME STEP LTIME
C
C*****
C
C      DIMENSION H1(0:250),H(0:250),X1(0:250),X(0:250),DELX(0:250)
C      DIMENSION DISS(0:250),QS(0:250),Q1(0:250),E(0:250),F(0:250)
C      DIMENSION SUMVOL(0:250),WSEL(0:250),WAVE(0:250)
C      REAL KQ
C      REAL KD
C      CHARACTER*8 PROF
C
C-----FORMAT STATEMENTS FOR INPUT/OUTPUT-----
C
920  FORMAT(1X, 'ERODED VOLUME EQUALS',F10.2, ' CUBIC YARDS/FT',/)
921  FORMAT(1X, 'TIME = ',F6.2,/)
925  FORMAT(1X,'GRID',1X, 'INITIAL',1X, 'INITIAL',1X, 'UPDATED',
1      2X,'UPDATED',2X, 'ENERGY',3X, 'SED.',4X, 'DELTA',4X, 'CUM.',/,
2      'POINT', 3X, 'ELEV',4X, 'DIST', 4X, 'ELEV',4X, 'DIST',
3      4X, 'DISS',4X, 'TRANS', 6X, 'X' ,6X, 'VOL',/)
930  FORMAT(I5,5F8.2,F8.4,2F8.2)
935  FORMAT(2X, 'TIME',3X, 'SURGE',3X, 'WAVE' ,21X,
1      'CONTOUR ADVANCE/RETREAT',21X, 'ERODED',4X, 'CHECK',/,
2      9X, 'HEIGHT' ,1X, 'HEIGHT' ,5X, 'DUNE' ,5X, '20 FT',
3      5X, '15 FT' ,5X, '10 FT' ,6X, '5 FT' ,6X, 'MSL' ,6X,
4      'VOLUME' ,3X, 'CONTINUITY',/)
940  FORMAT(F6.1,F8.2,F7.1,7F10.2,F10.1)
945  FORMAT(1X,/////)
950  FORMAT(7X,F7.2)
960  FORMAT(F6.2)
975  FORMAT('PROFILE', 5X, 'DUNE' ,10X, 'BERM' ,7X, 'BEACH',4X,
1      'DUNE' ,/,9X, 'ELEV' ,3X, 'DIST' ,3X, 'ELEV' ,3X, 'DIST',
2      3X, 'SLOPE' ,3X, 'SLOPE',/)
980  FORMAT(A8,F8.1,3F7.1,2F8.3,/)
990  FORMAT(A8,2F6.0,F6.1,F6.3,F6.1,2F6.0,F6.1,F6.3,F6.3)
C
C-----INPUT DATA-----
C
C      EQUILIBRIUM BEACH PROFILE SPECIFICATIONS
C
707  CONTINUE
C
      READ(10,990,END=777) PROF,XMSL,XBERM,HBERM,XMB,HDUNEF,XDUNEF,
1      XDUNET,HDUNET,XMD,SMULT
C
      WRITE(6,990) PROF,XMSL,XBERM,HBERM,XMB,HDUNEF,XDUNEF,
1      XDUNET,HDUNET,XMD,SMULT
C
      REWIND(1)
      WRITE(3,975)
      WRITE(4,975)
      WRITE(4,980) PROF,HDUNET,XDUNET,HBERM,XBERM,XMB,XMD
      WRITE(3,980) PROF,HDUNET,XDUNET,HBERM,XBERM,XMB,XMD
      WRITE(4,935)
C

```

```

DISSE=46.32*(A**1.5)
DH=0.5
C
C BERM AND DUNE SPECIFICATIONS
C
HDUNET=-HDUNET
HBERM=-HBERM
NMAX=51+IFIX((-HDUNET+30.)/0.5)
NBERM=1+IFIX(-(HDUNET-HBERM)/0.5)
NDUNEF=NBERM-1
C
C COEFFICIENTS FOR ENERGY DISSIPATION AND SEDIMENT TRANSPORT EQNS.
C
KD=55.24
KQ=0.001144
C
C TIME CHARACTERISTICS
C
T=0.0
LTMAX=25
C
C INITIAL VALUES
C
NSTOP=NBERM
NFLAG=0
MTWE=0
MFIF=0
NGOTO=1
IF(XBERM.LT.1.0) NGOTO=2
C
C SELECT INPUT FORMAT FOR WAVE HEIGHT
C IF IWAVE=1, USE CONSTANT WAVE HEIGHT, SET WH VALUE BELOW
C IF IWAVE=2, READ WAVE HEIGHT DATA AT ONE-HALF HOUR INTERVAL
C
IWAVE=1
C
IF(IWAVE.EQ.1) WH=15.0
C
C-----ESTABLISH INITIAL PROFILE-----
C
DO 110 N=1,NMAX
H1(N)=HDUNET+DH*(N-1)
WRITE(6,1120)N,H1(N),H1(N-1),HDUNET
1120 FORMAT(I5,F8.2,F8.2,F8.2)
IF(N.LE.NDUNEF) GO TO 103
IF(H1(N).NE.HBERM) GO TO 99
C
C IF PROFILE HAS WIDE BERM, USE 102 IN NEXT GO TO
C IF PROFILE DOES NOT HAVE BERM, USE 103 IN NEXT GO TO
C
GO TO(102,103) NGOTO
C
99 IF(H1(N).LE.HSTARI) GO TO 104
HA=H1(N)**2.5-H1(N-1)**2.5
HB=H1(N)+H1(N-1)
XH=(KD*HA)/(HB*DISSE)

```

```

      X1(N)=X1(N-1)+XH
      GO TO 109
102    X1(N)=XBERM
      GO TO 109
103    X1(N)=XDUNET+(H1(N)-HDUNET)/XMD
      GO TO 109
104    X1(N)=X1(NBERM)+(H1(N)-HBERM)/XMB
      GO TO 109
109    X(N)=X1(N)
      H(N)=H1(N)
      IF(H1(N).EQ.0.0) MSL=N
      IF(H1(N).EQ.-5.0) MFIV=N
      IF(H1(N).EQ.-10.0) MTEN=N
      IF(H1(N).EQ.-15.0) MFIF=N
      IF(H1(N).EQ.-20.0) MTWE=N
110    CONTINUE
C
C    RECORD INITIAL PROFILE
C
      IF(T.EQ.0.0) GO TO 999
997    CONTINUE
C
C*****
C
C    CALCULATE CHANGE IN PROFILE FOR GIVEN WATER LEVEL AND WAVE HEIGHT
C
C-----BEGIN MAIN TIME LOOP IN INCREMENTS OF ONE-HALF HOUR-----
C
      DO 1 LTIME=1,LTMAX
C
C    READ STORM SURGE LEVEL AT EACH TIME STEP
C
      READ(1,950) WSEL(LTIME)
      WRITE(6,950) WSEL(LTIME)
      WSEL(LTIME)=WSEL(LTIME)*SMULT
C
C    READ WAVE HEIGHT AT EACH TIME STEP UNLESS CONSTANT
C    FORMAT OPTION IS USED SUCH THAT WH=CONSTANT
C
      IF(IWAVE.EQ.1) GO TO 400
      READ(2,960) WAVE(LTIME)
      WH=WAVE(LTIME)
400    CONTINUE
C
C    UPDATE REAL TIME IN INCREMENTS OF 0.5 HOURS
C
      T=T+0.5
C
C    APPROXIMATE THE STORM SURGE TO NEAREST 0.5 FEET AND
C    DETERMINE INCREMENTAL CHANGE IN WATER LEVEL, DELWS
C    NOTE: FOR OUTPUT, WSELEV CONTAINS ACTUAL STORM SURGE LEVEL,
C          WSEL(LTIME) IS ALTERED TO CONTAIN APPROX. SURGE LEVEL
C
      WS=0.0
      WSEL(0)=0.0

```

```

WSELEV=WSEL(LTIME)
C
DO 200 K=1,50
  IF(WSELEV.LE.WS) GO TO 201
  WS=WS+0.5
200 CONTINUE
201 WSEL(LTIME)=WS
C
  DELWS=WSEL(LTIME)-WSEL(LTIME-1)
C
C UPDATE DEPTH AT EACH TIME STEP
C
DO 300 N=1,NMAX
  H(N)=H(N)+DELWS
300 CONTINUE
C
C-----SET SECONDARY TIME STEP TO AVOID NUMERICAL INSTABILITY-----
C
  IF(H(NBERM).GE.0.0) GO TO 111
  DT=600.0
  JTMAX=3
  GO TO 112
111 CONTINUE
  DT=100.0
  JTMAX=18
112 CONTINUE
C
C BEGIN SECONDARY TIME LOOP USING DT IN SECONDS
C NOTE: TOTAL REAL TIME SIMULATED IN FOLLOWING LOOP MUST
C EQUAL ONE-HALF HOUR
C
DO 2 JTIME=1,JTMAX
C
C
C-----DETERMINE BOUNDARY CONDITIONS LIMITING WIDTH OF ACTIVE PROFILE-----
C
C ESTABLISH OFFSHORE LIMIT TO SURF ZONE AT BREAKING DEPTH
C DEFINED BY THE SPILLING BREAKER ASSUMPTION
C
BDPT=1.30*WH
C
DO 113 N=1,NMAX
  IF((H(N).GE.BDPT).AND.(H(N-1).LT.BDPT)) NBREAK=N-1
113 CONTINUE
C
C ESTABLISH ONSHORE LIMIT TO SEDIMENT TRANSPORT AND ESTABLISH
C THE TRANSITION DEPTH, HSTAR, BETWEEN DYNAMIC AND GEOMETRIC
C SOLUTIONS
C
  IF(H(NBERM).LE.0.0) GO TO 114
  IF(H(NBERM).GT.0.0) GO TO 115
C
C IF WATER LEVEL IS ON BEACH FACE, SET HSTAR EQUAL TO ORIGINAL
C TRANSITION DEPTH, HSTAR1
C IF WIDE BERM IS PRESENT, SET NSTOP EQUAL TO NBERM
C IF BERM ERODES -OR- IF NO BERM IS PRESENT, NSTOP EQUALS 1 AT TOP

```

```

C      OF DUNE
C
114    HSTAR=HSTARI
      NSTOP=NBERM
      IF((X(NBERM)-X(NBERM-1)).LE.((0.5/XMD)+0.2)) NFLAG=1
      IF(NFLAG.EQ.1) NSTOP=1
      GO TO 118
C
C      IF WATER LEVEL IS ON DUNE FACE, TRANSITION DEPTH VARIES WITH
C      THE BERM WIDTH:
C      IF WIDE BERM IS PRESENT, HSTAR EQUALS WATER DEPTH AT NBERM, AND
C      NSTOP IS EQUAL TO NBERM-- THIS ALLOWS BERM TO ERODE QUICKLY.
C      IF BERM ERODES -OR- IF NO BERM IS PRESENT, HSTAR EQUALS ZERO
C      AND NSTOP IS EQUAL TO 1 AT TOP OF DUNE
C
115    HSTAR=H(NBERM)
      NSTOP=NBERM
      XHCRT=((H(NBERM)**2.5-H(NBERM-1)**2.5)*KD)/
1((H(NBERM)+H(NBERM-1))*DISSE)
      IF((X(NBERM)-X(NBERM-1)).LE.(XHCRT+0.2)) NFLAG=1
      IF(NFLAG.EQ.1) GO TO 116
      GO TO 118
116    HSTAR=0.0
      NSTOP=1
      GO TO 118
C
C      IF SOLUTION RESULTS IN DUNE ACCRETION, RESET HSTAR AND NSTOP
C      SUCH THAT ONLY BERM REBUILDS, THUS DUNE EROSION IS PERMANANT
C
117    CONTINUE
      IF(H(NBERM).GT.0.0) HSTAR=H(NBERM)
      NSTOP=NBERM
118    CONTINUE
C
C-----
C      BEGIN DYNAMIC SOLUTION
C-----
C
C      CALCULATE ENERGY DISSIPATION PER UNIT VOLUME AND
C      SEDIMENT TRANSPORT FLUX IN SURF ZONE
C
      DO 121 N=1,NMAX
        IF(H(N).LE.HSTAR) GO TO 119
        IF(H(N).GT.H(NBREAK)) GO TO 119
        HA=H(N)**2.5-H(N-1)**2.5
        HB=H(N)+H(N-1)
        HC=X(N)-X(N-1)
        DISS(N)=(KD*HA)/(HB*HC)
        QS(N)=KQ*(DISS(N)-DISSE)
        GO TO 120
119    DISS(N)=0.0
        QS(N)=0.0
120    Q1(N)=QS(N)
121    CONTINUE
C
C      APPLY SMOOTHING FUNCTION TO SEDIMENT TRANSPORT CURVE

```

```

C      FROM TRANSITION DEPTH, HSTAR, TO BEYOND BREAKING DEPTH
C
      DO 137 N=2,NMAX
        IF(H(N).LE.HSTAR) GO TO 138
        QS(N)=0.1*Q1(N-2)+0.15*Q1(N-1)+0.5*Q1(N)+
1        0.15*Q1(N+1)+0.1*Q1(N+2)
        IF(H(N).GT.H(NBREAK+2)) GO TO 138
        DISS(N)=DISSE+QS(N)/KQ
        IF((QS(N).NE.0.0).AND.(QS(N-1).EQ.0.0)) GO TO 139
        GO TO 137
138      QS(N)=Q1(N)
        DISS(N)=0.0
        GO TO 137
139      QQ=QS(N)
        NQQ=N
137      CONTINUE
C
C      EXTEND SEDIMENT TRANSPORT CURVE LINEARLY FROM TRANSITION DEPTH
C      TO ZERO AT NSTOP TO SATISFY CONTINUITY BETWEEN DYNAMIC
C      AND GEOMETRIC SOLUTION REGIONS.
C
        QQQ=QQ/(NQQ-NSTOP)
        QS(NSTOP)=0.0
        NA=NSTOP+1
        NB=NQQ-1
C
      DO 136 N=NA,NB
        QS(N)=QS(N-1)+QQQ
136      CONTINUE
C
C-----CALCULATE COEFFICIENTS FOR DOUBLE SWEEP SOLUTION-----
C      OFFSHORE SWEEP NUMBER 1
C
      BDT=DT/(2.0*DH)
      NB=NMAX-1
C
      DO 130 N=1,NB
        IF(N.EQ.1) GO TO 128
        XA=X(N)-X(N-1)
        XB=X(N+1)-X(N)
127      AN=-BDT*KQ*DISS(N)/XA
        BN=1.0+BDT*KQ*(DISS(N)/XA+DISS(N+1)/XB)
        CN=-BDT*KQ*DISS(N+1)/XB
        ZN=-(BDT/0.5)*(QS(N+1)-QS(N))
        GO TO 129
128      E(1)=0.0
        F(1)=-(BDT/0.5)*(QS(2)-QS(1))
        XB=X(N+1)-X(N)
        XA=XB
        GO TO 127
129      E(N+1)=-CN/(BN+AN*E(N))
        F(N+1)=(ZN-AN*F(N))/(BN+AN*E(N))
130      CONTINUE
C
C-----CALCULATE CHANGE IN POSITION OF EACH GRID POINT-----

```

```

C   ONSHORE SWEEP NUMBER 2
C
C   NB=NMAX-1
C   DELX(NMAX)=0.0
C
C   DO 140 M=1,NB
C       N=NMAX-(M-1)
C       DELX(N-1)=E(N)*DELX(N)+F(N)
140  CONTINUE
C
C-----
C   DYNAMIC SOLUTION IS COMPLETED, NOW APPLY GEOMETRIC CRITERIA
C   TO MAINTAIN SMOOTH PROFILE AND CONTINUITY
C-----
C
C   ESTABLISH OFFSHORE SLOPE TO LIMIT CELL GROWTH AT BREAKING DEPTH
C
C   XCRIT=0.33/XMB
C   NA=NBREAK-3
C   NB=NBREAK+10
C
C   DO 144 NN=1,5
C       KOUNT=0
C       DO 143 N=NA,NB
C           XFOR=X(N+1)+DELX(N+1)
C           XBAC=X(N)+DELX(N)
C           XCHECK=XFOR-XBAC
C           IF(XCHECK.LT.(0.8*XCRIT)) GO TO 142
C           GO TO 143
142      KOUNT=1
C           XDIFF=XCRIT-XCHECK
C           DELX(N)=DELX(N)-XDIFF/2.0
C           DELX(N+1)=DELX(N+1)+XDIFF/2.0
143      CONTINUE
C           IF(KOUNT.GT.0) GO TO 144
C           GO TO 145
144  CONTINUE
145  CONTINUE
C
C   ESTABLISH UNIFORM BEACH FACE SLOPE AND DUNE FACE SLOPE
C   SUCH THAT CONTINUITY IS SATISFIED AND ERODED VOLUME EQUALS
C   DEPOSITED VOLUME
C   NOTE: FROM THIS POINT ON, WE ARE ONLY CONCERNED WITH FINDING
C   PROFILE CHANGE IN BEACH-DUNE REGION
C
C
C   IF(DELWS.LT.0.0) GO TO 151
C   IF((H(NBERM).GT.0.0).AND.(NSTOP.NE.1)) GO TO 193
C   IF((H(NBERM).GT.0.0).AND.(DELWS.GE.0.0)) GO TO 150
C   GO TO 151
150  IF(HSTAR.EQ.H(NBERM)) HSTAR=H(NBERM-1)
151  CONTINUE
C
C   DETERMINE VOLUME REQUIRED TO SATISFY CONTINUITY
C   BY FINDING NET CHANGE IN VOLUME BETWEEN ORIGINAL
C   PROFILE AND CURRENT PROFILE IN DYNAMIC SOLUTION REGION

```



```

C   BETWEEN OFFSHORE POINT AND TRANSITION DEPTH, HSTAR.
C
C   SUMVOL(NMAX+1)=0.0
C
C   DO 160 M=1,NMAX
C       N=NMAX-(M-1)
C       VOL=DH*(X(N)+DELX(N)-X1(N))
C       SUMVOL(N)=SUMVOL(N+1)+VOL
C       IF(H(N).EQ.HSTAR) GO TO 161
160  CONTINUE
161  NSTAR2=N
C       DELSUM=-SUMVOL(NSTAR2+1)
C
C   DETERMINE VOLUME ERODED IN PREVIOUS TIME STEPS IN ONSHORE
C   ONSHORE PORTION OF THE PROFILE
C
C       HAVSUM=0.0
C
C       DO 170 N=1,NSTAR2
C           HAV=DH*(X(N)-X1(N))
C           HAVSUM=HAVSUM+HAV
170  CONTINUE
C       DSUM=DELSUM-HAVSUM
C
C   DETERMINE INCREMENTAL CHANGE IN VOLUME FOR CELLS ABOVE WATER LINE
C   TO SATISFY (1) UNIFORM SLOPE REQUIREMENT, AND (2) CONTINUITY
C
C       DELX(NSTAR2)=DSUM/((NSTAR2-NSTOP+1)*DH)
C
C       DO 180 M=1,NSTAR2
C           N=NSTAR2-(M-1)
C           DELX(N)=DELX(NSTAR2)
C           IF(N.LT.NSTOP) DELX(N)=0.0
C           VOL=DH*(X(N)+DELX(N)-X1(N))
C           SUMVOL(N)=SUMVOL(N+1)+VOL
180  CONTINUE
C
C   IF SOLUTION RESULTS IN DUNE ACCRETION, REPEAT CALCULATIONS
C   WITH ACCRETION LIMITED TO BERM AND BEACH FACE
C
193  IF(DELX(1).GT.0.0) GO TO 117
C
C   UPDATE POSITIONS OF EACH GRID POINT IN ENTIRE PROFILE
C
C       DO 666 N=1,NMAX
C           X(N)=X(N)+DELX(N)
666  CONTINUE
C
C*****
C   OUTPUT TO RECORD EROSION STATISTICS
C
C*****
999  CONTINUE

```

```

C
C   FIND CONTOUR LOCATION
C
      X20=0.0
      X15=0.0
      XDUNE=X(1)-X1(1)
      IF(MTWE.NE.0) X20=X(MTWE)-X1(MTWE)
      IF(MFIF.NE.0) X15=X(MFIF)-X1(MFIF)
      X10=X(MTEN)-X1(MTEN)
      X5=X(MFIV)-X1(MFIV)
      XMSL=X(MSL)-X1(MSL)
      VOLCHK=SUMVOL(1)
C
C   FIND ERODED VOLUME
C
      NVOL=1
      DO 500 N=1,NMAX
        IF(SUMVOL(N+1).LT.SUMVOL(N)) MVOL=N
        IF(SUMVOL(MVOL).GT.SUMVOL(NVOL)) NVOL=MVOL
500   CONTINUE
      VOLERO=SUMVOL(NVOL)/27.
C
C
      IF((T.NE.26.0).AND.(T.NE.30.0)) GO TO 998
      IF(JTIME.LT.JTMAX) GO TO 998
C
C-----WRITE STATEMENTS-----BEACH PROFILE DATA-----
C
      WRITE(3,921)T
      WRITE(3,920) VOLERO
      WRITE(3,925)
      WRITE(3,930)(N,H1(N),X1(N),H(N),X(N),DISS(N),QS(N),
1       DELX(N),SUMVOL(N),N=1,75)
      WRITE(3,945)
C
998   CONTINUE
C
C
2     CONTINUE
C
C-----WRITE STATEMENT-----TIME HISTORY OF STORM SURGE AND RECESSION-----
C
      WRITE(4,940) T,WSELEV,WH,XDUNE,X20,X15,X10,X5,XMSL,VOLERO,VOLCHK
C
      IF(T.EQ.0.0) GO TO 997
C
1     CONTINUE
C
      GO TO 707
C
777   CONTINUE
C
C
      STOP
      END

```